

**DEVELOPMENT OF GEOPOLYMER CONCRETES WITH  
CONSTRUCTION DEMOLITION WASTE**

**İNŞAAT YIKINTI ATIĞI İÇEREN JEOPOLİMER BETON  
TASARIMLARININ GELİŞTİRİLMESİ**

**EMİRCAN ÖZÇELİKÇİ**

**PROF. DR. MUSTAFA ŞAHMARAN**

**Supervisor**

Submitted to  
Graduate School of Science and Engineering of Hacettepe University  
as a Partial Fulfillment to the Requirements  
for be Award of the Degree of Master of Science  
in Civil Engineering

2020

## **ABSTRACT**

# **DEVELOPMENT OF GEOPOLYMER CONCRETES WITH CONSTRUCTION DEMOLITION WASTE**

**Emircan ÖZÇELİKÇİ**

**Master of Science, Department of Civil Engineering**

**Supervisor: Prof. Dr. Mustafa ŞAHMARAN**

**September 2020, 135 pages**

All around the world, sustainability of degrading infrastructures is a growing concern. Conventional concrete which is the main building block of these infrastructures consists of Portland cement as the main binding phase. Globally, there is an increasing trend in the cement consumption and as the emerging countries continue developing, the trend is expected to continue increasing. However, production of Portland cement is significantly energy-inefficient, carbon-intensive and accounts for 5 to 8% of total human-driven CO<sub>2</sub> emissions. Prolonged sustainability therefore necessitates the design and production of construction materials that are eco-friendly in nature. For true infrastructural sustainability, hence, a paradigm shift is necessary in terms of both greenness of conventional concrete material and improved infrastructural durability for the sake of less frequent repairs.

Construction and demolition applications have become one of the leading sectors in the world with the increased number of repetitive repair/renovation/maintenance of buildings, roads, bridges and other structures. However, each year, significant amounts of solid waste are generated as a result of the abovementioned applications requiring to be tackled properly. There are multiple adverse effects of construction and demolition waste (CDW) which include (i) waste landfilling of very large clean lands, (ii) causing hazardous pollution which jeopardize the surroundings and (iii) wasting of natural resources. Although “zero CDW”

seems unpractical since the waste generation is unavoidable, effective solutions to minimize the amount of CDW generated must be sought for the sake of environmental, social and economic benefits.

To counteract the negative effects of Portland cement production and favour increased materials' greenness, "geopolymers" are being researched widely nowadays. Geopolymer is a cement-free binding material obtained by the alkali-activation of certain aluminosilicate source materials. The source materials are generally obtained from industrial by-products including fly ash, slag, etc. Moreover, along with the significantly superior materials' greenness, geopolymers are being repeatedly reported to have high strength and enhanced durability performance (especially in terms of acid, corrosion, fire and frost resistance), although large-scale production and applications of geopolymer concretes are very restricted since the performance properties of ultimate geopolymeric materials are largely dependent on the selected aluminosilicate source material, availability of which is highly dependent on the geography.

The current research aims at developing "green" geopolymeric concrete whose constituents are entirely obtained from CDW for truly sustainable infrastructural development. For the purposes of the research, firstly, geopolymeric binding phases were developed using the inert portion of CDW which is largely composed of waste concrete, wall/roof members including different types of bricks/tiles and waste glass. Secondly, CDW-based aggregates with different sizes were incorporated into the geopolymeric binders to obtain "green" mortar and concrete mixtures. After evaluating the mechanical and micro-mechanical properties of geopolymer concretes, the focus was placed on the assessment of a set of durability properties. Successful outcomes and wide knowledge transfer of the current research are believed to make benefits in the lives of individuals by not only lowering the cost-inefficient and environment-unfriendly repairs of infrastructures but also completely recycling the CDW which is troubling all countries around the world with easy-to-implement, low-cost and energy-efficient techniques.

**Keywords:** Geopolymer Concretes, Alkali Activated Materials, Construction and Demolition Wastes, Mechanical Properties, Micro-Mechanical Properties, Durability of Geopolymer Concretes

## ÖZET

# İNŞAAT YIKINTI ATIĞI İÇEREN JEOPOLİMER BETON TASARIMLARININ GELİŞTİRİLMESİ

**Emircan ÖZÇELİKÇİ**

**Yüksek Lisans, İnşaat Mühendisliği Bölümü**

**Tez Danışmanı: Prof. Dr. Mustafa ŞAHMARAN**

**Eylül 2020, 135 sayfa**

Tüm dünyada, bozulmaya uğrayan altyapıların sürdürülebilirliği giderek artan bir endişe kaynağıdır. Bu altyapıların yapı taşı olan geleneksel beton, ana bağlayıcı faz olarak Portland çimentosundan oluşmaktadır. Küresel olarak, çimento tüketiminde artış eğiliminin olmasının yanında, gelişmekte olan ülkeler gelişmeye devam ettikçe, trendin artmaya devam etmesi beklenmektedir. Bununla birlikte, Portland çimentosunun üretimi, insan kaynaklı CO<sub>2</sub> emisyonlarının %5-8'ini oluşturur ve önemli ölçüde verimsiz enerji kullanımı ile yoğun karbon salınımından sorumludur. Bu nedenle uzun süreli sürdürülebilirlik, doğada çevre dostu yapı malzemelerinin tasarımını ve üretimini gerektirmektedir. Doğru altyapı sürdürülebilirliği kapsamında daha az sıklıkta yapılacak onarımlar için hem çevre dostu geleneksel betonlar hem de gelişmiş altyapı dayanıklılığı açısından köklü bir değişim gereklidir.

İnşaat ve yıkıntı uygulamaları, binaların, yolların, köprülerin ve diğer yapıların tekrar eden onarım/yenileme/bakımlarının artmasıyla dünyanın önde gelen sektörlerinden biri haline gelmiştir. Bununla birlikte, her yıl yukarıda belirtilen ve uygun bir şekilde ele alınması gereken uygulamalar sonucunda önemli miktarlarda katı atık ortaya çıkmaktadır. İnşaat ve yıkıntı atığının (İYA) (i) çok büyük temiz arazilerde depolanması, (ii) çevreye tehlikesi olan hava kirliliğe neden olması ve (iii) doğal kaynakların boşa harcanması gibi birçok olumsuz

etkisi vardır. Her ne kadar atık üretimi kaçınılmaz olduğu için “sıfır İYA” kavramı pratik olmasa da çevresel, sosyal ve ekonomik faydalardan ötürü İYA miktarını en aza indirecek etkili çözümler aranması gerekmektedir.

Portland çimentosu üretiminin olumsuz etkilerini minimize etmek ve çevre dostu malzemeleri desteklemek için, günümüzde “jeopolimerler” yaygın olarak araştırılmaktadır. Jeopolimer, alüminosilikat kaynaklı malzemelerin alkali aktivasyonu ile elde edilen çimento içermeyen bir bağlayıcı malzemedir. Uçucu kül, cüruf gibi bu tür alüminosilikat kaynaklı malzemeler genellikle endüstriyel yan ürünlerden elde edilir. Bunun yanı sıra, önemli ölçüde çevre dostu olmasına ve yüksek mukavemet ile gelişmiş dayanıklılık performanslarının (özellikle asit, korozyon, yangın ve dona dayanıklılık açısından) defalarca belirtilmesine karşın, jeopolimer malzemelerin nihai performans özellikleri önemli ölçüde seçilen alüminosilikat kaynağı malzemeye bağlı olduğundan, büyük ölçekli jeopolimer betonların üretimi ve uygulamaları çok kısıtlıdır.

Bu araştırma, tam olarak sürdürülebilir altyapı gelişimi için bileşenleri tamamen İYA'dan elde edilen “çevre dostu” jeopolimer beton geliştirmeyi amaçlamaktadır. Araştırmanın amaçları doğrultusunda, ilk olarak, büyük ölçüde beton atığından, farklı tipte tuğla/fayans atığı içeren duvar/çatı elemanlarından ve cam atığından oluşan İYA'nın kullanılmasıyla jeopolimer bağlayıcı fazlar geliştirilmiştir. Ardından, "çevre dostu" harç ve beton karışımları elde etmek için farklı boyutlarda İYA bazlı agregalar jeopolimer bağlayıcılara dahil edilmiştir. Üretilen jeopolimer betonların mekanik ve mikro-mekanik özellikleri değerlendirildikten sonra, bir takım dayanıklılık özelliklerinin değerlendirilmesine odaklanılmıştır. Mevcut araştırmanın başarılı sonuçlarının ve geniş bilgi aktarımının, sadece altyapıların maliyetlerini ve çevreye zararlı onarımlarını düşürmekle kalmayıp, aynı zamanda tüm ülkelerin sıkıntısı olan İYA'yı uygulaması kolay, düşük maliyetli ve enerji tasarruflu teknikler ile tamamen geri dönüştürerek bireylerin yaşamlarına fayda sağladığına inanılmaktadır.

**Anahtar Kelimeler:** Jeopolimer Betonlar, Alkali Aktif Malzemeler, İnşaat Yıkıntı Atıkları, Mekanik Özellikler, Mikro-Mekanik Özellikler, Jeopolimer Betonların Dayanıklılığı

## ACKNOWLEDGEMENT

First and foremost, I would like to express my sincere gratitude to my supervisor Prof. Dr. Mustafa ŞAHMARAN for the continuous support of my study and research, for his patience, motivation, and immense knowledge. His guidance helped me in all the time of research and writing of this thesis. I could not have imagined having a better advisor and mentor for my study.

Also, I have to give thanks to Prof. Dr. İsmail Özgür YAMAN, Assoc. Prof. Dr. Mustafa Kerem KOÇKAR, Assoc. Prof. Dr. Alper ALDEMİR for giving me the opportunity to defend my master thesis.

I have to express my gratitude to Assoc. Prof. Dr. Gürkan YILDIRIM for his valuable guidance and support. It was impossible to achieve this study without his help. Also, I would like to express my gratitude to all my colleagues at Hacettepe University for their support and valuable friendship.

The author gratefully acknowledges the financial assistance of the Scientific and Technical Research Council (TUBITAK) of Turkey provided under Project: 218M102.

Finally, I must express my very profound gratitude to my parents and to my family for providing me with unfailing support and continuous encouragement throughout my years of study and through the process of researching and writing this thesis. This accomplishment would not have been possible without them.

# TABLE OF CONTENTS

ABSTRACT .....	i
ÖZET .....	iii
ACKNOWLEDGEMENT .....	v
TABLE OF CONTENTS .....	vi
LIST OF TABLES .....	viii
LIST OF FIGURES .....	x
SYMBOLS AND ABBREVIATIONS .....	xiii
1. INTRODUCTION.....	1
1.1. General.....	1
1.2. Research Objectives and Scope .....	3
2. LITERATURE REVIEW .....	5
2.1. Portland Cement and Conventional Concrete .....	5
2.1.1. The Environmental Impact of Portland Cement and Conventional Concrete.....	6
2.2. Geopolymers as Alternative Binders .....	7
2.2.1. Alkali Activators of Geopolymers .....	9
2.2.2. Geopolymer Binders .....	11
2.2.3. Structure and Matrix Properties of Geopolymer Binders.....	16
2.3. Use of Construction and Demolition Wastes in Geopolymer Production.....	21
2.4. Construction and Demolition Waste Based Recycled Concrete Aggregate .....	24
2.4.1. Preparation of Recycled Aggregate.....	24
2.4.2. Composition of Recycled Aggregate .....	25
2.4.3. Properties of Recycled Aggregate.....	28
3. MATERIALS AND METHODOLOGY .....	43
3.1. Materials .....	43
3.1.1. Roof/Wall Wastes .....	44
3.1.2. Glass Waste (GW).....	46
3.1.3. Concrete Waste (CW) .....	47
3.1.4. Granulated Blast Furnace Slag (GBFS) .....	49
3.1.5. Fly Ash (FA) .....	50
3.1.6. Alkali Activators .....	51

3.1.7. Recycled Aggregate.....	53
3.1.8. Shrinkage Reducer Admixture .....	55
3.2. Methodology .....	56
3.2.1. Preparation of Mixtures .....	56
3.2.2. Casting and Placing .....	56
3.2.3. Curing Conditions .....	61
3.2.4. Consistency and Setting Time Analysis .....	61
3.2.5. Soundness Test on Recycled Aggregates .....	64
3.2.6. Flexural and Compressive Strength Tests .....	65
3.2.7. Mineralogical and Microstructural Analysis .....	65
4. EXPERIMENTAL RESULTS AND DISCUSSION .....	66
4.1. Development of Geopolymer Binders .....	66
4.2. Development of Geopolymer Mortars .....	76
4.3. Development of Geopolymer Concretes.....	83
4.4. Micro-Mechanical Analysis.....	93
4.4.1. X-ray diffraction (XRD) Analysis.....	93
4.4.2. Scanning Electron Microscope (SEM) and Energy Dispersive X-Ray (EDX) Analysis .....	98
4.5. Durability Studies of CDW-Based Geopolymer Concrete .....	108
4.5.1. Resistance to Sulphate.....	109
4.5.2. The Resistance to Wetting–Drying Cycles.....	111
4.5.3. Rapid Chloride Permeability Test .....	113
4.5.4. Sorptivity Test .....	113
5. CONCLUSION .....	116
REFERENCES .....	119



## LIST OF TABLES

<b>Table 2.1.</b>	CDW compositions for different grain sizes .....	26
<b>Table 2.2.</b>	CDW compositions for different grain sizes .....	26
<b>Table 2.3.</b>	Studies related to the water absorption capacity of CDW-based recycled aggregate .....	31
<b>Table 2.4.</b>	Studies related to the density of CDW-based recycled aggregate .....	36
<b>Table 3.1.</b>	Chemical composition of hollow brick .....	44
<b>Table 3.2.</b>	Chemical composition of red clay brick .....	45
<b>Table 3.3.</b>	Chemical composition of roof tile .....	46
<b>Table 3.4.</b>	Chemical composition of glass waste .....	46
<b>Table 3.5.</b>	Chemical composition of concrete waste.....	47
<b>Table 3.6.</b>	Specific gravity values of CDW-based precursors .....	48
<b>Table 3.7.</b>	Chemical composition of Granulated Blast Furnace Slag .....	49
<b>Table 3.8.</b>	Chemical composition of Fly Ash .....	50
<b>Table 3.9.</b>	Properties of Calcium Hydroxide Powder .....	51
<b>Table 3.10.</b>	Properties of Sodium Hydroxide Flakes .....	52
<b>Table 3.11.</b>	Chemical composition of Liquid Sodium Silicate .....	53
<b>Table 3.12.</b>	Minimum aggregate amount according to Dmax .....	54
<b>Table 3.13.</b>	Properties of the recycled aggregates.....	55
<b>Table 3.14.</b>	The proportions of geopolymer paste mixtures produced for the determining consistency and setting time .....	62
<b>Table 3.15.</b>	Consistency test results .....	62
<b>Table 3.16.</b>	Initial and final setting results .....	63
<b>Table 3.17.</b>	Aggregate soundness test results .....	65
<b>Table 4.1.</b>	Geopolymer paste mixtures containing 100% concrete waste.....	67
<b>Table 4.2.</b>	Geopolymer paste mixtures containing 100% concrete waste and binary alkali activator.....	69
<b>Table 4.3.</b>	Geopolymer paste mixtures containing concrete waste and glass waste .....	71
<b>Table 4.4.</b>	Geopolymer paste mixtures containing all CDW based precursors .....	74
<b>Table 4.5.</b>	Geopolymer mortar mixtures containing all CDW based precursors and recycled fine aggregates.....	77

<b>Table 4.6.</b>	Geopolymer mortar mixtures produced with the addition of GBFS .....	79
<b>Table 4.7.</b>	Geopolymer mortar mixtures produced with the addition of Ca(OH) <sub>2</sub> .....	81
<b>Table 4.8.</b>	Experiment to examine the effect of inert material between 0-100 microns in the recycled aggregate .....	84
<b>Table 4.9.</b>	Investigation of fly ash and aggregate amount in the scope of geopolymer concrete development.....	85
<b>Table 4.10.</b>	Mixtures produced by changing various parameters in the development of geopolymer concrete .....	86
<b>Table 4.11.</b>	Compressive strength results of mixtures produced by changing various parameters in the development of geopolymer concrete.....	86
<b>Table 4.12.</b>	Study on the shrinkage behavior of samples in the development of geopolymer concrete .....	88
<b>Table 4.13.</b>	Compressive strength results in the study on the shrinkage behavior of samples in the development of geopolymer concrete .....	89
<b>Table 4.14.</b>	Final mixtures in the development of geopolymer concrete .....	90
<b>Table 4.15.</b>	Compressive strength results of final mixtures in the development of geopolymer concrete .....	91
<b>Table 4.16.</b>	Mixtures produced for durability studies .....	109

## LIST OF FIGURES

<b>Figure 2.1.</b>	Representative three-fold diagram of fly ash composition .....	15
<b>Figure 2.2.</b>	Composition of recycling aggregate .....	25
<b>Figure 3.1.</b>	Hollow brick images (from left to right; raw state, crushed state, ground state, SEM micrograph).....	44
<b>Figure 3.2.</b>	XRD pattern of hollow brick .....	44
<b>Figure 3.3.</b>	Red clay brick images (from left to right; raw state, crushed state, ground state, SEM micrograph).....	45
<b>Figure 3.4.</b>	XRD pattern of red clay brick.....	45
<b>Figure 3.5.</b>	Roof tile images (from left to right; raw state, crushed state, ground state, SEM micrograph).....	45
<b>Figure 3.6.</b>	XRD pattern of roof tile .....	46
<b>Figure 3.7.</b>	Glass waste images (from left to right; raw state, crushed state, ground state, SEM micrograph).....	46
<b>Figure 3.8.</b>	XRD pattern of glass waste.....	47
<b>Figure 3.9.</b>	Concrete waste images (from left to right; raw state, crushed state, ground state, SEM micrograph).....	47
<b>Figure 3.10.</b>	XRD pattern of concrete waste .....	48
<b>Figure 3.11.</b>	Particle size distribution of CDW-based precursors.....	48
<b>Figure 3.12.</b>	Granulated Blast Furnace Slag image (from left to right; raw state, SEM micrograph).....	49
<b>Figure 3.13.</b>	XRD pattern of Granulated Blast Furnace Slag.....	49
<b>Figure 3.14.</b>	Fly ash images (from left to right; raw state, SEM micrograph) .....	50
<b>Figure 3.15.</b>	XRD pattern of Fly Ash.....	50
<b>Figure 3.16.</b>	Calcium Hydroxide Powder.....	51
<b>Figure 3.17.</b>	Sodium Hydroxide images (from left to right; 25 kg bag, flake form).....	52
<b>Figure 3.18.</b>	Liquid Sodium Silicate .....	53
<b>Figure 3.19.</b>	Granulometry analysis of Recycled Aggregate .....	54
<b>Figure 3.20.</b>	Shrinkage Reducer Admixture.....	55
<b>Figure 3.21.</b>	Geopolymer Pastes (Containing % 100 CW) .....	57

<b>Figure 3.22.</b> Geopolymer Pastes (Containing different proportions of CW, GW, HB, RCB, RT) .....	57
<b>Figure 3.23.</b> Geopolymer Mortars (Containing different proportions of CW, GW, HB, RCB, RT and Recycled Fine Aggregates) .....	58
<b>Figure 3.24.</b> Geopolymer Mortars (Addition of GBFS and Ca(OH) <sub>2</sub> to those containing different proportions of CW, GW, HB, RCB, RT and Recycled Fine Aggregates) .....	58
<b>Figure 3.25.</b> Geopolymer Concretes (the study carried out within the scope of the shrinkage behavior of the samples) .....	58
<b>Figure 3.26.</b> Geopolymer Concretes (GC1 and GC2 samples in final series).....	59
<b>Figure 3.27.</b> Geopolymer Concretes (in water curing GC1 and GC2 samples in final series) .....	59
<b>Figure 3.28.</b> Geopolymer Concretes (GC3 and GC4 samples in final series).....	60
<b>Figure 3.29.</b> Geopolymer Concretes (GC5 and GC6 samples in final series).....	60
<b>Figure 3.30.</b> Geopolymer Concretes (GC7 samples in final series) .....	60
<b>Figure 3.31.</b> Consistency and setting time measurements with Vicat apparatus.....	63
<b>Figure 3.32.</b> Test equipments prepared for aggregate soundness test .....	64
<b>Figure 4.1.</b> Compressive strength results of geopolymer paste mixtures containing 100% concrete waste .....	67
<b>Figure 4.2.</b> Compressive strength results of geopolymer paste mixtures containing 100% concrete waste and binary alkali activator .....	70
<b>Figure 4.3.</b> Compressive strength results of geopolymer paste mixtures containing concrete waste and glass waste.....	72
<b>Figure 4.4.</b> Compressive strength results of geopolymer paste mixtures containing all CDW based precursors .....	74
<b>Figure 4.5.</b> Compressive strength results of geopolymer mortar mixtures containing all CDW based precursors and recycled fine aggregates .....	78
<b>Figure 4.6.</b> Compressive Strength results of geopolymer mortar mixtures produced with the addition of GBFS .....	80
<b>Figure 4.7.</b> Compressive strength results of geopolymer mortar mixtures produced with the addition of Ca(OH) <sub>2</sub> .....	82
<b>Figure 4.8.</b> XRD analysis of WCF-1 mixture after heat curing at 75 ° C for 72 hours.....	93
<b>Figure 4.9.</b> XRD analysis of WCF-9 mixture after heat curing at 125 ° C for 48 hours....	94
<b>Figure 4.10.</b> XRD analysis of WCF-S-6 mixture after 28 days of ambient curing .....	94

<b>Figure 4.11.</b> XRD analysis of CDWF-1 mixture after heat curing .....	94
<b>Figure 4.12.</b> XRD analysis of CDWF-9 mixture after heat curing .....	95
<b>Figure 4.13.</b> XRD analysis SW-6 mixture after 28 days of ambient curing .....	95
<b>Figure 4.14.</b> XRD analysis SS-6 mixture after 28 days of ambient curing .....	95
<b>Figure 4.15.</b> XRD analysis SS6-2 mixture after 28 days of ambient curing .....	96
<b>Figure 4.16.</b> XRD analysis E-2 mixture after 28 days of ambient curing .....	96
<b>Figure 4.17.</b> XRD analysis GC-7 mixture after 28 days of moisture curing .....	96
<b>Figure 4.18.</b> SEM-EDX analysis of WCF-1 mixture (75 ° C for 72 hr) .....	99
<b>Figure 4.19.</b> SEM-EDX analysis of WCF-9 mixture (125 ° C for 48 hr) .....	100
<b>Figure 4.20.</b> SEM-EDX analysis of WCF-S-6 mixture (28 days at ambient) .....	100
<b>Figure 4.21.</b> SEM-EDX analysis of CDWF-1 mixture after heat curing .....	101
<b>Figure 4.22.</b> SEM-EDX analysis of CDWF-9 mixture after heat curing .....	102
<b>Figure 4.23.</b> SEM-EDX analysis SW-6 mixture (28 days at ambient) .....	103
<b>Figure 4.24.</b> SEM-EDX analysis SS-6 mixture (28 days at ambient) .....	104
<b>Figure 4.25.</b> SEM-EDX analysis SS6-2 mixture (28 days at ambient) .....	105
<b>Figure 4.26.</b> SEM analysis E-2 mixture (28 days at ambient) .....	106
<b>Figure 4.27.</b> SEM analysis GC-7 mixture (28 days at ambient) .....	106
<b>Figure 4.28.</b> Masses of the samples for Resistance to Sulphate .....	110
<b>Figure 4.29.</b> Compressive strength results of the samples for Resistance to Sulphate ....	110
<b>Figure 4.30.</b> Masses of the samples for Wetting-Drying Cycles .....	111
<b>Figure 4.31.</b> Compressive strength results of the samples for Wetting-Drying Cycles ...	112
<b>Figure 4.32.</b> Coulomb values of the samples for RCPT .....	113
<b>Figure 4.33.</b> Absorption results of the F-coded samples for Sorptivity test .....	114
<b>Figure 4.34.</b> Absorption results of the W-coded samples for Sorptivity test .....	114

## SYMBOLS AND ABBREVIATIONS

### Abbreviations

BA	Bottom Ash
BFS	Blast Furnace Slag
Ca(OH) <sub>2</sub>	Calcium Hydroxide
CDW	Construction Demolition Wastes
CW	Concrete Waste
EDX	Energy Dispersive X-Ray Analysis
FA	Fly Ash
GBFS	Ground Granulated Blast Furnace Slag
GW	Glass Waste
HB	Hollow Brick
Na <sub>2</sub> SiO <sub>3</sub>	Sodium Silicate
NaOH	Sodium Hydroxide
RCB	Red Clay Brick
RT	Roof Tile
SEM	Scanning Electron Microscopy
XRD	X-ray Diffraction Analysis
XRF	X-ray Fluorescence Analysis

# 1. INTRODUCTION

## 1.1. General

Portland cement is the most energy-intensive, costly and environmentally-unfriendly ingredient of conventional concrete. The energy required to produce one kilogram of clinker is 850 kcal. To produce a tonne of clinker, 1.7 tonnes of rock is needed (Pacheco-Torgal and Jalali, 2010). Producing one tonne of cement is responsible of the emission of 0.94 tonnes of CO<sub>2</sub> – 0.55 tonnes from calcination of raw clinker materials and 0.39 tonnes from fuel emissions (Gartner, 2004) The cement industry is responsible for 5-8% of the total anthropogenic CO<sub>2</sub> in the atmosphere (Scrivener and Kirkpatrick, 2008), and the cost of cement represents more than 45% of the overall cost of conventional concrete (Pacheco-Torgal and Jalali, 2010). Despite its drawbacks, the place of conventional concrete did not change over the years and the material is still the most commonly used construction material and is the second mostly consumed material in the world following water (Woodward and Duffy, 2011). It is therefore appropriate to state that, for the time being, no construction activity can be imagined without concrete.

On the other hand, considering the ever-increasing population and the economy and industry of developing countries, construction and demolition management has become one of the most important factor by generating the greatest amount of waste. At the root of significantly increased amounts of CDW around the globe, there mostly stand the structural and infrastructural projects, renovation, repair/maintenance and demolition work. In cases where these waste materials are not controlled, it is inevitable that there will be irreversible effects on the natural habitat due to the filling of clean landfills and the accumulation of toxic substances. Consequently, the management of CDW in an appropriate manner for the sake of environmental, economic and social benefits is of great importance. This is not only important in terms of reducing the CDW amount for clean landfills but also to remarkably reduce the amount of cement-based material that is, otherwise, going to be used to build/renovate/repair/maintain new and/or existing infrastructures.

Among major CDW components, concrete and masonry units (different types of bricks/tiles) are of greater importance given the fact that these account for more than 50% of total waste

generated (Patel et al., 2016). To illustrate the situation, yearly concrete production of EU member countries is nearly 50 million tons while the same values were reported to be 60 and 10-12 million tons for the USA and Japan, respectively (Arslan et al., 2012). On the other hand, other units such as metals, wood-based materials, pipes, conduits etc. can more easily be reused and/or recycled. Moreover, concrete and masonry units should be considered as one because, during demolition, it is almost impossible to separate the individual pieces from each other, making reuse and/or recycling of these materials more difficult.

The current practice of waste concrete reuse and recycling is predominantly limited to the basic crushing process which creates coarse aggregates together with concrete fines. Usage of final recycled coarse aggregates from the concrete crushing process is limited to low-specification applications and mostly allocated to the landfilling of road base courses and non-structural filling (Hack and Bryan, 2006). Furthermore, recycled coarse concrete aggregates are generally of low quality. This is originated due to cement paste and/or mortar particles remaining on the recycled aggregate surface. Recycled aggregates have higher crushability, abrasion loss, water absorption and amount of dusty particles in comparison to natural aggregates which cause concrete mixtures incorporating these recycled aggregates to have lower strength, durability and shrinkage properties. This, therefore, results in limited rates of recycled aggregate utilization in the production of fresh structural concrete. In addition to the inferior performance, fine aggregates generated as a result of waste concrete crushing generally buried to clean landfills as well.

However, for the sake of prolonged sustainability, complete recycling of waste concrete is highly desirable which is very challenging even for the researchers working in the related area. It is therefore with the current research to focus on recycling of inert portion of CDW (concrete, masonry, window glass etc.) to manufacture “green” concrete.

The principal aim of this thesis is to develop globally applicable solutions to counteract the undeniable negative effects of CDW on environment, economy, society and to gain maximum possible favour from CDW by the development of “green” construction materials, and hence to promote and popularize the notion of reusing and/or recycling in the construction industry.



The successful outcomes of this research are highly likely to contribute to deceleration of the pace of global warming which is of the main challenges facing humanity nowadays. To achieve the overall goal of the research, the specific objectives listed below are identified:

- Development and performance characterization of novel and environmentally-friendly geopolymeric binders produced completely out of the inert portion of CDW including waste concrete, wall/roof elements and waste glass (whose reuse is restricted to low-tech technologies such as direct crushing) by considerably less energy-intensive, more economical and easily applicable techniques of alkali-activation to be actively used in the production of “green” concrete materials.
- Development and detailed durability/mechanical property characterization of “green” concrete materials incorporated with novel geopolymeric binders (from the first specific objective) and fine/coarse waste aggregates acquired completely from CDW to maximize the amount of reused/recycled CDW material and in favour of contributing prolonged sustainability and enhanced materials’ greenness without compromising the expected properties from ultimate materials.

## **1.2. Research Objectives and Scope**

In the current thesis study, a major objective is to completely recycle the inert portion of CDW (i.e. concrete waste, masonry and glass cullets). The first stage of this objective is to manufacture binding agent that is capable of holding the recycled aggregate particles together, similar to ordinary Portland cement. To entirely recycle the inert portion of CDW herein, an emerging methodology called “geopolymerization” was utilized. In the material and methodology section, the physical and chemical properties of all materials used in the study were examined. In addition, the methodology of all processes within the scope of the study is presented in detail.

As the first step of the study, concrete waste (CW) obtained in the powdery form after the crushing and grinding of waste concrete and masonry units was used singly as the aluminosilicate source for geopolymeric binder production. If the expected performance is not obtained, CW will be combined with powdered waste bricks/tiles/glass cullets which will be acquired after the selective demolition of infrastructures. At this stage, the types of alkali activators (sodium hydroxide and sodium silicate), molar concentrations of activators (10M, 15M and 19M), different curing conditions (lab. environment, dry and moist curing)

and curing temperatures (ambient temperature, 75 °C, 100 °C and 125 °C) was primarily focused. In the second step to produce geopolymeric binders, the abovementioned approach was taken one step further by optimizing the ingredients with another CDW participant, glass waste (GW). GW's high amorphous silica and alkali contents make it an excellent material source and activator for the production of cement-free geopolymeric binder. Eventually, to further improve the usability of completely CDW-based geopolymeric binders, concrete waste and glass waste was combined with waste roof/wall elements to design mixtures with completely including CDW-based materials. Afterward, the development of CDW-based geopolymeric binders, compressive strength test results were considered for the performance assessment of geopolymeric binders.

In the following step of the study, different geopolymeric binders produced with sufficient mechanical properties were incorporated with recycled coarse and fine aggregates. As part of the development of CDW-based mortar and concrete mixtures, the study focused entirely on ambient curing. In this scope, sodium hydroxide, sodium silicate and calcium hydroxide were used as alkaline activators in ternary in various proportions and 20% blast furnace slag was combined with CDW-based materials to evaluate the performance of several mixture designs in terms of compressive strength. In the development of CDW-based geopolymer mortar, the recycled fine aggregate / binder ratio was chosen as 0.35 and the water / binder ratio was kept constant as 0.35. In the ongoing phase, CDW-based geopolymer concrete mixtures were developed by adding coarse recycled aggregate to the mixtures that provide the best performance out of 30 designed geopolymer mortar mixtures. Finally, 7 CDW based geopolymer concrete mixtures were designed and their compressive strength, flexural strength, Scanning Electron Microscope (SEM), Energy Dispersive X-Ray (EDX) X-ray Diffraction (XRD) analysis were examined.

At the final stage of the study, the mixtures with the best performance in terms of mechanical and micro-mechanical properties were subjected to durability tests such as resistance to sulfate, sorptivity, rapid chloride permeability test (RCPT) and resistance of wetting-drying cycles to examine their durability performance. Eventually, all the data acquired within the scope of the study are summarized in the conclusion section.

## **2. LITERATURE REVIEW**

### **2.1. Portland Cement and Conventional Concrete**

Portland cement is the mostly used building material worldwide, as its easy, accessible and economical, suitable properties for all construction applications. It is generally used when cement and/or concrete is not exposed to specific exposures such as sulfate attack from soil or water, or to an unfavorable temperature increase due to hydration. Usage areas are reinforced concrete buildings, bridges, railway structures, tanks, reservoirs, culverts, sewers, in short, all building systems.

The first work was carried out by Isaac Johnson in 1844 to produce Portland cement using high heat treatments. Within this procedure, Johnson went to heat treatment until the materials used in cement production partially melt. This method not only shortened the calcination time, but also enabled cement production with more reliable setting times and strength properties. In the following years, cement production continued with an easier method by the pulverizing the solid clinker produced with the mentioned process using jaw crushers. (Klemm, 1989). Limiting the use of clay and lime in Portland cement production with a certain ratio was discovered in the following years and volumetric rates were used until this discovery. In 1887, Le Chatelier researched cement chemistry within the scope of his studies and proposed upper and lower limits for the amount of lime to be used in quality of cement production (Klemm, 1989). Production of modern Portland cement and traditional concrete applications based on Portland cement has began to become widespread in 1880. In the following process, the use of steel reinforcement with high tensile strength and concrete with high compressive strength together in reinforced concrete systems has become widespread.

Although Portland cement has high mechanical properties, it is an insufficient material from the point of durability. In the years when Portland cement was still considered to be a young building material, the serious damages seen in the rail tunnels made in France are an important example in terms of these weak durability properties. When the damages are examined, it is seen that there are sulphate attacks originating from groundwater. In order to overcome this problem, sulfur-resistant high aluminate cement was produced by melting

bauxite (aluminum hydroxide) and lime together. It was used quite widely in that period through these properties of the product. However, in the following period, the use of high aluminated cement remained at a limited level due to the damages when exposed to high humidity and temperature effects (Neville, 1975).

For more than a century, cement, aggregate and water are the main part of the concrete used in construction. The characteristic of concrete in this mixture depends mainly usage of the water. Sufficient water must be included in the system to ensure cement hydration takes place and acquire sufficient workability for placement in fresh concrete. This condition often requires more water to be used and an increase in water has a direct impact on the characteristics of concrete. Since the 1980s, there have been two important developments regarding the manufacture of high strength concrete with many additives. The first was to improve the mix design by optimizing the gradation of the grains used in the concrete mix with the addition of extremely fine nanoscale microsilica particles that fill the gaps between the larger cement particles. With this approach, increases in compressive strength performances have been achieved by ensuring that the matrices of the mixes are more compact and dense. The second development was to minimize water demands by the addition of organic components into the mixture, which would improve the fresh concrete mixtures' fluidity. The compressive strength has risen to the rate of 80-120 MPa from 20-40 MPa as a result of using these additives. This led to substantial improvements in urban architecture and construction practices. In the following process, studies were carried out on optimizing these two developments and obtaining more effective combinations.

### **2.1.1. The Environmental Impact of Portland Cement and Conventional Concrete**

Increasing social awareness about the threats caused by global warming raised more concern about the impact of anthropogenic carbon dioxide (CO<sub>2</sub>) emissions on the global climate. Considering the results of cement production, water management and air pollution are the most urgent areas of action. At the Copenhagen Climate Summit, a common idea was expressed that 2020 and 2050 were critical turning points for climate change and it was decided to speed up action plans. The current atmospheric CO<sub>2</sub> level approaches 380 ppm according to the data obtained from recent studies. Even if parameters directly affecting CO<sub>2</sub> emissions such as high commercial volume, technological and social changes are not taken

into account, CO<sub>2</sub> concentration is estimated to increase above 800 ppm at the end of the century (Feely et al. 2004, Sabine et al. 2004).

In addition to CO<sub>2</sub> emissions, the cement industry is responsible for its emission in other dangerous compounds such as carbon monoxide (CO), nitrogen oxides (NO<sub>x</sub>), sulfur dioxide (SO<sub>2</sub>) and heavy metals (Lei et al., 2011, Wang, 2013). Many of the substances that cause air pollution by releasing during cement manufacturing arise with high temperatures in the rotary kiln and it is necessary to control its emissions to prevent environmental pollution. Because of the growing volume of cement in the global market and the negative environmental effects it causes, the necessity for control over cement production has become inevitable. Attempts at all stages of service life to estimate and reduce environmental impacts caused by products manufactured globally like cement are increasingly becoming more and more relevant. Within the scope of these evaluations, environmental awareness should be increased by making realistic inferences about the damages of cement.

Considering the damages of cement, it is an undoubted fact that alternative binders that are not as aggressive as the cement to the environment should replace cement. However, information that can be obtained on why cement remains such a successful building material can assist in the design of strategies for producing alternative materials in the future.

## **2.2. Geopolymers as Alternative Binders**

The term geopolymer was first introduced by Joseph Davidovits in the 1970s to describe the type of material formed with reactions between aluminosilicate powder and alkali solution (Davidovits 1982a). They were first developed as the fire-resistant alternative to heat-curing polymers after conflagrations in European countries. It has been used as a protective resin layer for carbon fiber composites at high temperatures and as a protective material in many different areas such as providing thermal protection to wooden structures. In the future, much research has centered on the usability of this kind of materials as building materials as a result of the reliable and high-performance properties of geopolymers produced by fly ash activation (Wastiels et al., 1993).

The first study for the development of constructive materials with alkali-activation of different materials from cement was carried out by Purdon in 1940, and in his studies, he

activated the types of metallurgical slag. In the future, the main difference to be made regarding the alkali activation of slags and the geopolymer products obtained is the formation of a one-dimensional calcium silica hydrate based gel structure in which the Al-Si and Mg-Ca exchanges can take place (Duxson et al. 2007b).

The term geopolymer is defined in the literature in quite different forms such as alkali ash materials, inorganic polymers, hydroceramics, inorganic polymer glasses, mineral polymers, soil cement, alkali-bonded ceramics. Geopolymers have been identified as a subset of alkali-activated materials, which includes materials that can be constituted through the activation of metallurgical slags by alkali, silicate, sulfate or carbonate and gives a product that can be defined as calcium silicate hydrate (Shi et al., 2006). It can be shown as a defining feature of geopolymers that the binding phase of the geopolymer contains an alkali aluminosilicate gel bonded with aluminum and silicon in the frame of a three-dimensional tetrahedral gel (MacKenzie, 2003; Rees et al., 2007). Davidovits stated the 'sialate' terminology to define aluminosilicate structures, and within the scope of this terminology, Si-O-Si was named as a siloxo bond and Si-O-Al as a sialate bond (Davidovits, 1982a). Thanks to this terminology, it has become possible to define the geopolymer compositions according to Si/Al ratios. These ratios are defined as bond polysialate when 1.0, polysialate-siloxo when 2.0 and polysialate-disiloxo when 3.0. Although this nomenclature system enables a certain classification, it is inadequate because it only expresses the Si/Al ratios as an integer and defines a three-dimensional network structure as one-dimensional.

Geopolymers are a complicated class of material. The main way to synthesize geopolymers is to combine an alkaline activator with an aluminosilicate material (especially metakaolin, fly ash or calcined kaolinite-clay). The result of this combination is an irregular alkaline aluminosilicate gel known as the geopolymer gel binder. This phase also contains the void structure incorporating unreacted solid precursors embedded in the matrix and water. Unlike the CSH gel produced in cementitious systems, water does not form an integral component of the geopolymer binder, and practically this has both the pros and cons. The basic structural framework of the geopolymer gel consists of a highly bonded 3-dimensional aluminate and silicate tetrahedral network formed by the alkaline metal cations from the activator solution and negative charge from  $Al^{3+}$  ions in four-fold coordination localized in one or more of the bridging oxygen in each aluminate tetrahedron. In some cases, this similarity is so high that

the nanocrystalline formation in the geopolymeric gel can be seen, especially in the high water content, high temperature and low Si/Al ratio (Provis et al., 2005). However, even if none of these factors exist and the geopolymer does not show a structural order at a length scale exceeding 1 nm, strong structural motifs can be detected that show a good correlation with those observed in zeolites at an atomic length scale (Bell et al., 2008).

## **2.2.1. Alkali Activators of Geopolymers**

### **2.2.1.1. Alkali Hydroxides**

Sodium and/or potassium can be considered as the most widely used alkaline hydroxide as the alkali activator. Lithium, rubidium and cesium hydroxides have been limited in use due to their costs, shortage and the relatively low solubility of LiOH in water (Monnin and Dubois, 2005). In comparison, both sodium and potassium hydroxide can be dissolved in water at even higher molarity such as 20 mol/kg (Kurt and Bittner, 2006). Sodium hydroxide is produced mainly by the chlorine alkali process. This has significant environmental impacts for using as an alkaline activator, both with regards to greenhouse emissions and emissions of components used in this production process. Potassium hydroxide is produced by the electrolysis of KCl solutions. In terms of the production process, besides the obvious corrosive properties of concentrated hydroxide solutions, the most important features to consider are the viscosities and heat that are released by dissolving alkalies hydroxide particles throughout the solution phase. Alkaline hydroxide solutions viscosity is quite low compared to alkaline silicate solutions used to the same purpose, which can be an advantage for alkaline hydroxide solutions.

Efflorescence is a common problem in the binders produced with alkaline hydroxide solutions where excess alkaline reacts with ambient CO<sub>2</sub> when an extremely high concentration of hydroxide solution is used. This phenomenon leads to visual esthetic issues, but it doesn't always detrimental to the structural integrity of the product. In hydroxide activated binders, efflorescence are typically more prevalent in Na than K.

### **2.2.1.2. Alkali Silicates**

Similar to alkali hydroxides, sodium and potassium silicates are also known as the most commonly used activators in alkaline activation. High costs and limited amounts of rubidium and cesium silicate constitute an impediment to the use of such silicates. Alkali silicates are

typically formed with carbonate salts and calcine silica, afterward dissolved in water. This process of production is responsible for energy consumption and emissions of CO<sub>2</sub>. However, since almost any alkaline-activated binders have relatively low activator mass levels, the CO<sub>2</sub> emission rate due to carbonate calcination in the alkaline silicate manufacturing process remains considerably lower than the Portland cement production CO<sub>2</sub> emissions.

Vail classified most of the silicate compositions formed in different regions of the Na<sub>2</sub>O-SiO<sub>2</sub>-H<sub>2</sub>O trilateral system and used materials prone to crystallization, partially crystalline mixtures, high viscous solutions and/or hydrated sodium metasilicates (Vail, 1952). Transportation and storage of these solutions must be done carefully and the storage for long period of silicate solutions (laboratory experiments or larger-scale manufacturing) before to use can have unforeseen and/or negative impacts. Since the precipitation of hydrated potassium silicate phases can maintain a wider range of stable and homogeneous aqueous solution stability compared to sodium, these issues usually do not occur in potassium silicate solutions.

Silica chemistry has more complex features for all phases than any element except carbon, and the explanations on their properties remain relatively weak. Silica polymerizes into a number of small species in concentrated alkaline solutions (Provis et al., 2005; Knight et al., 2007), and the careful application of the <sup>29</sup>Si NMR obtained by Nuclear Magnetic Resonance (NMR) (Engelhardt et al., 1974; Cho et al., 2006) spectroscopy only and can be resolved by mass spectroscopy analysis (Pelster et al., 2006; Petry et al., 2009). Although infrared spectroscopy analyzes have also been carried out to identify silica chemistry, the information obtained on the spectral properties is sometimes incompatible with the results of NMR experiments (Halasz et al., 2007, 2010). The most important consequence of the distribution of silicate types in terms of geopolymerization reactions is the variability in the instability between silicate types and different types.

During the activation process, the majority of the silicate types used for alkaline activation are deprotonated (White et al., 2011). Considering the distribution of existing species and their relative pK<sub>a</sub> value, many silicate-based activator solutions are buffered at a pH of about 11-13.5 by the silicate deprotonation balance (Phair and van Deventer, 2002; Nordström et



al., 2011). Considering the similar pH value, availability of alkalinity is much higher comparing with the hydroxide-solutions. The pH value of the hydroxide based solutions is relatively high before the alkali-activation process, but the optimum amount of silica dissolves from the precursor into the system will rapidly bring the pH to this level as the reactions take place (Provis and van Deventer, 2013).

Potassium silicate solutions have significantly less viscosity comparing to similarly composed sodium silicates. This feature may present problems when casting and placing alkali activated concrete that is still freshly which activated with sodium silicate. Studies on silicates also show that sodium silicate solutions' viscosity decreased significantly with elevating temperature (Yang et al., 2008). The enthalpy of a high concentration of activator solution prepared using solid sodium metasilicate decreases due to the fact that the dissolved species cannot reach full hydration at very high concentrations.

## **2.2.2. Geopolymer Binders**

### **2.2.2.1. Metakaolin**

The simplest and most understandable chemistry among the geopolymer systems is the geopolymers obtained by the activation of metakaolin with alkali hydroxide/silicate. Initially, the term geopolymer was used for these materials but this term soon began to involve fly ash and other aluminosilicate sources, and it has gradually expanded in scope (Davidovits, 1982, 1991, 2008). The alkali activation of metakaolin at elevated temperatures to form various zeolites is a type of reaction known before the determination of the term geopolymerization (Barrer and Mainwaring, 1972a, 1972b). Research related alkali activation of metakaolin has been increased, and the importance of this system, which is a model for some complex geopolymerization systems, has become much prominent in identifying these new systems.

Various methods of experimental and modeling have been studied in the last 20 years for metakaolin geopolymerization. Observing geopolymerization directly on site is quite difficult due to the effect of different elements. However, the process can be summarized in this way:

- Alkaline attacks on the metakaolin structure contribute to the dissolve and release into the solution of silicate and aluminate forms. During this dissolution, 5- and

6- coordinate Al passes to 4- coordinate phase (Duxson et al., 2005c). In the metakaolin structure, the first oscillation of Al occurs faster than Si since the Al layers form an additional cross-joint compared to the Si layers (Weng and Sagoe-Crentsil, 2007).

- The interaction of pieces dissolved from the precursor and silicate sources provided by the activator solution form aluminosilicate oligomers.
- The dissolution continues until the concentration of dissolved aluminum is sufficient as much as to stabilize the silicate solution. Factors such as mechanical degradation and additional surfaces that can cause nucleation may also influence this stage. Since the dissolution will continue in the gel formation process, dissolution kinetics can be affected by the gel coating of the particles. Leaching tests, therefore, fail to provide full details on kinetic dissolution. One of the key reasons for this is the continued precipitation of dissolved particles.
- Geopolymeric gel expands to the point where the solidification of the reacting paste. Factors such as mixture design, any additives and curing condition directly affect the gel formation process and setting time of the mixture. The reaction process continues after the end of the setting period, as seen by the growth of X-ray observable zeolitic crystals and ongoing compressive strength development.

#### **2.2.2.2. Granulated Blast Furnace Slag**

According to some literature studies, slag of different source yields cementitious hydration products by alkaline activation. Slag is formed in different types: blast furnace, phosphor, steel slag. Granulated blast furnace slag (GBFS) is one of the most preferable precursor in alkali-activated material class. Slag is formed by combining 'clay' acid gang in coke sulfur ash and iron ore with magnesium and lime (Fernandez-Jimenez, 2000; Shi et al., 2006).

Acidic ( $\text{Al}_2\text{O}_3$  and  $\text{SiO}_2$ ) and Basic ( $\text{MgO}$  and  $\text{CaO}$ ) components are formed by high-temperature fusion ( $1600\text{ }^\circ\text{C}$ ) and subsequently cooling to ambient temperature from  $1400\text{ }^\circ\text{C}$ . When the liquid slag is suddenly cooled to below  $800\text{ }^\circ\text{C}$ , the solidified material, which does not have time to form crystals, gains a glassy structure and it has a wide range of use in alkali activation with these properties (Provis and van Deventer, 2009).

Slag's composition primarily depends on the type and production process of steel. When examined mineralogically, besides the glassy phase consisting of a depolymerized calcium silicate network, GBFS is normally defined as a mixture with a weak crystal structure in a range from akermanite ( $2\text{CaO} \cdot \text{MgO} \cdot 2\text{SiO}_2$ ) to gehlenite ( $2\text{CaO} \cdot \text{Al}_2\text{O}_3 \cdot \text{SiO}_2$ ). Afterward, the crystal phase can be considered practically inert, while the slag contains the hydraulically active component. However, some researchers argue that the reactivity of slag can increase with the presence of a small amount of crystals, considering the amorphous structure formation in the early stages of crystallization (Smolcyk, 1980).

Blast furnace slag can exhibit potential hydraulic characteristics. In other words, its products can be similar to Portland cement's, when finely ground and combined with water even with very long reaction times. The hydraulic binding properties of the slag develop very slowly compared to Portland cement. However, the slag hydrates rapidly and forms adhesive cement products when activated by various methods and activating agents. Alkali compounds are also regarded as activating agents which increase the hydraulic slag binding property more effectively (Wang et al., 1995).

Also, the slag reactivity highly depends on the grain size. Slag react very slowly if has a grain size above 20 microns and slag with grain size below 2 microns reacts completely when mixed with alkali activators for 24 hours (Wang et al., 2005).

For being an alternative to cement, primarily requirements for the slag are listed as follows (Fernandez-Jimenez, 2000; Sih et al., 2006; Provis and van Deventer, 2009):

- Granulation and 85-95% glassy phase must be required.
- It should have a greatly amorphous shape.
- It should have  $\text{MgO} + \text{CaO} / \text{SiO}_2 > 1$  composition. Due to the lime content controls the degree of activation, basic slag has great hydraulic potential. However, acidic slag can be activated with alkali.
- It should be grinded until the surface area is 400-600  $\text{m}^2/\text{kg}$ .

CASH gel formed by activation of GBFS shows a very similar feature with the gel formed by of cement hydration with lower C/S ratio (generally using as 1.0) (Wang and Scrivener,

1995). Hydrotalcite ( $Mg_6Al_2CO_3(OH)_{16} \cdot 4H_2O$ ) is the other product, which can usually be precipitated with phases of type C4AH13, C4AcH11- and C8A2cH24.

Alkalis play an important role in specifying gel properties due to higher alkali molarity in alkali-activated materials, which in some cases may be as much as 5-6 mol/kg (but generally about 1-2 mol/kg binder) (Shi et al., 2006). However, at very high pH values, still, there is not a consensus to determine the interactions between the precursor components and the species in the pore solution. Conceptually, this interaction is most likely due to the Ca/(Si+Al) and Si/Al ratios in the gel, but more studies are necessary to resolve both the equilibrium and kinetic effects on this kind of system.

In the activation of GBFS, alkali incorporation into the CASH gel begins in early periods of reaction. The alkaline consumption of these early formed products is generally supposed to be much more than the gels produced by traditional Portland cement systems. However, researchers also stated that alkali consumption and increment of Si/Ca ratio are inversely proportional. This may provide a slow reaction of ongoing Ca-supply (Hong and Glasser, 1999).

Blast furnace slag particles can cause to alkali-release from the alkaline-rich gels. This process can have important consequences for the long-term structure of the binders; In the presence of aluminum, structures such as tobermorite-like have been stable for centuries, as evidenced by the examination of old Roman structures (Jackson et al., 2013). Microstructural examination of 8-30 years old concrete containing alkali active slag, (Ilyin, 1994; Xu et al., 2008; Bernal, 2014), has indicated increases in mechanical properties with high stability and any reaction by the harmful chemical that will cause CASH gel instability was not observed.

### **2.2.2.3. Fly Ash**

During the combustion stage, fly ash consists of residue of sand, coal and organic materials at the chimney of the furnace. These compounds rapidly cooled in the air to obtain micronized and usually glassy spherical particles. At the same time, the existing crystal particles have heterogeneity at both intraparticle and interparticle phases (Hemmings and Berry 1988, Hower et al. 1999, Nugteren 2007). So that, the properties of ashes are not only highly dependent on impurities in materials before combustion but also combustion and cooling

process. The low calcium-containing fly ashes are the most commonly used for geopolymerization. For instance, F class fly ashes may be said in standard ASTM C618. Studies published on high Ca (Class C) fly ashes are generally less due to a quick setting in 'standard' geopolymer design systems.

The chemical composition of fly ash and the structure of fly ash based alkali-activated products differ significantly. In this context, some additional approaches can be indicated by comparing the fly ash composition and strength values as presented in Figure 2.1. According to Figure 2.1, the strength values can be achieved according to the different percentages of oxide components. Since the values are acquired from different research groups created by various sources in literature, exact strength data can not be compared directly, as the samples are very different in terms of their formulation and curing process. Nevertheless, it does provide some useful information to categorize "high", "medium" or "low" strength.

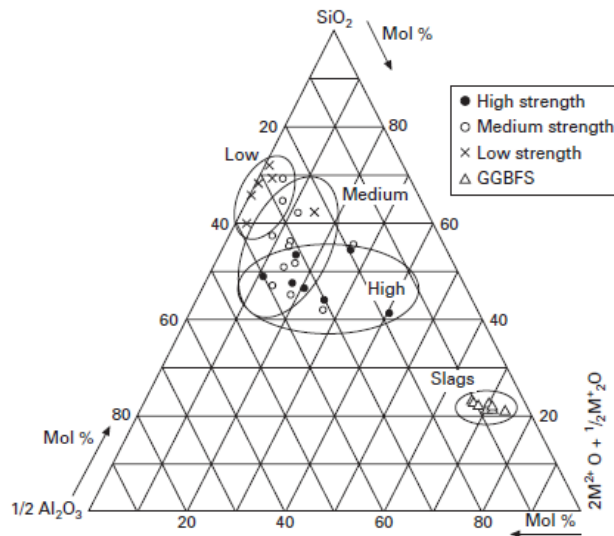


**Figure 2.1.** Representative three-fold diagram of fly ash composition (Provis ve van Deventer, 2009)

As can be clearly seen in Figure 2.1, fly ashes with low network modifying content cause the formation of low performance products. Strength usually increases with depending network modifying content. C Class fly ash is seen to the far right of the black dot, gives high strength products with alkali activation (Keyte et al. 2005). Additionally, Figure 2.1 indicates the composition of representative GGBFS containing high calcium and less

aluminum compared to fly ash. In Figure 2.1, there is an important overlap between the 'high' and 'medium' classes. This shows that there could be additional significant factors that affect strength as expected, not described in Figure 2.1, particularly crystallinity, particle size, and other features.

The fact that the network modifier content is an indication of the potential benefit of fly ash in activation draws attention to the usage of high calcium fly ash. Class C fly ash in the scientific literature has not been evaluated at the same level as Class F, except for a few academic publications (Roy et al., 1996, Perera et al., 2004, Xu et al., 2004, Keyte et al., 2005, Chindaprasirt et al., 2007). Roy et al. (1996) and Lukey et al. (2006) have demonstrated that in addition to the fact that Class C fly ash is usable in geopolymers, it is also highly preferable when the mixture rheology is sufficiently controlled.

In short the process and structure of the geopolymerization mechanism would depend on the chosen fly ash type and the same mechanism will not occur for all fly ashes. Therefore, the analysis should be aimed at understanding the structure and details of the different phases that occur throughout the geopolymerization mechanism. Experiences and information such as phase availability and accessibility during geopolymerization would then allow the required mechanical examination to all different fly ashes.

### **2.2.3. Structure and Matrix Properties of Geopolymer Binders**

#### **2.2.3.1. High-Calcium Geopolymer Binders**

Structural development of blast furnace slag-based geopolymers is quite complex reaction processes with four steps, and this reaction proceeds in the following steps.

- Dissolution of precursor's components
- Nucleation and formation of solid phases
- Interactions of phases and forming mechanical structures
- Formation of products in consequence of ongoing reactions through dynamic chemical balance (Fernandez-Jimenez et al., 1998; Bernal et al., 2011)

According to studies for evaluating the reaction products obtained from alkaline activation of high Ca-source materials, the main product is CASH type, which has a very similar type to that of CSH (I) amorphous tobermorite gel and additionally includes aluminum in its bonds (Zhou et al. 1993, Wang et al. 1995; Myer, et al., 2013).

The composition of the CASH product produced by the GBFS activation is highly relating to the type of activator. For instance, in sodium hydroxide based geopolymers, the Ca/Si ratio of the matrix is greater compared to sodium silicate based geopolymers and a more homogeneous matrix is formed (Escalante-Garcia et al., 2003; Fernandez-Jimenez, 2003).

In studies of Ben Haha et al., on the alkali activation of GBFS, some of the  $\text{Ca}^{+2}$  ions in the structure of the CASH gel formed in both sodium silicate and hydroxide activated slag can be replaced with  $\text{Na}^+$  ions and as a result, a C-(N)-ASH type gel is reported (Ben Haha et al., 2011).

It is important to analyze the chemistry of the structure of reaction products of GBFS and water without any alkali activators. Even if the blast furnace slag has a very coarse-grained structure and 20 years have passed since the hydration reactions took place, it can react 22% if sufficient reactive component is present. This structure, which continues to harden when sufficient time is provided, also forms a highly alumina-substituted C-S-H phase (Taylor et al., 2010).

Reaction between GBGF and water would provide hardened binder forming after a long period of time. Alkali activator's key role then is to improve the efficiency of the reactions in question by maintaining a sufficient pH condition within a suitable timeframe. The most common activators for alkali activation and raise atmospheric pH values to higher levels than other kinds of activators are alkali silicates and hydroxides. There are also free hydroxides for activation attributable to calcium-containing reactions from the dissolution of slags. Carbonates and sulfates provide moderately alkaline conditions compared to other activators.

Once an assessment was carried out in the first 24 to 48 hours of the reaction kinetics of alkaline silicate, carbonate, or hydroxide activated GBFS based binders, it was determined that the heat flow curves were quite similar to Portland cement as a result of isothermal calorimetric tests (Fernandez- Jimenez et al., 1997, 1998; Bernal et al., 2011).

The characteristic feature of the alkali activator used is the most important parameter that affects the GBFS activation product both mechanical and durability properties (Wang et al.,

1994). Activator solutions can generally be considered as alkali silicate salts  $R_2O \cdot rSiO_2$  (Here R is  $Na^+$ ,  $K^+$  or etc. ), strong acid salts ( $Na_2SO_4$ ,  $CaSO_4 \cdot 2H_2O$ ), weak salts ( $R_2S$ ,  $R_2CO_3$ ,  $RF$ ) and alkaline hydroxides ( $ROH$ ,  $Ca(OH)_2$ ). The most widely used for activating GBFS among them are sodium-based hydroxides, silicates, carbonates and sulfates.

In the activator, efficiency directly depends on ambient pH level and also the pH level controls the effectiveness of the dissolution rate of the precursors used for alkaline activation and the resulting condensation reactions (Fernandez-Jimenez & Puertas, 2003; Shi, 2003; Shi & Day, 1996). The impact of pH about alkaline activation of GBFS is directly related to activator. At high pH conditions, silica and alumina solubility increases while calcium solubility decreases. Although NaOH based alkaline solutions have higher pH comparing to sodium silicate based ones with the same molarity and products activated with silicate generally exhibit higher performances than products activated with NaOH (Wang et al., 1994; Duran Atiş et al., 2009; Ben Haha et al., 2011). This situation is a result of the addition of silicate types to the system in order to reaction with Ca-sources obtained from blast furnace slag, but it also provides the formation of dense CASH reaction products and dissolves more Ca from the solution phase (Fernandez-Jimenez et al., 2003). For this reason, during the selection of the most suitable alkali activator, the dissolution capability of the Ca-sources in the pore water pH and interactions of cations provided by activators must be considered.

The development of the mechanical properties of the silicate activated GBFS depends on the modulus ( $SiO_2/Na_2O$  molar ratio) of the activator solution and the nature of the blast furnace slag used. In activation of GBFS, the reaction kinetics were less affected by activator concentration and water/binder ratio when activated with NaOH and  $Na_2CO_3$  compared to  $Na_2SiO_3$  (Shi ve Day, 1996).

The selection of precursors, activator chemistry and optimization for binders obtained from alkaline activation is essential for the literature, but a single assessment of the precursors in most studies in this area restricts their applicability to others. Yet the impact of heterogeneity in the chemical components of blast furnace slag among precursor sources is not yet fully understood. Calcium-rich materials are the most used for alkali activation materials all around the world, with the effect of calcium is increasingly understood in beneficial effects



on strength-related properties, but as mentioned above, the properties of these systems originating from the precursor material are still subject that needs to be investigated.

### **2.2.3.2. Low-Calcium Geopolymer Binders**

The first studies of development of low-calcium or calcium-free geopolymer binders are included in the literature as the studies carried out by Davidovits (Davidovits, 2008). However, although the advancements of concrete manufacture increased the tendency to Ca-rich sources in a short time, it has been replaced by studies based on high-temperature applications and the use of clay-based alkali-activated pastes for other ceramic-like scenarios. Academic investigations on alkali activation of the aluminosilicate sources to obtain a binding material began in the early 1990s (Palomo et al., 1992; Palomo and Glasser, 1992), and the first examples of the formation of the high-pressure and durable product by alkali activation of fly ash were declared by Wastiels et al., (1993, 1994). In the field of fly ash activation, which provides better mechanical property than other clayey sources, interest in the production has increased again and there have been many developments continued in industry and academia. In low calcium alkali-activated systems, the basic binder structure is a highly amorphous and cross-linked alumino silicate gel. In several studies, Glukhovsky, who uses zeolites to establish similarity of alkaline active binders and old roman cement, has documented comparison of the structure of aluminosilicate gel and zeolite (Glukhovsky, 1994).

Alkali hydroxides are usually prepared in the liquid solution and combined with the aluminosilicate source, due to the high heat dissipation caused by dissolution of alkali hydroxides in water; If the high level of heat release occurs in the binder where the reactions continue during the geopolymerization phase, it may cause important problems due to the formation of thermal tensions (Provis, 2009). In the production of alkaline activated materials, only the water addition method is possible by calcining aluminosilicate sources with alkalies (Kolousek et al., 2007, Feng et al. 2012), but this process is yet two-part (adding alkali solution to the solid mixture) could not be developed on a large scale system.

Crystalline phase formation is primarily dependent on Na as an alkaline source in this kind of system. Studies on KOH-activated aluminosilicate binders are limited, in addition, the tendency to crystallize is lower than Na-containing hydroxide activators (Duxson et al., 2007). Crystallites in sodium hydroxide activated metakaolin (where total Si / Al is nearly

1.0) are mostly feldspathoids within hydro-hydroxy sodalite system (usually zeolite NaA and/or low silica faujasite). However, other zeolitic products are seen as temporary or later stages of reaction when the metakaolin reacts with the same activators and for greater liquid/binder amounts (Provis et al., 2009; Rowles et al., 2003; Zhang et al. 2009).

Thanks to their low calcium content, some possible effects have been discovered for some raw materials. With hydroxide based activators, calcium can be rapidly released into the solution, reaching over-saturation compared to calcium hydroxide and therefore this phase can precipitate into nanosized particles (Provis et al., 2009). This is not seen in silicate-activated systems. Because higher Si level initially found in solution will cause to formation of complex C-S products rather than achieving supersaturation compared to a hydroxide phase.

The binder gel structure of low Ca content aluminosilicate raw material formed by silicate activation is quite similar to the binder gel structure formed by hydroxide activation of the same raw material (by applying NMR, FTIR and other spectroscopic techniques). The main differences observed in the atomic length scale of the gel products are caused by the Si/Al ratios of the products. Considering many academic literature studies, it is concluded that silicate activation of fly ash and metakaolin shows an extensive mix of design and curing conditions and acceptable strength development compared to hydroxide activation.

Silicate activation of binders with low calcium content was more effective when using dissolved silicates. In the literature, solid silicate was evaluated in binders based on fly ash but fairly slow growth in strength was observed (Yang et al., 2008). In the case of the changes in silica modules between 1.0 and 2.0 depending on the binding raw material, the use of silicate solution instead of hydroxide solution causes an increase in compressive strength and less porous structure (Lloyd et al., 2009). Optimum compressive strength results were observed in cases where the Na/Al ratio was around 1.0, depending on the Si/Al ratio in the binder pulp (Rowles et al., 2003). The effect of the alkaline ion is quite a similar with hydroxide activation, but it was concluded that the alkalis which providing the best performance in alkali activation of fly ash depend on the composition are Na and K mixtures, but the chemical composition and grain size of the fly ash also affect this situation (van Jaarsveld and et al., 1999).

Considered the complication of gel formation produced by silicate activation of low calcium precursors in the past years, several approaches have been developed for the analysis of the gel binder. For example, important information about the setting and consistency processes is obtained using calorimetry and rheology tests, but some features are still arguable (Palomo et al., 2005). Moreover, some techniques used in binding systems with alkali activation material go far beyond the laboratory analytical techniques often used in traditional cement studies. X-rays and neutron applications were applied to silica-activated metakaolin binders before applying to Portland cement systems (Skinner et al., 2010). The first neutron pair distribution function study that characterizes a reaction process was also performed by examining of metakaolin based alkali-activated systems. In this context, X-ray fluorescence microscopy (Provis et al., 2009), X-ray nanotomography (Provis et al., 2011), and synchrotron infrared microscopy (Hajimohammadi et al., 2011) have been applied to alkali-activated binders before traditional cement systems (Hajimohammadi et al., 2011).

### **2.3. Use of Construction and Demolition Wastes in Geopolymer Production**

Construction industry consumes natural resources day by day and creates significant amounts of construction wastes. Construction and demolition wastes make up largest volume of volume among all solid wastes. In America, nearly 100 million tons of demolition wastes are generated annually from construction industry and cover approximately 29% of the total solid waste (Mills et al., 1999). In England, construction wastes make up more than 50% of waste storage volume and 70 million tons are added to it every year (Sealey et al., 2001). Between 1993 and 2004, annual construction demolition waste production in Hong Kong doubled, and it has been reported to reach about 20 million tons (Poon, 2007). That amount of construction waste from around the world has reached serious environmentally and economically levels and has shown the importance of local initiatives for its management, recycling and reuse.

The increase in construction waste has brought out severe problems locally and globally. Therefore, construction demolition waste management has become one of the most significant environmental problems. Construction waste management is aimed at reducing negative environmental consequences and minimize existing wastes. Since construction waste is seen as a serious environmental problem all around the world, a set of regulations have been introduced regarding this matter. Construction waste management has been

counted as part of government policies and specifications have been prepared on these issues. In addition, the European Union states have numerous studies and papers on construction waste management and recycling.

Considering the economic activities, the construction sector in Turkey is a very important position. Recently, the role of the construction industry has gained significantly with new housing and infrastructure investments throughout the country. Furthermore, the demolition, maintenance, reconstruction and strengthening of severely risky buildings proceeded intensively due to high earthquake risks. Considering Turkey's existing building stock, a large part of the housing stock needs to be recycled urgently via devastation, reinforcement and renovation activities due to earthquake risk (Turkey Building Materials Sector Outlook Report, 2011). All these activities would also increase construction waste and make it more necessary to effectively handle waste flows in the process of turning it into sustainable building stock.

Although not yet widely commercialized, among the "green" binders, alkali-activated binders are interested in research. The only sample case on the commercialization of a binder with alkaline activation comes from Australia under the brand E-Crete (van Deventer et al., 2010). Various industrial wastes and by-products have been frequently evaluated under the name of the alkali activation mechanism until today. On the other hand, there are very few studies about the evaluation of construction demolition waste, which can be substantial resource for the manufacture of green binders.

Recently, geopolymerization technology, which has been successfully used for industrial by-products and wastes is considered an important option for recycling of inorganic compounds inherent in construction wreckage wastes. Puertas et al. (2006) worked on alkaline activation of ceramic wastes that containing NaOH and Na<sub>2</sub>SiO<sub>3</sub> in the molarity of 6 M and stated a 13 MPa compressive strength result at 8th day, and they associate that consequence to the semi-crystalline structure of such precursors. Allahverdi and Hani (2009) used brick waste from construction and demolition and sodium hydroxide alkaline solution containing 8% Na<sub>2</sub>O and obtained 40 MPa compressive strength in 28 days after cure. Additionally, Allahverdi and Hani (2013) activated the concrete and brick waste mixture by using the Na<sub>2</sub>SiO<sub>3</sub> in order to provide 1.4 silica module of the mixture and 8% of the binder amount of Na<sub>2</sub>O and

reached compressive strengths of 50 MPa. Sun et al. (2013) obtained a 71.1 MPa performance applying a 60 ° C for 28 days cure with ceramic waste activated by NaOH and KOH. Similarly, Reig et al. (2013) used brick wastes as a precursor and activated by 7M NaOH and achieved 30 MPa result after 7 days of 65 ° C cure. Lampris et al. (2009) studied construction wastes obtained at recycling facilities and after alkali activation, they obtained 18.7 MPa result after 7 days ambient curing; and they observed that the geopolymer compressive strength increased 112% and 63%, respectively, with 24-hours curing at 105 °C with the adding 20% metakaolin that a source of alumina. Komnitsas et al. (2015) examined the geopolymerization potential of brick, tile and concrete wastes as different building wastes and reported results of the alkali activation of brick and tile wastes up to 49.5 and 57.8 MPa respectively; In addition, they found that the performance of concrete wastes remained at 13 MPa by applying 90 °C for 7 days curing and using with 14 moles of NaOH. Khater (2013) examined the silica fume addition to concrete waste and metakaolin mixtures and stated that there were significant increases in the ages over 90 days the specimen cured at ambient condition. Ahmari et al. (2012) activated 50% concrete waste and 50% fly ash mixture with Na<sub>2</sub>SiO<sub>3</sub> and NaOH (10M NaOH, SS / N = 2) and reached a 35 of MPa compressive strength. Salazar et al. (2017) activated 100% red clay brick using Na<sub>2</sub>SiO<sub>3</sub> and NaOH as an activator and reached 54.38 MPa after curing at room conditions. Moreover, they reported 25.57 MPa result when activating 100% concrete waste as a precursor. Komnitsas and Zaharaki (2015) stated that industrial and construction demolition wastes are suitable for geopolymerization and can be obtained compressive strengths nearly 76 MPa by proper use of alkali. In addition, they obtained 76, 54 and 51 MPa of compressive strengths by making a mixture of 50% blast furnace slag- 20% brick- 20% tile- 10% concrete, 90% tile- 10% fly ash and 90% tile- 10% red mud, respectively. According to these results, using the construction demolition wastes in geopolymerization technology is of considerable interest now, especially in countries with having issues in waste management. Especially thanks to this technology, the environmental impact of these residues can be reduced by utilizing waste.

The alkaline activation of construction demolition wastes (waste brick and concrete) with the correct proportion of alkaline activators can be enabled to manufacture geopolymer binders with satisfactory properties. One of the important problems is the efflorescence in construction and demolition based products. Previous studies showed that the formation of

efflorescence is a result of secondary reaction when unreacted sodium hydroxide leaks onto the surface and reacts with CO<sub>2</sub> in medium to form sodium carbonate (Allahverdi et al., 2009; Najafi et al., 2012). Efflorescence is sometimes a problem in construction demolition waste-based alkali-activated binders, but this problem can be eliminated by adding aluminum-rich additives or applying hydrothermally curing (Najafi et al., 2012). In addition, applying a 45 °C or higher degree of curing process have a greatly positive impact on efflorescence.

## **2.4. Construction and Demolition Waste Based Recycled Concrete Aggregate**

The use of CDW as aggregates in the manufacture of concrete has been a major concern of researchers. The effective use of CDW as an aggregate has the potential to lowering the natural aggregate usage, minimize the energy usage used to manufacture the natural aggregates, minimize harm to nature caused by mines, and to prevent environmental damage and economic damages directly. Recycling of CDW is potentially the most significant aspect that can pave the way for sustainable construction systems by increasing the life cycle of building materials on both binder and aggregate basis.

Since the aggregates obtained from CDW constitute at least 75% of the concrete mix, they play a significant role in the formation of the characteristics of the new material to be produced. The CDW aggregates are classified into 2 categories according to BS 8500 (2002) norm. Aggregates made of crushed concrete if 95% and higher, are classified as recycled concrete aggregates and aggregates from 100% masonry as recycled aggregates, in accordance with the standard mentioned above.

### **2.4.1. Preparation of Recycled Aggregate**

Although research concerning the use of CDW as an aggregate is not new, recycling plants are currently working in several countries for the processing of CDW. The procedure required to make the CDW usable as an aggregate mainly involves the production of small parts by crushing the waste concrete elements, separating the aggregates of different sizes from sieves into certain sizes. The separation of foreign materials such as plastic, metal, wood, etc., which may have harmful effects, from the crushed CDW is one of the important steps within the scope of this procedure. Concerning the processing of recycling aggregates, even the concrete produced in the laboratory can be used, and it is also a key role in deciding

the characteristics of the new concrete to be manufactured (Fonseca et al. 2011). The quality and composition of origin concrete in the processing of recycled aggregates is significantly determining aspects of the properties of the aggregates produced (Nagataki et al., 2004).

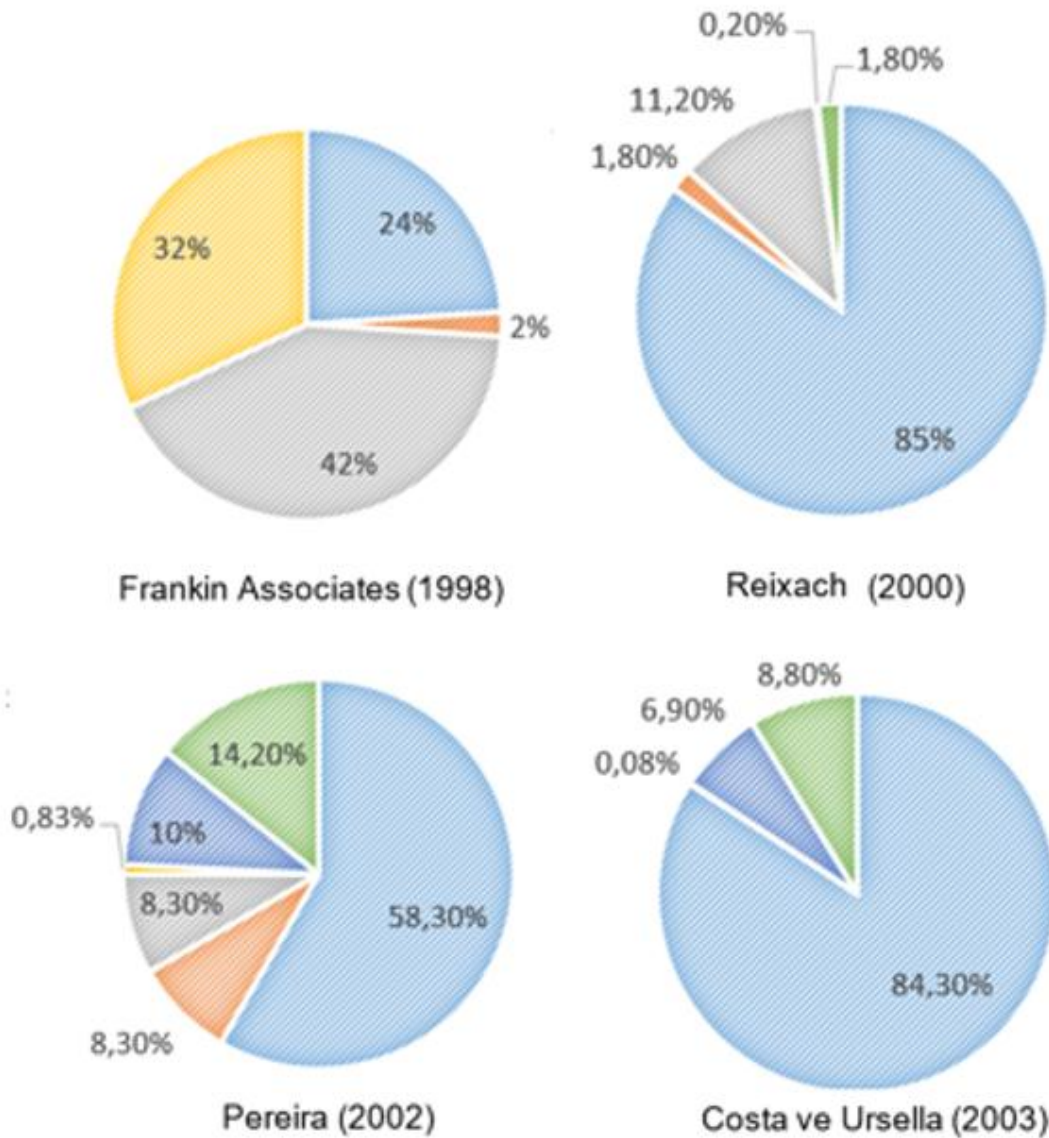


**Figure 2.2.** Composition of recycling aggregate (Frankin Associates, 1998; Reixach et al., 2000; Pereira, 2002; Costa and Ursella, 2003)

#### 2.4.2. Composition of Recycled Aggregate

CDW aggregates are classified into two as natural aggregates with mortar adhering and natural aggregates with mortar adhering that contain impurities such as plastic, brick, tile, bituminous materials. A graph of the material distribution included in the recycling

aggregate is given in Figure 2.2. In general CDW aggregate is obtained from concrete blocks containing 30% cement paste and 70% aggregates (Poon et al., 2004a, b). A study has been performed to examine the distribution of the CDW aggregate composition for certain grain sizes produced from the rubble obtained from real destruction in Spain (Table 2.1). Especially for 0-40 mm grain size, the ratio of concrete and stone is 72% and 20%, respectively, for 10-25 mm, these rates are 53% and 37% respectively, for 4-12 mm, these rates are 51% and 42%, respectively.

**Table 2.1.** CDW compositions for different grain sizes (Gonzalez-Fonteboa ve Martinez-Abella, 2008)

(%)	0-40 mm	10-25 mm	4-12 mm
Concrete	72	53	51
Stone	20	37	42
Asphalt	6		
Betuminous		7	5
Masonry	2	3	2

CDW aggregates may have varying compositions in various grain sizes and materials that influence the pureness of the aggregate in the presence of materials of different origins (Sani et al. 2005). Factors such as source material type, conditions and composition in the recycling aggregate are accepted as the most important parameters controlling the concrete quality producing with using recycling aggregate. The distribution of different types of pollution sources for the sand and gravel size in the aggregate composition are given in Table 2.2.

**Table 2.2.** CDW compositions for different grain sizes (Sani et al., 2005)

(%)	Sand (0-5 mm)	Aggregate (5-15 mm)
Masonry	32	25
Inert	30	29
Concrete	35	45
Bitumen	2	0,5
Glass, plastic, wood	1	0,5



The amount of mortar adhered around the aggregates is one of the most important criteria for determining the properties of the recycling aggregate. Factors such as the crushing procedure, the number of crushing are the preliminary parameters that determine the amount of the adhered mortar. Although the repetition of the crushes is made for removing the adhered mortar from the aggregate as much as possible, it is an important issue to optimize the relationship between the quality and production cost of the recycling aggregate due to its increased costs. In addition, the type of crusher device is another important factor in the separation of the mortar adhered to the aggregate.

Some researchers stated that the amount of adhered mortar of aggregate obtained from CDW is 33-55% for 4-8 mm grain size and 23-44% for 8-16 mm grain size (De Juan and Gutiérrez, 2009). Additionally, with the range of grain size of aggregate decreasing, the amount of adhered mortar is increasing, and moreover, recycling aggregates from the origin concrete with poor compressive strength contain less adherent mortar than the aggregates obtained from high compressive strength concretes (Etxeberria et al., 2007a).

In the literature, there are four different approaches for assessing the amount of adhered mortar. First method is a procedure of keeping the recycling aggregate in dilute hydrochloric acid and dissolving cement pulp without detriment to aggregate (Nagataki et al., 2000). Nevertheless, this is not a feasible method for the recycling of several CDWs based aggregates, such as limestone, that are highly sensitive to acid and can be dissolved in the presence of acid. The second process uses colored cement to prepare samples containing CDW recycling aggregates, and then the thin mortar can be determined by analyzing the thin segments taken from the samples (Ravindrarajah and Tam, 1985). The third method consists of the procedure of keeping the aggregate in water, then heating it until the adhered mortar parts are completely separated (De Juan and Gutiérrez 2009). The last step involves exposing the aggregate for a few days into a sodium-sulfate solution with applying the freeze-thaw cycle which performs more rapidly than other processes. In addition, methods such as heat curing, thermal-mechanical curing, acid soaking, chemical-mechanical curing are among the recommended methods for cleaning aggregate from adhered mortar.

### **2.4.3. Properties of Recycled Aggregate**

#### **2.4.3.1. Water Absorption Capacity**

Recycling aggregate studies indicate that water absorption capacity is the most obvious difference between the standard and recycled aggregates. Adhered mortar contents of recycling aggregate are highly related with the high water absorption capacity of it. Another common conclusion is that concretes including recycling aggregates have poorer compressive strength values by comparison of control mixtures. Also flexural strength shows the same results within the limited data. There is a limited study showing that the effect of strength properties of the original concrete, which will be used as a recycling aggregate source, on the strength properties of new concrete. However, it is also a known fact that in the case of breaking the concert, the weakest zone is cement paste, which adhered to the aggregate. With using the recycling fine aggregate, no major difference in compressive strength was found, but losses with regards to workability were found compared with control samples.

The water absorption quantity of recycling aggregate is a reason for the porous structure of the adhered cement. It is generally below 1% for normal aggregates, may increase up to 30 times in some cases for the recycled aggregate. Although the water absorption is highly related to adhered cement, presence of materials with high water absorption capacity such as roof tiles and bricks is also one of the important parameters determining this property. Vieira et al. (2011) stated that the absorption rate reached 80% only 5 minutes in the water, and then the absorption rate slowed down and reached 84% in a 30-minute period. Considering this behavior of the recycling aggregate, the water absorption capacity can be used as an auxiliary parameter in determining the additional water to meet the extra absorption percentage during the mixture.

Recycling aggregates from concretes with low water/binder ratio have lower water absorption capacity as they reflect the low porosity and high mechanical strength properties of origin concrete (Hansen & Narud, 1983). The grain size of the recycling aggregate highly important in determining the water absorption capacity. The main reason for the recycled fine aggregate to have a greater capacity of absorption compared to the coarse recycled aggregate is having higher amount of adhered mortar within it (Santos et al., 2002b).

Ferreira et al. (2011), indicated another approach to maintain w/b ratio, within this approach, expected to be the absorption water amount by the recycled aggregate during the mixture directly added to the mixture for the meet actual water/binder ratio. This extra water equivalent is referred to as the effective absorption of water. Santos et al. (2002b) determined the water absorption percentages as 1.7% and 1.82% for two different mixtures.

Malhotra (1976) carried out several studies to determine the characteristics of CDW aggregates such as water absorption capacities, strengths and relative densities. As a result of these studies, the major distinction between natural aggregates and CDW aggregates is capacity of water absorption. This has been associated with the increased porosity of cement paste. He also stated that although the CDW aggregates have low density compared to normal aggregates, this difference in density is not as pronounced as in their water absorption rates. In the analyzes carried out by Malhotra to examine the morphological properties of recycled aggregates, it was seen that they have more rounded and smooth surface texture compared to the limestone aggregate used as a reference.

The high water absorption capacity shown by CDW aggregates has been associated with 2-4  $\mu$  wide cracks between the aggregate and hydrated cement paste. On examination of concrete samples produced with these aggregates, it was found that there were small variations in the composition of the samples, as in the aggregate densities. Malhotra also stated that examination of low, medium and high strength samples showed a lower strength of mixtures having recycled aggregates. Additionally, Malhotra examined the workability of mixtures using natural fine sand and recycled coarse aggregate in different water/binder ratios and stated that mixtures using only natural aggregate had almost even workability. He stated that the need for water greatly rises in the mixtures used to recycle fine aggregates, particularly when the grain size is less than 150  $\mu$ , and the reason for this is the hydrated parts that make up the majority of the grains under 150  $\mu$ .

Frondistou-Yannas (1977) examined the effects aggregates both natural and recycled on workability in mixtures it prepared in certain w/c ratios, and he confirmed that the effects of using only coarse aggregate as a recycled aggregate on the workability comparing to completely natural aggregate can be neglected. Also, they found that mixtures having recycled aggregates had a lower modulus of elasticity.

The studies carried out in the literature on the water absorption capacity of recycled aggregates were given in Table 2.3.

**Table 2.3.** Studies related to the water absorption capacity of CDW-based recycled aggregate

	Source	Type	Size (mm)	Water absorption (%)	
				CDW aggregate	Natural aggregate
Topcu ve Guncan, (1995)	Construction site	Coarse	8-31,5	7	
Gonzalez-Fonteboa and Martinez-Abella (2008)	Clean waste	Coarse	4-12 10-25	4,82 4,59	
Courard et al. (2010)	Bituminous pavements	Fine and Coarse	2-20 (%86,5 10-20 mm)	4,58	
Poon et al. (2007)	Unwashed demolition waste	Coarse	10 (max. diameter)	4,3	
			20 (max. diameter)	3,5	
Rao et al. (2011)	CDW from culvert	Coarse	-	3,1	
Corinaldesi et al. (2002)	Rubble from recycling plant	Fine	0-5	10	
Corinaldesi and Moriconi (2009a)	Precast concrete	Fine	0-5	8,8	
	Rubble from recycling plant			7,1	
	Crushed red brick			16,2	
Miranda and Selmo (2006)	Ceramic Wall	Fine	4,8 (max. diameter)	11,5	
	Mortar (laboratory)		0,55 (max. diameter)	1,0	
	Concrete (laboratory)		4,8 (max. diameter)	2,0	

Poon and Chan (2007)	Concrete (Recycled)	Coarse	-	10,3	
	Brick (Recycled)		-	30,9	
	Tiles (Recycled)		0-5	16,9	
Eguchi et al. (2007)	CDW (Laboratory)	Coarse	20	5,69-7,92	
			(max. diameter)		
Tangchirapat et al. (2008)	CDW (Laboratory)			6,22-7,66	
		Fine	0-4,5	11,91	
		Coarse	4,5-25	5,61	
Li et al (2009)	Old concrete pavement	Coarse	5-31,5	8,7	
Corinaldesi and Moriconi (2009b)	Rubble from recycling plant	Coarse	15 (max)	8	
		Fine	5 (max)	10	
Katz (2003)	CDW (Laboratory)	Coarse	>9,5	1 day: 3,2	
				2 day: 3,4	
				28 day: 3,3	
		Medium	2,36-9,5	1 day: 9,7	
				2 day: 8,1	
				28 day: 8,0	
Fine	<2,36	1 day: 11,2			
		2 day: 11,4			
		28 day: 12,7			
Tam et al. (2007)	Recycling Plant	Coarse	20	1,65	0,77
			10	2,63	0,57

Fonseca et al. (2011), Amorim et al. (2011)	Concrete (Laboratory)	Coarse	4-25,4	6,1	1,5
Evangelista and de Brito (2007, 2010)	Concrete (Laboratory)	Fine	<4	13,1	0,8
Gomes and de Brito (2009)	Concrete (Laboratory)	Coarse	<25,4	8,49	2,29
	Brick and mortar mixture from old wall	Coarse	<25,4	16,34	
Ferreira et al. (2011)	CDW (mobile plant)	Coarse	4-25,4	5,8	1,2
Santos et al. (2002a)	CDW (stadium)	Coarse	4-25,4	6,0	0,8
	Concrete (Laboratory, 56 MPa)	Coarse	19 (max)	4,9	1,14
	Concrete (Laboratory, 45 MPa)	Coarse	19 (max)	5,5	

### **2.4.3.2. Porosity**

Most of the attributes of CDW-based recycling aggregate are essentially related with presence of pores with a higher rate than the natural aggregate. Poon et al. (2004a) subjected the aggregates obtained from different sources to the mercury intrusion porosimeter (MIP) test to determine the porosity of the aggregate. According to the results obtained porosity values are 1.6%, 7.86% and 16.81% for natural aggregate, high-strength concrete based recycled aggregate and normal concrete based recycled aggregate, respectively. The high porosity property of them has been associated with the residual cement paste. The pore sizes of the normal aggregate vary between 0.01-1 mm, while the pore sizes of the high performance concrete aggregate are less than 0.1 mm. The reasons of low pore sizes of the high-performance concrete aggregate are the improvement of cement paste microstructure and interface transition area due to presence of the pozzolanic binders contained in concrete (Poon et al., 2004a).

### **2.4.3.3. Density**

In the design of concrete mixtures and other properties of the product, density is the most significant aspect. The density values of recycled aggregates obtained from the studies carried in the literature are shown in Table 4. For the aforementioned reasons the density of recycled aggregates obtained from CDW is quite low compared to the density of natural aggregates. Therefore, the CDW aggregate has different density values depends on the source, size and residual mortar phase. In addition, CDW aggregates with having a small amount of residual mortar have a greater density.

Santos et al. (2002a) stated that the recycling aggregates obtained from samples with different compressive strengths are similar in terms of density and other parameters. The compressive strength results of the two different concretes used as the aggregate source were determined as 56 MPa and 45 MPa after 28-day cure, and the mortar contents as 36.3% and 49.4%, respectively.

The unit volume weight of the CDW aggregate is not much compared to the normal aggregate and generally has a unit volume weight within 1.100-1.450 kg/m<sup>3</sup>, except for some exceptional cases. Ferreira et al. (2011) determined void content of natural and CDW aggregates as 48.8% and 50.4%, respectively. General information about the literature



studies on the density of CDW aggregates obtained from different types of sources were given in Table 2.4.

**Table 2.4.** Studies related to the density of CDW-based recycled aggregate

	Source	Type	Size (mm)	Density kg/m <sup>3</sup>	
				CDW aggregate	Natural aggregate
Watanabe et al. (2007)	-	Coarse		2,520	
		Sand		2,470	
Topcu and Guncan, (1995)	Construction site	Coarse	8-31,5	2,450	
Gonzalez-Fonteboa and Martinez-Abella (2008)	Clean CDW	Coarse	4-12	2,350	
		Coarse	10-25	2,370	
Courard et al. (2010)	Bituminous pavements	-	2-20	2,634	
Poon et al. (2007)	Unwashed demolition waste	Coarse	10 (max. diameter)	2,490	
		Coarse	20 (max. diameter)	2,570	
Rao et al. (2011)	CDW from culvert	Coarse	-	2,470	
Corinaldesi et al. (2002)	Rubble from recycling plant	Coarse	-	2,150	
Corinaldesi and Moriconi (2009a)	Precast concrete	Coarse	0-5	2,290	
Miranda and Selmo (2006)	Rubble from recycling plant	Fine	4,8 (max. diameter)	2,680	
	Crushed red brick		0,55 (max. diameter)	2,600	
	Ceramic Wall		4,8 (max. diameter)	2,670	

Poon and Chan (2004a, b)	CDW (Normal concrete)	Coarse	-	2,409	
	CDW (High performance concrete)	Coarse	-	2,390	
Poon and Chan (2007)	Concrete (CDW)	Fine	0-5	2,310	
	Tiles (CDW)			2,199	
	Brick (CDW)			2,042	
Eguchi et al. (2007)	CDW (Laboratory)	Coarse	20 (max. diameter)	2,220-2,280	
	CDW (Power plant)			2,221-2,231	
Tangchirapat et al. (2008)	CDW (Laboratory)	Fine	0-4,5	2,310	
		Coarse	4,5-25	2,450	
Courard et al. (2010)	Bituminous pavements	Fine and Coarse	2-20 mm (%86,5 10-20mm)	2,634	
Topcu (1997)	C16 Concrete (Laboratory)	Coarse	-	2,450	
Gomez-Soberon	Concrete (Laboratory after 150 days curing)	Coarse	10-20	2,280	
			5-12	2,260	
		Fine	0-5	2,170	
Fonseca et al. (2011), Amorim et al. (2011)	Concrete (Laboratory, 39.6 MPa)	Coarse	4-25,4	2,310	2,550
				(Oven dry)	(Over dry)
				2,450	2,580
				(SSD)	(SSD)

Evangelista and de Brito (2007, 2010)	Concrete (Laboratory, 29.6 MPa)	Fine	<4	1,913 (Oven dry) 2,165 (SSD)	2,544 (Oven dry) 2,564 (SSD)
Gomes and de Brito (2009)	Concrete (Laboratory, C30)	Coarse	<25,4	2,448 (Oven dry) 2,526 (SSD)	2,550 (Oven dry) 2,573 (SSD)
Gomes and de Brito (2009)	Brick and tiles mixture from old wall	Coarse	<25,4	2,160 (Oven dry) 2,301 (SSD)	
Ferreira et al. (2011)	CDW (Recycling plant)	Fine	4-25,4	2,300 (Oven dry) 2,440 (SSD)	2,600 (Oven dry) 2,640 (Oven dry)

Santos et al. (2002a)	Concrete wastet (stadium)	Coarse	4-25,4	2,460 (SSD)	2,660
	Concrete (Laboratory, 56 MPa)	Coarse	19 (max.)	2,364 (Oven dry)	2,620 (Oven dry)
				2,480 (SSD)	2,657 (SSD)
	Concrete (Laboratory, 45 MPa)	Coarse	19 (max.)	2,329 (Oven dry)	
				2,458 (SSD)	

#### **2.4.3.4. Durability**

In the studies carried out in the literature, for the evaluations made in terms of durability, examinations on the freeze-thaw resistance were carried out. According to the stated results, if the recycled concrete is pure and uncontaminated, it is observed that the freeze-thaw resistance is not adversely affected. Even in cases where the aggregate is porous and sensitive to frost, improvements in freeze-thaw resistance can be seen as a result of sealing pores by cement paste. In addition, it is stated that drying shrinkage is high for concrete mixtures using recycling aggregate. In the studies carried out on the effects of sulphate contamination (mostly originated from gypsum plaster) of recycled aggregate on the final product, it is stated that recycling may cause problems due to the demolition without material classification of the structures. It is stated that the soluble sulphate amount of the aggregate can be 1% provided that it is used with conventional cement if the origin concrete is found in conditions where it can remain wet for a long time.

Gluzhge (1946) reported that crushed concrete aggregates have a lower specific weight comparing with normal aggregates, and concrete samples produced using crushed concrete aggregates have lower performance than concretes produced using normal aggregates. However, bending strengths of concretes containing crushed concrete aggregates for compressive strength grades were higher than that of normal aggregate samples.

Newman (1946), in his studies, examined the effects of soluble sulfates on crushed-brick aggregate. As a result, he stated that the presence of  $SO_3$  did not cause any harmful effects up to 1% by weight.

Gaede (1952) added fine ground gypsum or magnesium sulfate to the gravel-sand aggregate system and determined a critical range for  $SO_3$  to determine the effects of the state of the aggregate contamination on concrete. When this range is exceeded, the compressive strength decreases rapidly, and if the addition of gypsum is increased, it remains stable. For this reason, he stated that the amount of 1%  $SO_3$ , which is accepted as the limit value, should be reduced to 0.5%.

Graf (1973) added certain amounts of gypsum to the CDW in a controlled manner to investigate the contamination effect of the gypsum plaster on CDW. As a result of his

studies, he stated that the maximum tolerable level for SO<sub>3</sub> in gypsum form is 1% by weight and that the powdered gypsum causes larger volumetric expansion in a shorter time compared to gypsum material has a particle size of 1-7 mm. Additionally, he reported that gypsum tends to concentrate in fine-grained material.

The study of the compressive strength with the same workability of concrete using recycling aggregates was carried out by Buck (1973, 1976). In his studies, he lowered the w/c ratio for the two mixtures with the usage of fly ash substitution and water-reducing additives, while keeping this ratio constant for others. According to the results obtained, mixtures containing recycled aggregates have lower compressive strength than to the control mixture. The use of water reducing admixture and high cement rate is also suggested to be effective in manufacturing high compressive strength concrete. In his analysis, Buck found that the slump values of these mixtures were greater than the control samples and had more cement content. He claimed that recycled aggregate mixtures tend to be wet even though they have a harder structure than control samples. However, the differences found in terms of slump, void content, and cement content have been reduced to very low levels by using natural sand together with recycled coarse aggregate in these systems. It is also stated that similar workability can be achieved at lower water/cement rates thanks to the use of water reducing additives. In his study (1973), Buck researched the freeze-thaw performance of concrete produced from recycled aggregates and he stated that freeze-thaw performance of these mixtures was very similar to control mixtures after the 300 freeze-thaw cycles were applied to the mixtures. Moreover, he stated that mixtures, where siliceous schist containing concretes are used as recycling aggregates, have better freeze-thaw resistance compared to concrete containing normal siliceous schist. This is due to old mortar covering the siliceous schist seals the pores, preventing water from reaching the parts of the schist sensitive to freezing. In addition, Buck determined the 28-day linear thermal expansion coefficient of concrete mixes produced with recycled aggregate and observed the lengthening of the cubic samples it prepared at  $22.5 \pm 1$  °C and 90% relative humidity conditions. As a result of these tests, he stated that concrete mixtures containing recycled aggregates showed very similar results with control mixtures. In the continuation of his studies, Buck stated that if the cement contains more than 5% C<sub>3</sub>A and the mixtures are subjected to water curing, it will be sufficient to contain gypsum as much as 5% of the total aggregate in case of internal expansion that will adversely affect the concrete strength. When these samples were dried,

volumetric expansion decreased but neither the use of cement with reduced C<sub>3</sub>A content nor fly ash substitution prevented the expansion.

Samurai (1976) examined the values of length change, compressive and flexural strength of mortar prisms by adding gypsum and using different types of cement. He stated that the mixtures prepared with traditional Portland cement and recycling aggregate should not exceed the maximum total sulphate amount of 0.6%. This rate is 0.7% for sulphate resistant cement. In addition, he noted that the use of pozzolanic cement reduced volumetric expansion, especially at high SO<sub>3</sub> levels, but did not set a limit value for the amount of SO<sub>3</sub>.



### 3. MATERIALS AND METHODOLOGY

In this section, the procedure for obtaining all materials used in the study, their size and chemical contents, and various analysis methods performed while determining these characteristics are described in detail. In addition, mixing methods, production procedures and test parameters are presented in full detail.

#### 3.1. Materials

In the study, materials such as hollow brick (HB), red clay brick (RCB), roof tile (RT), glass waste (GW), concrete waste (CW) (which constitute the important part of CDW), and by-products such as granulated blast furnace slag (GBFS) and fly ash (FA) were used as the precursor phase. For the mortar and concrete designs, recycling aggregates obtained from the concrete part of CDW were used. For the alkali activation of these precursors, sodium hydroxide and sodium silicate, which commonly using in the literature, and also calcium hydroxide and shrinkage reducer admixture as additive materials, were used.

CDW-based precursors are obtained from different structures demolished according to the selective demolition procedure located in different parts of Ankara. CDW-based precursors obtained in a dissociated form within the framework of the selective demolition procedure was brought to a size of approximately 1 mm using the laboratory type jaw crusher as per the pre-crushing process and then ground in the laboratory type ball mill for 1.5 hours, accordance with the data obtained from the preliminary studies performed.

Chemical compositions of precursors were analyzed by performing X-ray fluorescence (XRF) analysis, and the crystal structure of precursor and produced geopolymer mixture were analyzed by performing X-ray diffraction analysis (XRD). Additionally, Scanning Electron Microscope (SEM) and Energy Dispersive X-Ray (EDX) Analysis were performed to make visual examinations on microstructures of geopolymer mixtures and to perform chemical analysis of the variable regions of microstructures.

### 3.1.1. Roof/Wall Wastes

Clay-based bricks and tiles as roof/wall wastes are basically produced by grinding different types of clays, shaping them with water and drying artificially or naturally for a certain period then firing in kilns between 800-1000 °C. Clay-based brick and tile products, which are used as building materials in roof and wall elements and have a significant volume in structures, become inert after the maintenance-repair or demolition of structures. Recycling of these materials stored in waste storage areas is not possible and the waste-management is becoming a difficult issue to deal with day by day.

#### 3.1.1.1. Hollow Brick (HB)

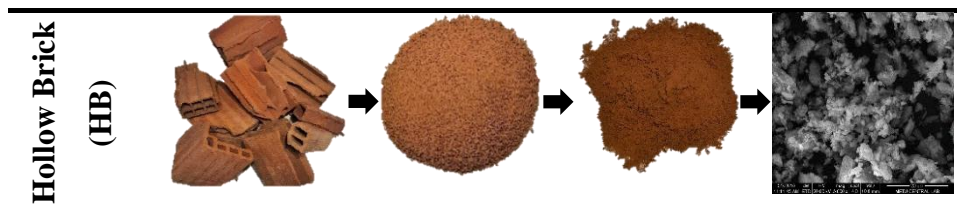


**Figure 3.1.** Hollow brick images (from left to right; raw state, crushed state, ground state, SEM micrograph).

**Table 3.1.** Chemical composition of hollow brick

Chemical Composition (%)	SiO <sub>2</sub>	Al <sub>2</sub> O <sub>3</sub>	Fe <sub>2</sub> O <sub>3</sub>	CaO	MgO	SO <sub>3</sub>	TiO <sub>2</sub>	K <sub>2</sub> O	Na <sub>2</sub> O	LOI
<b>Hollow Brick</b>	39.7	13.8	11.8	11.6	6.45	3.4	1.65	1.55	1.45	7.8

LOI: Loss of Ignition

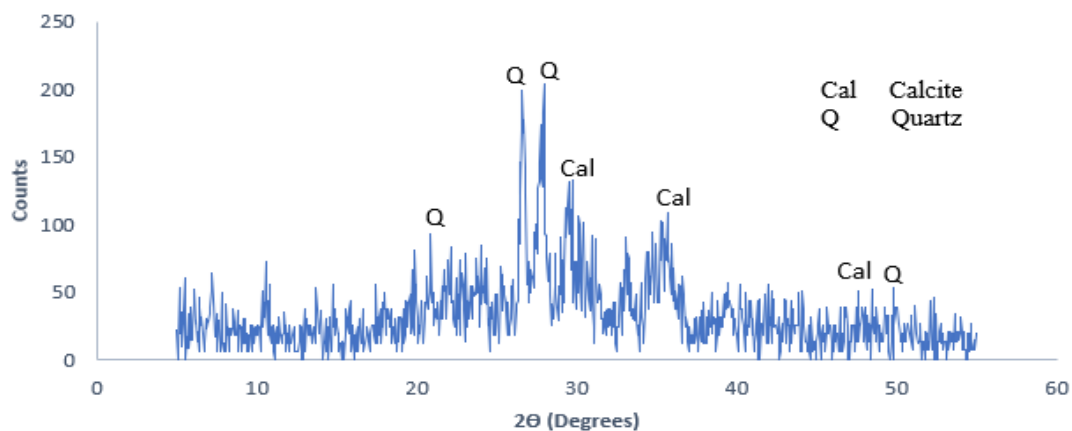


**Figure 3.2.** XRD pattern of hollow brick

### 3.1.1.2. Red Clay Brick (RCB)

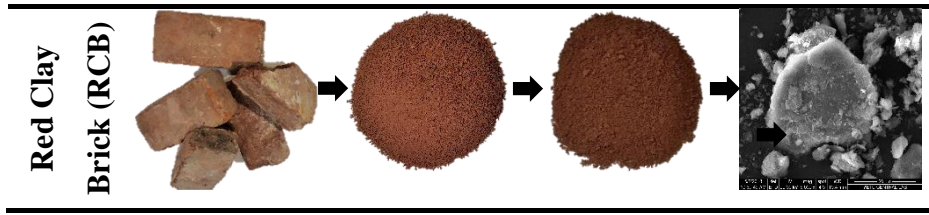


**Figure 3.3.** Red clay brick images (from left to right; raw state, crushed state, ground state, SEM micrograph)

**Table 3.2.** Chemical composition of red clay brick

Chemical Composition (%)	SiO <sub>2</sub>	Al <sub>2</sub> O <sub>3</sub>	Fe <sub>2</sub> O <sub>3</sub>	CaO	MgO	SO <sub>3</sub>	TiO <sub>2</sub>	K <sub>2</sub> O	Na <sub>2</sub> O	LOI
<b>Red Clay Brick</b>	41.7	17.3	11.3	7.69	6.49	1.41	1.57	2.66	1.15	7.96

LOI: Loss of Ignition

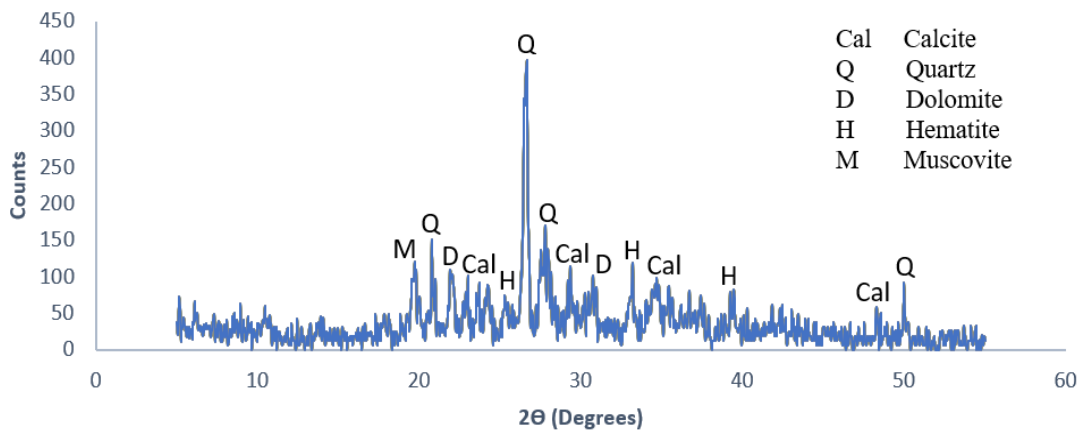


**Figure 3.4.** XRD pattern of red clay brick

### 3.1.1.3. Roof Tile (RT)



**Figure 3.5.** Roof tile images (from left to right; raw state, crushed state, ground state, SEM micrograph)

**Table 3.3.** Chemical composition of roof tile

Chemical Composition (%)	SiO <sub>2</sub>	Al <sub>2</sub> O <sub>3</sub>	Fe <sub>2</sub> O <sub>3</sub>	CaO	MgO	SO <sub>3</sub>	TiO <sub>2</sub>	K <sub>2</sub> O	Na <sub>2</sub> O	LOI
Roof Tile	42.6	15.0	11.6	10.7	6.26	0.71	1.82	1.6	1.6	7.49

LOI: Loss of Ignition

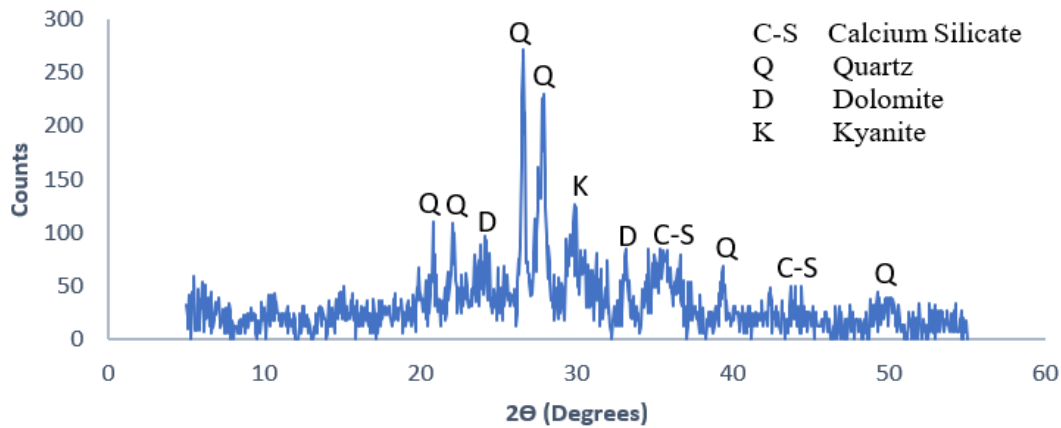


**Figure 3.6.** XRD pattern of roof tile

### 3.1.2. Glass Waste (GW)

Glass waste is the SiO<sub>2</sub>-richest material among CDWs according to XRF analysis. Major oxide components are SiO<sub>2</sub> (66.5%), Na<sub>2</sub>O (13.6%) and CaO (10.0%). Despite it is expected that glass waste will not show adequate performance if it is used as a precursor by virtue of its low Al<sub>2</sub>O<sub>3</sub> ingredient in terms of the Si/Al balance, the fact that the SiO<sub>2</sub> ingredient is largely amorphous indicates that it can be a good source for geopolymerization.



**Figure 3.7.** Glass waste images (from left to right; raw state, crushed state, ground state, SEM micrograph)

**Table 3.4.** Chemical composition of glass waste

Chemical Composition (%)	SiO <sub>2</sub>	Al <sub>2</sub> O <sub>3</sub>	Fe <sub>2</sub> O <sub>3</sub>	CaO	MgO	SO <sub>3</sub>	TiO <sub>2</sub>	K <sub>2</sub> O	Na <sub>2</sub> O	LOI
Glass Waste	66.50	0.93	0.25	10.00	3.93	0.24	0.06	0.20	13.60	4.15

LOI: Loss of Ignition

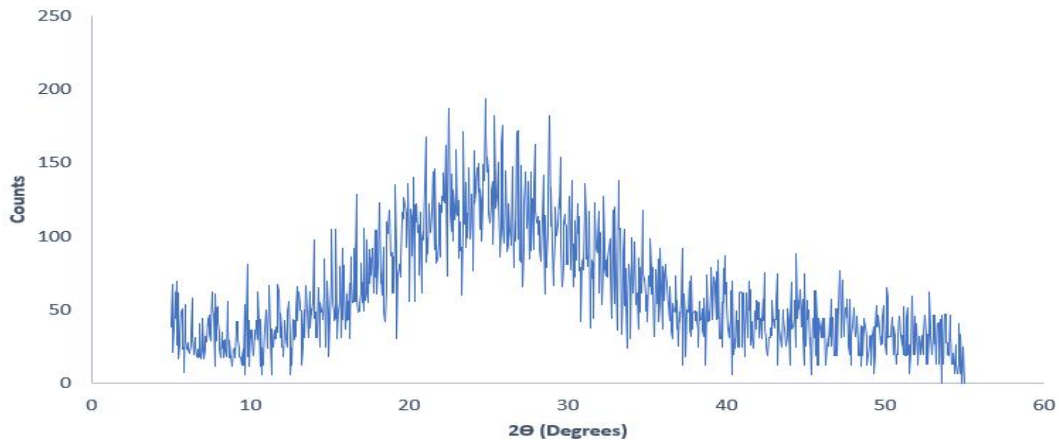


**Figure 3.8.** XRD pattern of glass waste

### 3.1.3. Concrete Waste (CW)

Concrete waste was obtained by crushing and grinding processes of various concretes generated from construction and demolition and whose strengths are not known. The chemical composition of concrete waste clearly shows that the CaO content is at the expected level. It is thought that 20% loss of ignition concrete waste may be caused by carbonated parts of concrete.



**Figure 3.9.** Concrete waste images (from left to right; raw state, crushed state, ground state, SEM micrograph)

**Table 3.5.** Chemical composition of concrete waste

Chemical Composition (%)	SiO <sub>2</sub>	Al <sub>2</sub> O <sub>3</sub>	Fe <sub>2</sub> O <sub>3</sub>	CaO	MgO	SO <sub>3</sub>	TiO <sub>2</sub>	K <sub>2</sub> O	Na <sub>2</sub> O	LOI
Concrete Waste	31.60	4.76	3.50	31.30	5.12	0.92	0.24	0.71	0.45	20.90

LOI: Loss of Ignition

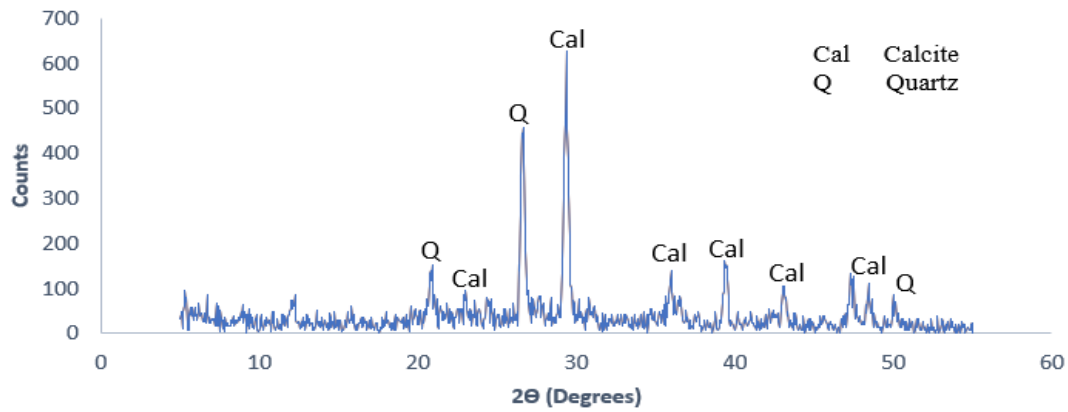


**Figure 3.10.** XRD pattern of concrete waste

The particle size distribution and specific gravity values of CDW-based precursors are presented in Figure 3.11, and Table 3.6, respectively.

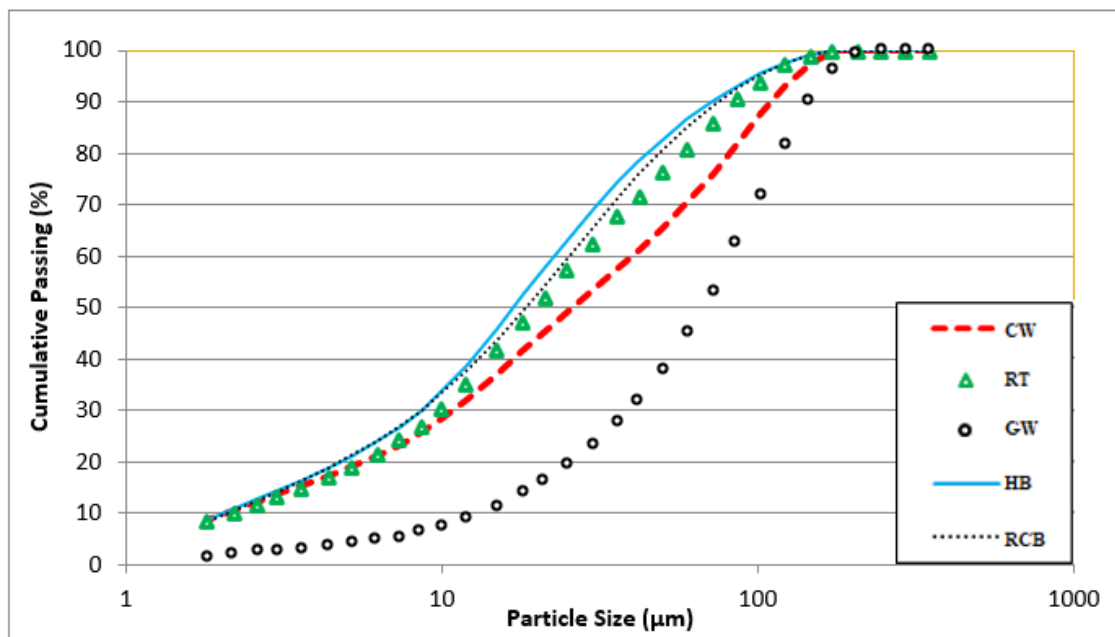


**Figure 3.11.** Particle size distribution of CDW-based precursors

**Table 3.6.** Specific gravity values of CDW-based precursors

Precursor	Specific Gravity (g/cm <sup>3</sup> )
Roof Tile	2.88
Red Clay Brick	2.81
Hollow Brick	2.89
Glass Waste	2.51
Concrete Waste	2.68

### 3.1.4. Granulated Blast Furnace Slag (GBFS)

In this experimental work, granulated blast furnace slag (GBFS) was obtained from Hatay-Iskenderun, Turkey. In order to decrease handicaps of the CDW arising in the geopolymerization process, the decision was made for the use of GBFS to supply the mixture with the elevated calcium content. When CDW based geopolymers are produced along with high-calcium GBFS, the compressive strength of geopolymer products is considered to be increased under ambient conditions. In this study, it is planned to use blast furnace slag up to 20% of the binder ratio in the mixture.



**Figure 3.12.** Granulated Blast Furnace Slag image (from left to right; raw state, SEM micrograph)

**Table 3.7.** Chemical composition of Granulated Blast Furnace Slag

Chemical Composition (%)	SiO <sub>2</sub>	Al <sub>2</sub> O <sub>3</sub>	Fe <sub>2</sub> O <sub>3</sub>	CaO	MgO	SO <sub>3</sub>	TiO <sub>2</sub>	K <sub>2</sub> O	Na <sub>2</sub> O	LOI
<b>GBFS</b>	32.1	11.2	0.62	36.10	5.64	1.21	1.07	0.83	0.31	9.09

LOI: Loss of Ignition

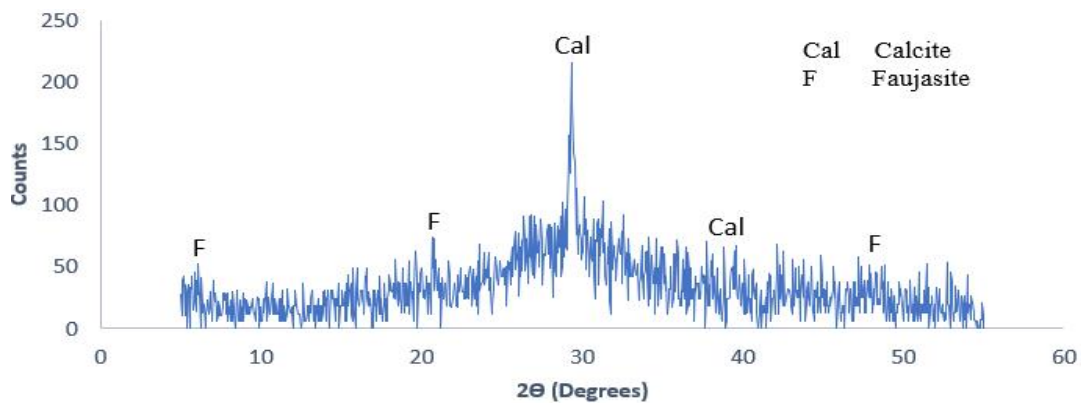


**Figure 3.13.** XRD pattern of Granulated Blast Furnace Slag

### 3.1.5. Fly Ash (FA)

The fly ash (FA) used in the mixes was obtained from Hatay-Iskenderun, Turkey. The fly ash used is type F class according to ASTM C 618. The explanation for the use of fly ash, the most widely used precursor in literature in geopolymer development, is its favorable effect on workability. This favorable effect can be divided into two groups, physically and physicochemically. In the first group, 3 effects can be said to be useful together; (1) prevents agglomerated by entering among the particles, (2) reduces bleeding in plastic concrete by limiting the movement of free water in capillar void, (3) increases workability with the lubricating effect caused by spherical shape. The effect in the second group, thanks to its hydrophilic character, leads to a more homogeneous and widespread distribution of water to the concrete as a result of adsorbing a thin water film on their surface. In this context, it was determined to use up to 5% of the binder ratio in the mixtures.



**Figure 3.14.** Fly ash images (from left to right; raw state, SEM micrograph)

**Table 3.8.** Chemical composition of Fly Ash

Chemical Composition (%)	SiO <sub>2</sub>	Al <sub>2</sub> O <sub>3</sub>	Fe <sub>2</sub> O <sub>3</sub>	CaO	MgO	SO <sub>3</sub>	TiO <sub>2</sub>	K <sub>2</sub> O	Na <sub>2</sub> O	LOI
<b>Fly Ash</b>	60.07	21.35	7.41	0.99	1.82	0.22	0.94	2.91	0.99	2.61

LOI: Loss of Ignition

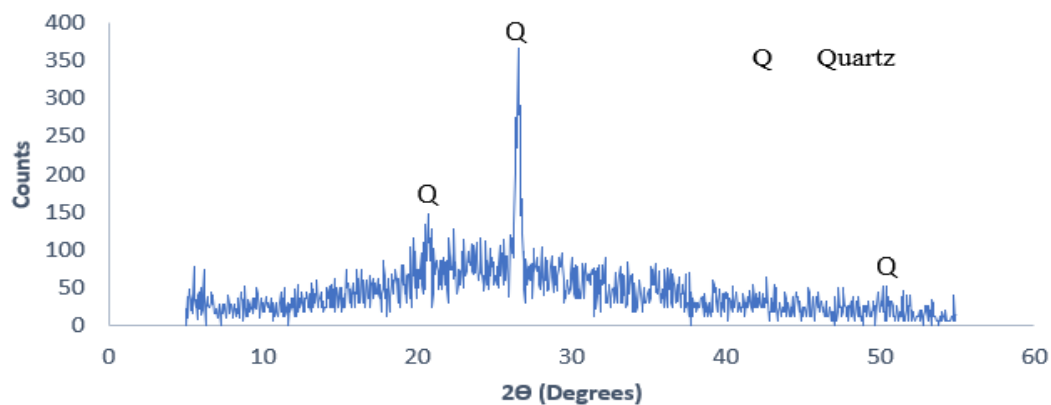


**Figure 3.15.** XRD pattern of Fly Ash



### 3.1.6. Alkali Activators

As a consequence of the extensive literature analysis and preliminary studies, sodium hydroxide (NaOH) in flake form, sodium silicate in liquid form (Na<sub>2</sub>SiO<sub>3</sub>) and calcium hydroxide in powder form (Ca(OH)<sub>2</sub>) were used as activators. The characteristics of the different activators used are presented in the titles below.

#### 3.1.6.1. Calcium Hydroxide (Ca(OH)<sub>2</sub>)

Calcium hydroxide (Ca(OH)<sub>2</sub>) is the chemical compound obtained by adding water to the quicklime. It is available in crystal white powder form and looks pasty when dissolved in water. Its traditional name is slaked or hydrated lime. Ca(OH)<sub>2</sub> used in the studies was supplied by "Tekkim Kimya San. ve Tic. Ltd. Sti." in powder form in 5 kg buckets.



**Figure 3.16.** Calcium Hydroxide Powder

**Table 3.9.** Properties of Calcium Hydroxide Powder

<b>Analyzes</b>	<b>Results</b>
<b>Molecular Weigth</b>	74.09 g/mol
<b>Melting Point</b>	550 °C
<b>Purity (%)</b>	min. 87
<b>MgO (%)</b>	max. 1
<b>Acid-insoluble (%)</b>	max. 1
<b>Loss of ignition (%)</b>	max. 3
<b>Particle size (&lt;90 mm) (%)</b>	min. 90

#### 3.1.6.2. Sodium Hydroxide (NaOH)

Sodium hydroxide (NaOH) is a basic compound used in chemistry and many industries. Sodium hydroxide, also called caustic, is a white-colored moisture-absorbing substance, easily dissolves in water and forms a soft, slippery and soapy solution. Available in liquid or solid form. It is solidly shaped like flakes, prills, and cast blocks. In liquid form, it is generally aqueous solution form. The temperature increases to 100 ° C in around 5 minutes when its solid forms react with water and retain its temperature for a period of time, depending on solution volume and molarity. Sodium hydroxide used in the studies was

supplied by "Koruma Klor Alkali San. Tic. A.Ş. " in granular form and supplied in 25 kg bags in flake forms.

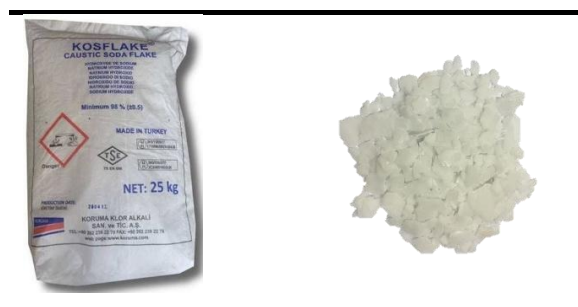


**Figure 3.17.** Sodium Hydroxide images (from left to right; 25 kg bag, flake form)

**Table 3.10.** Properties of Sodium Hydroxide Flakes

Analyzes	Specifications	Unit	Results
Appearance	White flake		White flake
Sodium Hydroxide	min. 98	%	98.27
Sodium Chloride	max. 0.10	%	0.02
Sodium Carbonate	max. 0.40	%	0.35
Iron (Fe)	max. 15	ppm	13.17

### 3.1.6.3. Sodium silicate ( $\text{Na}_2\text{SiO}_3$ )

Sodium silicate is the common name for the chemical compounds represented by its general formula  $\text{Na}_2(\text{SiO}_2)_n\text{O}$ . Sodium silicate solutions likewise named "glass water". It produced by the dissolution of alkali silicate pellets in hot water or by the dissolution of a reactive source of silica in the corresponding alkaline hydroxide solution hydrothermally. Pure compositions are colorless or white in color, but with the containing of iron-based materials, their colors are usually greenish or blue. Sodium silicate is generally used in soap, detergent, paper, timber and ceramic sectors. Apart from the specified areas of use, it is also common to use them as alkaline activators for the development of geopolymeric binders. Different modules ( $\text{SiO}_2/\text{Na}_2\text{O}$ ) can be used for the development of geopolymeric binders that are produced using sodium silicates. After sodium hydroxide, sodium silicate in the alkaline activation of aluminosilicate based materials is the second most commonly used activator. The soluble silica content of sodium silicate affects the many mechanical properties such as workability, consistency and setting time and as well as composition and microstructure. Glass water (liquid sodium silicate) used within the scope of the study is a commercial product produced by "Emir Kimya" and supplied with 5-liter canisters.



**Figure 3.18.** Liquid Sodium Silicate

**Table 3.11.** Chemical composition of Liquid Sodium Silicate

Parameter	Value
<b>SiO<sub>2</sub> (%)</b>	23
<b>Na<sub>2</sub>O (%)</b>	11
<b>Module (SiO<sub>2</sub>/Na<sub>2</sub>O)</b>	1.9
<b>Baume (20 °C, Be<sup>1</sup>)</b>	40
<b>Density (20°C, gr/cm<sup>3</sup>)</b>	1.39
<b>H<sub>2</sub>O (%)</b>	66

### 3.1.7. Recycled Aggregate

Throughout the study, 100% recycling aggregates was used as aggregate to be used in mortar and concrete mixtures. Various concrete wastes obtained from buildings demolished within the province of Ankara, whose ages and strengths are unknown, were divided into smaller pieces by hammer drill and brought to the desired size range by jaw crusher.

In order to provide minimum workability, strength and durability properties of the mixtures, the requirement of the geopolymer paste in the mixture should be minimized. Therefore, the granulometry of the aggregate to, in other words, the grain size distribution, is also significant property in determining the geopolymer paste required for workable concrete. The amount of geopolymer pulp is directly related to the amount of space to be filled between aggregate grains and to be coated of the surface area of aggregates. The composition of granulometry defines the proportion of grains whose sizes are within certain limits. For this reason, the granulometric composition should be determined before using the aggregate by means of a sieve analysis experiment and the condition should be tested within certain limits.

### 3.1.7.1. Sieve Analysis

In this context, by adjusting the jaw intervals of 1 mm and 10 mm through the jaw crusher, concrete waste divided into smaller pieces to achieve the ideal aggregate particle size distribution. The aggregate stack broken from 1 mm gap is called group A and the aggregate stack broken from 10 mm gap is called group B. Aggregate stacks broken in two intervals were then mixed in different proportions and sieve analyzes were performed according to TS 130 “Sieve Analysis Test of Aggregate Mixtures” standard. The curve nearest to the ideal grain size curve has been obtained by mixing uniformly 1 unit group A and 3 unit group B. According to  $D_{max}$ , the amount of aggregate to be used in the experiment is presented in Table 3.12, and the final recycled aggregate gradation curve is presented in Figure 3.19.

**Table 3.12.** Minimum aggregate amount according to  $D_{max}$

$D_{max}$ (mm)	Amount of Aggregate (kg)
63	40
32	10
16	2,6
8	0,6
<4	0,2

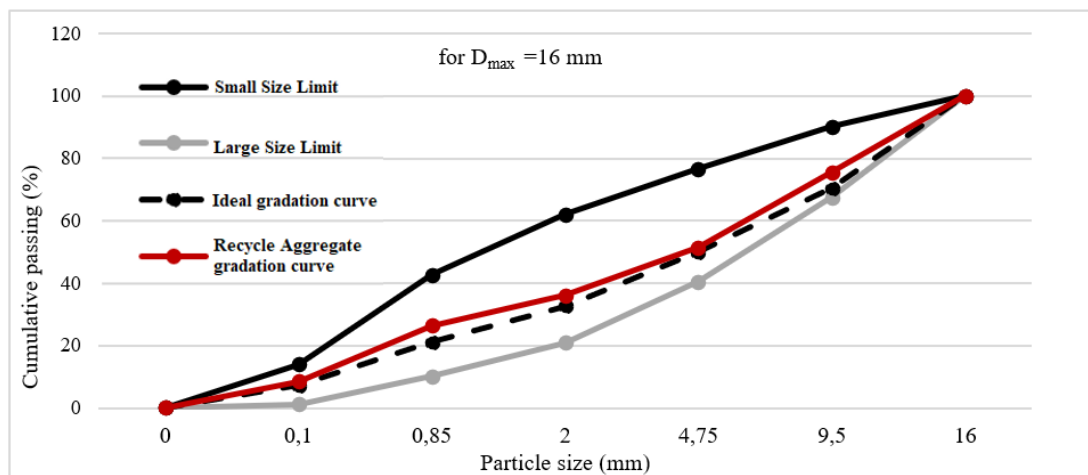


**Figure 3.19.** Granulometry analysis of Recycled Aggregate

The unit volume weight of the recycling aggregate was calculated according to the TS 3529, “Determination of Unit Weights of Concrete Aggregates” standard, and the water absorption capacity and specific gravity were calculated according to the TS EN 1097–6, “Experiments for mechanical and physical properties of aggregates, part 6: determination of particle density and water absorption rate”. Since the recycled concrete aggregate contains some adhered cement mortar, recycled aggregates have a high water absorption capacity. It can be said that the lower specific gravity is due to its porous structure. The physical properties of the coarse and recycled fine aggregates are presented in Table 3.13.

**Table 3.13.** Properties of the recycled aggregates

<b>Size (mm)</b>	<b>16.00-4.75 mm</b>	<b>4.75-0.00 mm</b>
<b>Dry Specific Gravity (g/cm<sup>3</sup>)</b>	2.23	1.86
<b>SSD Specific Gravity (g/cm<sup>3</sup>)</b>	2.32	2.11
<b>Apparent Specific Gravity (g/cm<sup>3</sup>)</b>	2.46	2.51
<b>Water Absorption (%)</b>	4.2	13.8
<b>Loose unit weight (g/cm<sup>3</sup>)</b>	1.22	1.44
<b>Dense unit weight (g/cm<sup>3</sup>)</b>	1.35	1.58

### 3.1.8. Shrinkage Reducer Admixture

One of the methods to reduce shrinkage in concrete is to use shrinkage reducing additives. Within the scope of the study, the product of Plustechno brand named PLUS SR, used to reduce shrinkage.



**Figure 3.20.** Shrinkage Reducer Admixture

## **3.2. Methodology**

All procedures from the powder phase to the final product, including design of the mixtures, the aggregate soundness test, the casting and placement of the samples into the molds, consistency and setting time analysis are presented in detail in this section.

### **3.2.1. Preparation of Mixtures**

The solid materials used in the mixtures were weighed on a 0.1 g precision scale and poured into the Hobart mixer vessel. Sodium hydroxide was mixed with city water to provide the targeted molarity, and then it was allowed to cool for 1 day under room conditions. Sodium Silicate, which is a liquids solution at room temperature, has been removed from the container, weighed, and used in the appropriate blends immediately before the mixture.

### **3.2.2. Casting and Placing**

All mixtures designed within the scope of the study were mixed via Hobart mixer. Mixing processes were initially performed for 1 minute in such a way that the solid particles were mixed homogeneously. Then, by completing the cooling process, the sodium hydroxide solution was added to the mixture. By the sodium hydroxide addition, the mixer was launched at low speed for 1 minute, then sodium silicate was added in mixtures containing sodium silicate. After the addition of the alkali activator is completed, the mixing process for 2 minutes at high speed took place and the mixing process is completed. The material produced after mixing was cast into 50x50x50 mm cubic molds for paste and mortar samples, 100x100x100 mm cubic molds for concrete samples, and 80x80x400 mm molds for beam samples. The casting was carried out in two stages, firstly slurry was divided into three equal layers and 25 strokes applied each these layers. Secondly after placing the slurry into molds, the compaction process applied to the specimens via the vibration table for 1 minute. After the casting process is finished, the samples are ready to be subjected to the curing process determined beforehand. Pictures of the samples produced after casting are presented below. The contents of all these mixtures prepared within the scope of the study are presented in the experimental results and discussion section.

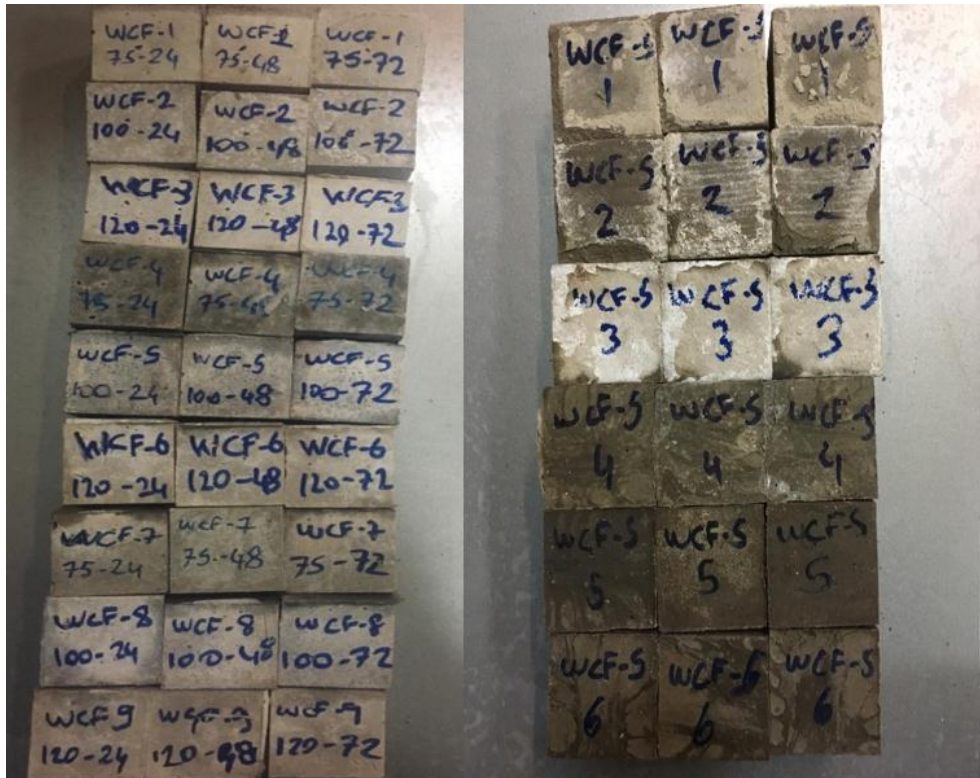


Figure 3.21. Geopolymer Pastes (Containing %100 CW)

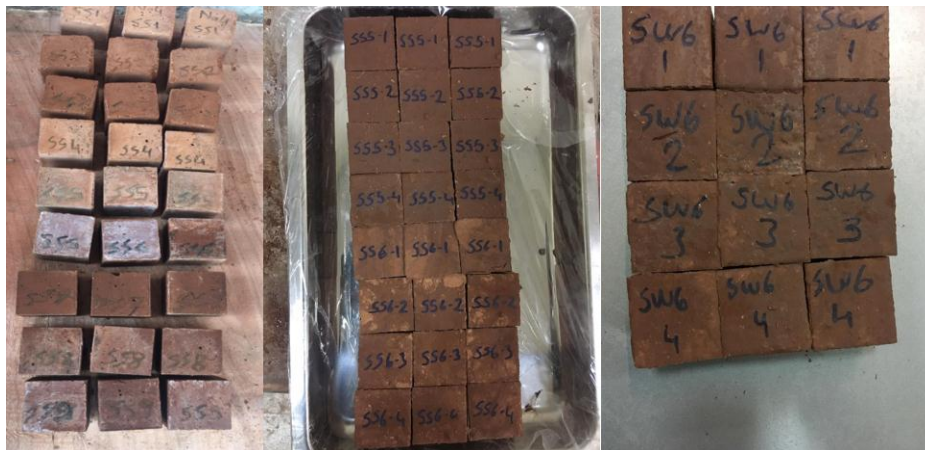


Figure 3.22. Geopolymer Pastes (Containing different proportions of CW, GW, HB, RCB, RT)





**Figure 3.23.** Geopolymer Mortars (Containing different proportions of CW, GW, HB, RCB, RT and Recycled Fine Aggregates)



**Figure 3.24.** Geopolymer Mortars (Addition of GBFS and  $\text{Ca}(\text{OH})_2$  to those containing different proportions of CW, GW, HB, RCB, RT and Recycled Fine Aggregates)



**Figure 3.25.** Geopolymer Concretes (the study carried out within the scope of the shrinkage behavior of the samples)





**Figure 3.26.** Geopolymer Concretes (GC1 and GC2 samples in final series)



**Figure 3.27.** Geopolymer Concretes (in water curing GC1 and GC2 samples in final series)



**Figure 3.28.** Geopolymer Concretes (GC3 and GC4 samples in final series)



**Figure 3.29.** Geopolymer Concretes (GC5 and GC6 samples in final series)



**Figure 3.30.** Geopolymer Concretes (GC7 samples in final series)

### **3.2.3. Curing Conditions**

Several curing applications have been applied for the samples produced within the framework of the study, such as heat curing, moisture curing, water curing and dry ambient curing. For the heat curing, four different ovens are used that can reach up to 200 ° C. In the moisture curing, the samples are wrapped in a wet cloth regularly with water supplements and sealed on each side for prevent moisture loss. Specimens were placed into water tank for wafter curing and water was renewed at certain intervals. In the dry ambient curing, the samples were kept at 25 ° C room conditions without any change in temperature and humidity in the laboratory.

### **3.2.4. Consistency and Setting Time Analysis**

Consistency is a measure of the fluidity of the paste produced. The amount of water used and the fluidity of the paste phase are directly proportional, which affects the workability of the mixture. However, excessively increased water content causes a decrease in the mechanical properties.

The paste samples produced by the combination of the precursor material and the alkali activator are plastic (shapeable) for a while. After this combination, the paste sample loses its plasticity over time and hardens with the beginning of geopolymer reactions. The elapsed time from the beginning of the geopolymeric reactions to hardens of paste phase by losing plasticity is called setting time.

Within the scope of the study, the most important factor affecting the consistency and setting time was the use of sodium silicate in mixtures. The w/b ratio was chosen as 0.35 for all studies to be the most appropriate in terms of consistency and setting time. However, with the addition of sodium silicate, although the consistency of the mixes was positively affected, there was a dramatically decrease in setting times. It has been also observed in some other studies that sodium silicate has lowered the setting times of the mixtures in consequence of rapid reactions due to its excessive reactive silica content (Goberis and Antonovich, 2004). For these reasons, two different mixes were prepared to determine the consistency and setting time. The prepared mixes will be the basis of the final mortar and concrete mixtures to be produced in general within the scope of the study. The only difference between these two mixtures is sodium silicate usage. In the mixture design containing sodium silicate, the

mixture water was adjusted to have a w/b ratio of 0.35, considering the water content in the sodium silicate solution.

### 3.2.4.1. Standard Consistency Test of Geopolymer Pastes

The consistency of the geopolymers to be produced within the scope of the study was measured by the “Consistency Of Standard Cement Paste (Is: 4031-Part4-1988)” standard. In this context, as mentioned earlier, since the rheological properties of mixtures are generally related to the use of sodium silicate, two similar mixtures were designed with and without sodium silicate, and the content of these mixtures were presented in Table 3.14. The results obtained after conducting consistency tests for paste mixtures were given in Table 3.15.

**Table 3.14.** The proportions of geopolymer paste mixtures produced for the determining consistency and setting time

<b>Code</b>	<b>HB</b>	<b>RCB</b>	<b>RT</b>	<b>GW</b>	<b>CW</b>	<b>GBFS</b>	<b>FA</b>	<b>Ca(OH)<sub>2</sub></b>	<b>Na<sub>2</sub>SiO<sub>3</sub></b>	<b>NaOH</b>	<b>Water</b>
<b>CS-1</b>	240	320	400	160	160	240	80	80	358	179.2	323.4
<b>CS-2</b>	240	320	400	160	160	240	80	80	0	268.8	560

Note: The unit of all materials is kg/m<sup>3</sup>.

**Table 3.15.** Consistency test results

	<b>CS-1</b>	<b>CS-2</b>
<b>Distance to the glass sheet (mm)</b>	0	7

According to the results given in Table 3.14, it was observed that the mixture with CS-1 code was very fluid. It is aimed to eliminate the problem by preparing a fluid mixture due to the very fast setting and hardening before the finished casting and placement processes of mixtures containing sodium silicate. As a result of the consistency test of the CS-2 coded mixture, it was quite similar to the consistency of the traditional Portland cement and since the mixture had no fast setting, the mixture was designed to be less fluid than the mixture with the CS-1 coded mixture.

### 3.2.4.2. Initial and Final Setting Time of Geopolymer Pastes

The initial setting time is known as the time from the moment that the water is poured into the cement until the paste begins to lose plasticity. And also the time between the addition of water and losing all plasticity of slurry is called a final setting time.

As mentioned in consistency experiments, the use of sodium silicate is also the most important factor in setting times. For this reason, the setting time tests were carried out in the same way for the mixes prepared in consistency tests. Images of these experiments and the results are presented in Figure 3.31 and Table 3.16, respectively.

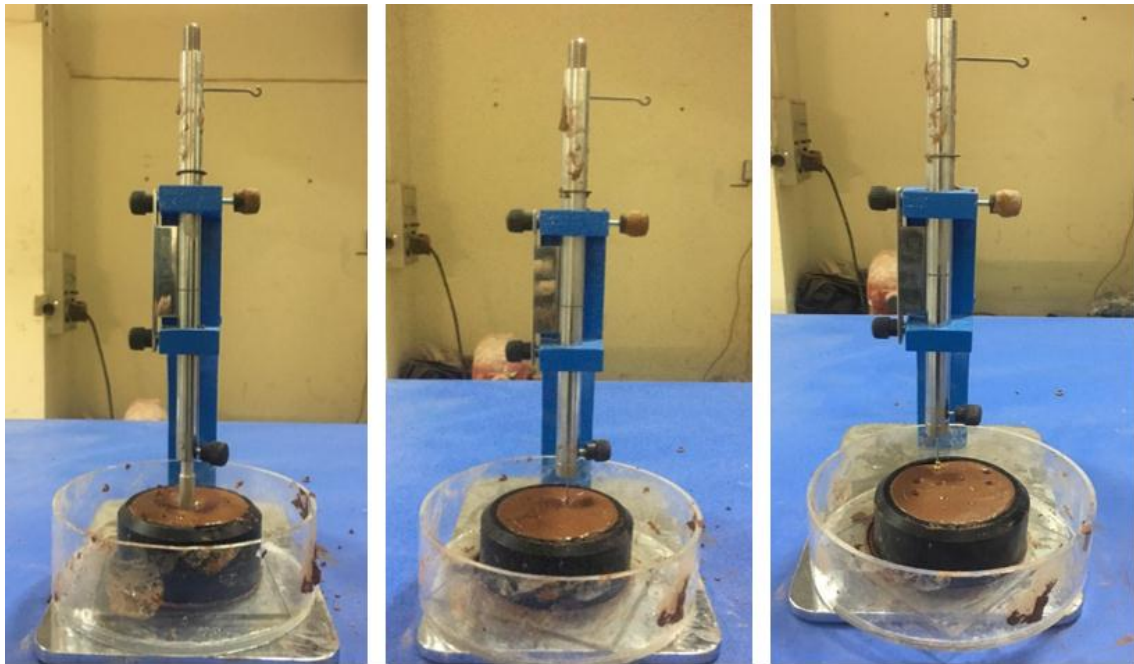


**Figure 3.31.** Consistency and setting time measurements with Vicat apparatus

**Table 3.16.** Initial and final setting results

	<b>Initial</b>	<b>Final</b>
<b>Code</b>	<b>setting</b>	<b>setting</b>
<b>CS-1</b>	7 min	15 min
<b>CS-2</b>	15 min	75 min

In the setting time experiments, the initial and final setting time of the CS-1 coded mixture containing sodium silicate was 7 minutes and 15 minutes, respectively. It is seen that the CS-2 coded mixture, which does not contain sodium silicate, has an initial setting time of 15 minutes and an final setting time of up to 75 minutes. In this case, it is obvious that the

mixtures including sodium silicate harden quite early, while it is obvious that this will be the basis for the mixtures to be made in the continuation of the study.

### 3.2.5. Soundness Test on Recycled Aggregates

The soundness test determines the resistance of an aggregate to degradation through decomposition and, especially freeze-thaw cycles. Durable (weather resistant) aggregates are less likely to deteriorate on site.

In the soundness test, the aggregates are repeatedly immersed in sodium/magnesium sulphate solution. As a result of that process, salty crystals are formed in the porous parts of the aggregate. These crystal compositions create internal forces that will cause the aggregate disintegration by force a pressure. After a certain immersing and drying cycles, the soundness test ends by determining the percentage of material loss.

Within the scope of the study, weight loss in the  $\text{Na}_2\text{SO}_4$  solution was defined in terms of 19% for fine aggregates and 15% for coarse aggregates according to ASTM-C88 standards. In this context, the soundness test for aggregates was carried out by the methods specified in ASTM-C88 standards for the recycled aggregates. The test results are presented in Table 3.17.



**Figure 3.32.** Test equipments prepared for aggregate soundness test

**Table 3.17.** Aggregate soundness test results

	Aggregate size (mm)	Initial Weight (gr)	Final Weigh (gr)	Weight Loss (%)	Average Weight Loss (%)	Weight Loss Limits according to ASTM-C88 (%)
<b>Recycled</b>	0.10-0.85	100	84.7	15.30		
<b>Fine</b>	0-85-2.00	100	86	14.00	13.4	19%
<b>Aggregate</b>	2.00-4.75	100	89.1	10.90		
<b>Recycled</b>	4.75-9.50	300	272	9.33		
<b>Coarse</b>	9.50-16.0	500	459	8.20	8.77	15%
<b>Aggregate</b>						

According to the results given in Table 3.17, the recycled fine aggregates used in the study lost an average of 13.4% weight as a result of the soundness test. Thus, it has been concluded that it is utilizable according to the weight loss value stated in ASTM-C88 standards as maximum 19%. Coarse recycled aggregates have been determined to be also utilizable with an average weight loss of 8.77% after the soundness test, which is limited to 15% in the standard.

### 3.2.6. Flexural and Compressive Strength Tests

Based on the specifications defined in the standard ASTM C78 and ASTM C109, compressive and flexural strength testing were performed with three of each were produced for paste and mortar samples, and two of each were produced for concrete and beam sample, and the weighted average values were taken as final strength values.

### 3.2.7. Mineralogical and Microstructural Analysis

SEM, EDX and XRD analyses were performed on a set of geopolymer specimens to evaluate the effects of parameters such as curing condition, alkali activator type and molarity, and precursor material on the microstructure of samples. These analyzes were carried out in the Advanced Technologies Application and Research Center Laboratory at Hacettepe University.



## **4. EXPERIMENTAL RESULTS AND DISCUSSION**

In this section, the results and findings obtained from the studies carried out in the context of the development of CDW-based paste, mortar and concrete mixtures are examined in detail. Studies were initially performed to acquire binder properties by using different alkaline activators as a result of the geopolymerization of waste materials. In this case, minimum compressive strength of 30 MPa was aimed in 28 days by using 100% concrete waste and, and if this goal cannot be achieved, it was intended to combining concrete waste with glass waste and eventually adding all the materials from a construction demolition wastes such as hollow brick, red clay brick and roof tile to this combination to achieving satisfactory mechanical performance. The formulated mixtures were subjected to the oven, ambient and water curing, and their performances and optimum rates to be used in the mixture were evaluated. Following the development of the binding phase, mortar and concrete samples were produced by adding the most suitable aggregates to the mixtures after various tests and gradations. In addition to 100% CDW-based mortar and concrete mixtures, various mixtures containing GBFS and fly ash were designed to reach final products with highest performance.

### **4.1. Development of Geopolymer Binders**

Within the scope of the development of geopolymer binders as the first step of the study, the concrete waste powder obtained after crushing and grinding CDW-based waste concrete was mixed with NaOH solutions at 10M, 15M and 19M concentrations and then cast in 50x50x50 mm cubic molds. The samples were put in ovens at 75 ° C, 100 ° C and 125 ° C for curing for 24, 48 and 72 hours immediately, without being removed from the molds. The content of these mixtures with a 0.35 water/binder ratio is presented in Table 4.1 and the compressive strength results are presented in Figure 4.1.



**Table 4.1.** Geopolymer paste mixtures containing 100% concrete waste

<b>Note: The unit of all materials is kg/m<sup>3</sup>.</b>				
<b>Code</b>	<b>CW</b>	<b>NaOH (M)</b>	<b>Water</b>	<b>Curing Temperature (°C)</b>
<b>WCF-1</b>	1600	10	560	75
<b>WCF-2</b>				100
<b>WCF-3</b>				125
<b>WCF-4</b>	1600	15	560	75
<b>WCF-5</b>				100
<b>WCF-6</b>				125
<b>WCF-7</b>	1600	19	560	75
<b>WCF-8</b>				100
<b>WCF-9</b>				125

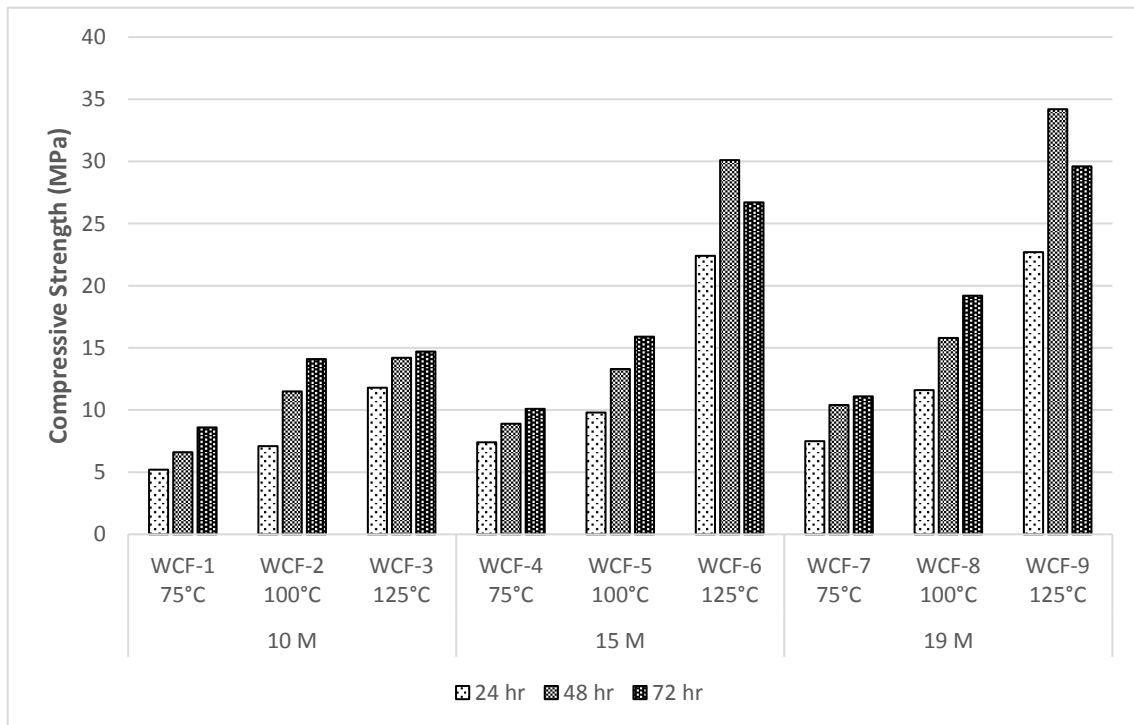


**Figure 4.1.** Compressive strength results of geopolymer paste mixtures containing 100% concrete waste

According to the results given in Figure 4.1, the usage of 10M of NaOH yielded the lowest compressive strengths. An improvement in compressive strength was observed when the alkali concentrations were increased to 15 moles and 19 moles. Alkaline activator, which provides dissolution of aluminosilicate-based waste materials during the reaction, when used in high concentrations, but not excessively, increases the performance of the final product as a result of greater NASH formation in the matrix by enhancing polymerization reactions (Ahmari et al., 2012). On the other hand, excessive increases in alkali concentrations are considerably detrimental to the geopolymer mechanism and diffusions of low-mobility alkaline ions from the solution are significantly reduced. In addition, reaction products occurring very rapidly in mixtures containing high alkali concentrations cause an irregular non-homogeneous structure in the matrix that prevents the completion of the geopolymerization process by disrupting the kinetics of the ongoing reaction (Alonso and Palomo, 2011).

In addition to the influence of alkali activator concentration on compressive strengths, curing temperatures and durations applied to the samples have an also significant effect on the mechanical performance. Results in Figure 4.1 demonstrate that the temperature elevation generally increases the compressive strengths of samples. The increment in curing temperatures accelerate the polymerization reactions and enabling the geopolymer paste to reach high compressive strengths within a short period. However, elevated temperatures applied beyond a certain value cause sudden moisture loss in the samples, resulting in a non-homogeneous matrix with a high void ratio and decreasing in compressive strength. Moreover, extremely high temperatures cause shrinkage due to volume loss in the samples, which causes shrinkage cracks in the samples, resulting in poor performance of the geopolymer products. The increment in curing time typically led to an increase in terms of compressive strength of the samples. Nevertheless, the increment in curing duration caused performance losses in samples curing at high temperatures. After 48-hour curing duration at 125 ° C, the compressive strengths of WCF-6 and WCF-9 mixtures have reached above 30 MPa. As a consequence of the optimization of parameters such as alkaline concentration and curing conditions, the geopolymer paste samples produced with concrete waste can exceed 30 MPa values. However, the compressive strengths were not adequate due to their low aluminosilicate content compared to other CDW components that were to be used in the later stages of the study. In this context, it is thought that in the development of geopolymer paste,

higher results can be obtained if concrete waste is combined with glass and brick wastes in appropriate proportions.

In another study, unlike the WCF-1-9 series, sodium silicate ( $\text{Na}_2\text{SiO}_3$ ) was added to the mixtures as another alkali activator, and the samples produced were left ambient curing under laboratory conditions. The contents of the mixtures containing sodium hydroxide solutions prepared as 4M, 8M and 12M and the sodium silicate prepared as 1 and 2 times of the sodium hydroxide amount are presented in Table 4.2, and results are presented in Figure 4.2. The amount of water in the mixtures was calculated by subtracting the water present in the sodium silicate content from the mix water.

**Table 4.2.** Geopolymer paste mixtures containing 100% concrete waste and binary alkali activator

<b>Note: The unit of all materials is kg/m<sup>3</sup>.</b>				
<b>Kod</b>	<b>CW</b>	<b>NaOH (M)</b>	<b>Na<sub>2</sub>SiO<sub>3</sub></b>	<b>Water</b>
<b>WCF-S-1</b>	1600	4	89.6	500.8
<b>WCF-S-2</b>	1600	4	179.2	441.6
<b>WCF-S-3</b>	1600	8	179.2	441.6
<b>WCF-S-4</b>	1600	8	358.4	323.47
<b>WCF-S-5</b>	1600	12	268.8	382.67
<b>WCF-S-6</b>	1600	12	537.6	205.07

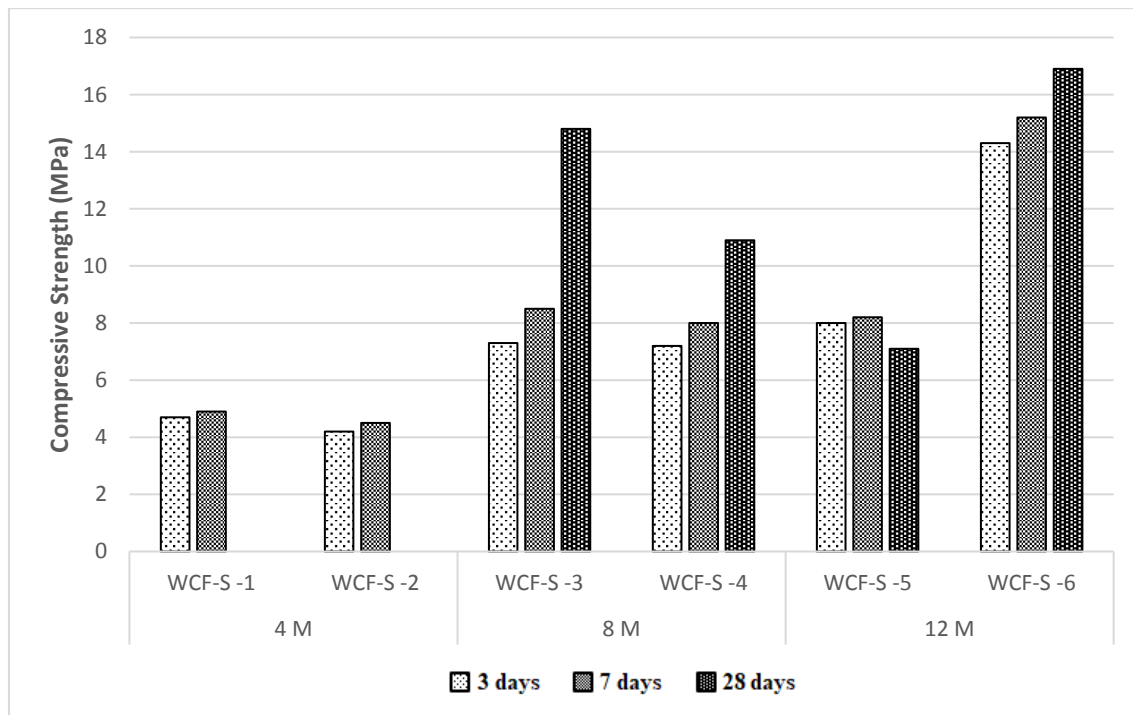


**Figure 4.2.** Compressive strength results of geopolymer paste mixtures containing 100% concrete waste and binary alkali activator

The compressive strength results of WCF-S-1 and WCF-S-2 mixtures containing 4 moles of sodium hydroxide and low amount sodium silicate have been relatively low as shown in Figure 4.2. Furthermore, the results could not be obtained after 28 days of curing due to crack formation and degradation of these samples. In addition, the WCF-S-3 and WCF-S-4 mixtures have reached relatively high strength values. WCF-S-6 mixture has reached the compressive strength of 14 MPa on the 3rd day and became the best performing mixture in the shortest time. However, the growth of compressive strength has remained limited and in the following days, compressive strength could not exceed 16 MPa. Consequently, the compressive strength results of the samples produced only with concrete waste did not reach the desired values in 28 days. Development of geopolymer paste has continued with the addition of other CDW components to the mixtures to reaching higher values. On the other hand, sodium silicate has been used in mixtures as a secondary activator, as it has a significant effect on the ambient curing, with its reactive silica content and being an additional sodium source. Samples that were only developed using sodium hydroxide and left to the curing were not gain sufficient strength and no results were obtained.

At this stage of the study, various geopolymer paste mixtures were produced by combining concrete waste with glass waste. These mixtures with 0.35 water/binder ratio have been combined in three different ways: 75% concrete waste- 25% glass waste, 50% concrete waste- 50% glass waste and 25% concrete waste- 75% glass waste. As the alkali activator, sodium hydroxide was prepared as 10M, 15M and 19M, and the curing conditions were chosen as 24 hours, 48 hours and 72 hours while keeping the temperatures constant at 125 °C based on the samples reaching the highest compressive strength values in the previous study. The contents of the mixtures are presented in Table 4.3 and the compressive strength results are presented in Figure 4.3.

**Table 4.3.** Geopolymer paste mixtures containing concrete waste and glass waste

<b>Note: The unit of all materials is kg/m<sup>3</sup>.</b>					
<b>Code</b>	<b>CW</b>	<b>GW</b>	<b>NaOH (M)</b>	<b>Water</b>	<b>Curing Temperature (°C)</b>
<b>WCF-GW-1</b>	1200	400	10	560	125
<b>WCF-GW-2</b>	800	800			125
<b>WCF-GW-3</b>	400	1200			125
<b>WCF-GW-4</b>	1200	400	15	560	125
<b>WCF-GW-5</b>	800	800			125
<b>WCF-GW-6</b>	400	1200			125
<b>WCF-GW-7</b>	1200	400	19	560	125
<b>WCF-GW-8</b>	800	800			125
<b>WCF-GW-9</b>	400	1200			125

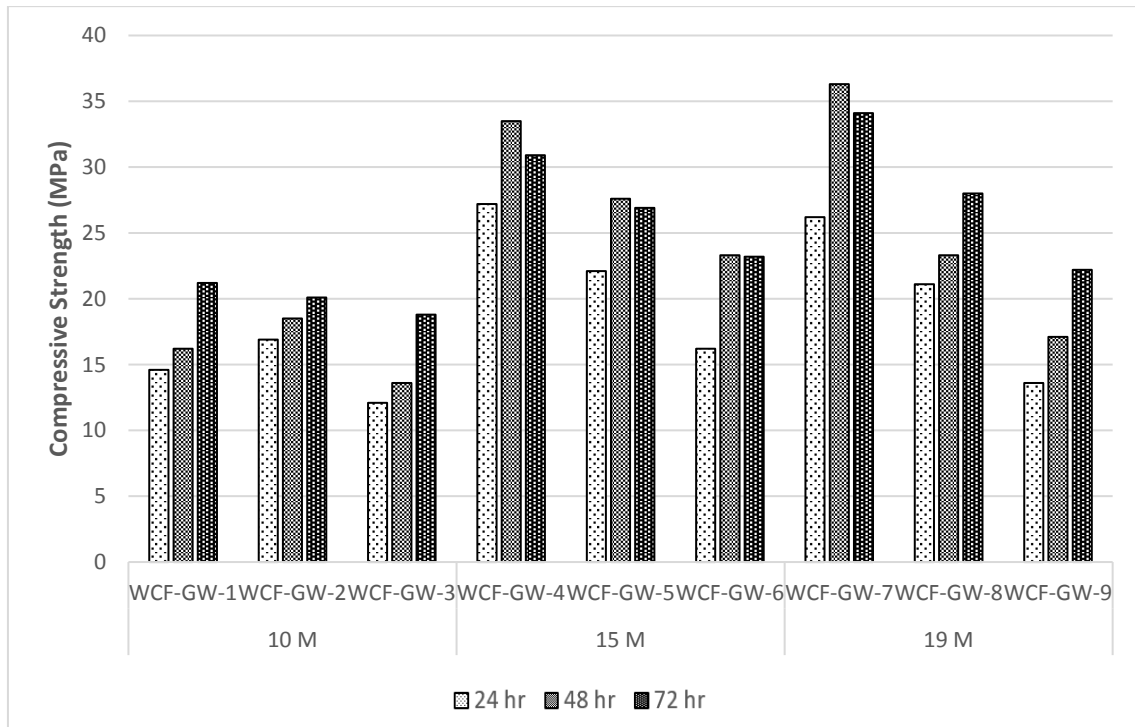


**Figure 4.3.** Compressive strength results of geopolymer paste mixtures containing concrete waste and glass waste

According to the results in Figure 4.3, mixtures containing 15 and 19 moles of alkaline activator showed higher compressive strengths than mixtures containing 10 moles of alkaline activators as expected. However, while the increase in curing period has a positive effect on compressive strengths in general, 48 hours curing period in some mixtures (WCF-GW-4,5,7) was sufficient to obtain the highest compressive strengths. The key aspect to be investigated in these mixtures is the impact on the compressive strength of geopolymer paste of glass waste mixed with concrete waste. In general, the compressive strength of the mixtures in which glass waste substituted 75% and 50% was lower than those in which it substituted 25%. Although glass powder is expected to lead to higher strengths with being generally fairly amorphous in nature, glass powder substitution can lead to decreases in strength due to its partially coarser size and inadequate to form products with the ability to dissolve and bind these particles with the selected alkali activator. In addition, glass waste with high Si / Al content can affect the compressive strength results significantly even in small changes in Si / Al ratio, and when it is activated with sodium hydroxide, it forms sodium silicate gels that have a higher tendency to shrink and crack (De Silva et al., 2007; Redden and Neithalath, 2014; Oyler, 1984).

In the current process of study, various roof/wall elements obtained from CDW components such as hollow brick, red clay brick and roof tile have been added to concrete waste and glass waste mixtures. As these brick elements with high aluminosilicate content are materials that are very suitable for geopolymerization and constitute an important part of CDW, they are considered significant for the production of mortar and cement mixtures under the appropriate alkali concentrations and cure conditions. In this series within the scope of the development of geopolymer paste mixtures, firstly, in the first three mixtures (CDWF-1,2,3), concrete waste and glass waste have been kept constant by 20%, and in the remaining 60%, the ratios of brick wastes were tested for assessment of the compressive strength. After the appropriate ratio of roof/wall elements between each other was found, the effect of the increase of roof/wall elements on the final product was examined in the next four mixtures (CDWF-4,5,6,7), and the ratios of concrete and glass wastes between each other were examined in the last four mixtures. CDWF-8,9,10,11). After various preliminary studies for the mixtures, the water/binder ratio was selected as 0.32, the curing temperature and duration were determined as 115 ° C and 48 hours, respectively, and sodium hydroxide solution used as alkali activator was chosen as 15M. The contents of the mixtures are presented in Table 4.4 and the compressive strength results are presented in Figure 4.4.

**Table 4.4.** Geopolymer paste mixtures containing all CDW based precursors

**Note: The unit of all materials is kg/m<sup>3</sup>.**

Code	HB	RCB	RT	GW	CW	NaOH (M)	Water	Curing Conditions
CDWF -1	320	320	320	320	320	15	512	115 °C 48 hr
CDWF -2	426.67	213.33	320	320	320			
CDWF -3	213.33	320.00	426.67	320	320			
CDWF -4	142.13	213.33	284.53	480	480			
CDWF -5	177.87	266.67	355.47	400	400			
CDWF -6	248.80	373.33	497.87	240	240			
CDWF -7	284.53	426.67	568.80	160	160			
CDWF -8	284.53	426.67	568.80	106.67	213.33			
CDWF -9	284.53	426.67	568.80	80	240			
CDWF -10	284.53	426.67	568.80	213.33	106.67			
CDWF -11	284.53	426.67	568.80	240	80			

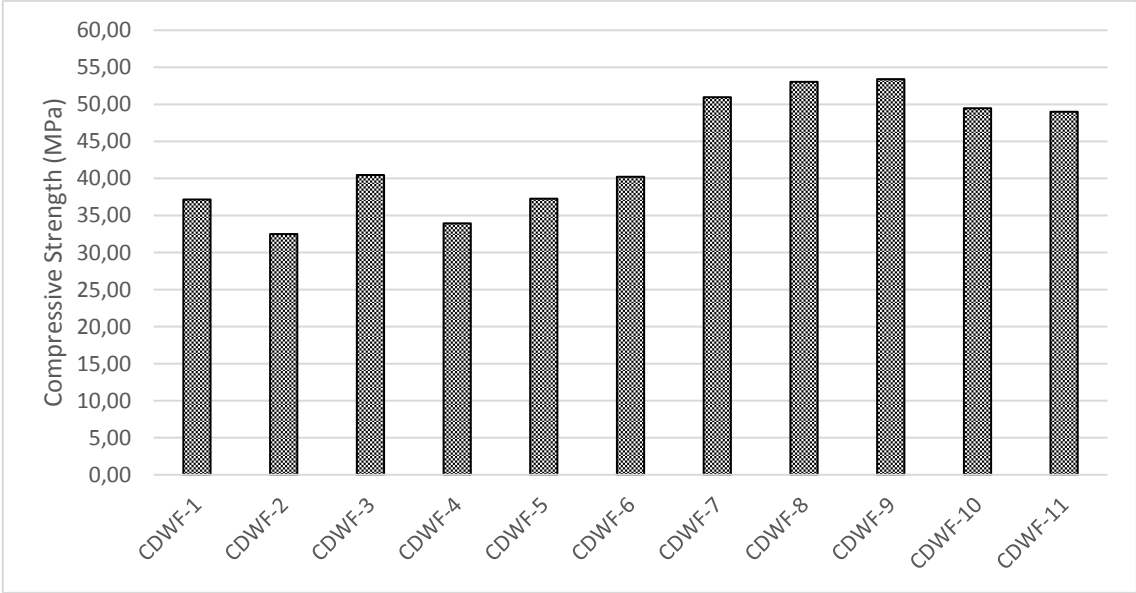


**Figure 4.4.** Compressive strength results of geopolymer paste mixtures containing all CDW based precursors



The CDWF-3-coded mixture, which has the roof tile substitution is the highest and followed by the red clay brick and hollow brick amounts respectively, has the greatest compressive strength result, according to the results shown in Figure 4.4 when the CDWF-1,2,3-coded mixtures are considered. The roof tile is the material with the highest silicon dioxide ratio and having a very fine grain size compared to other waste brick materials used in the study and provides better mechanical performance than others in its high substitution usage. After the ideal brick-element ratio was determined between the brick-elements, CDWF-4,5,6,7 mixtures were produced for observe the influence of all roof/wall elements on the compressive strength compared to concrete and glass wastes. The findings show that there is an increment in the compressive strength of the mixtures as the substitution of the brick components increases. CDWF-7 coded mixture with 80% roof/wall element substitution among these four mixtures exceeded 50 MPa compressive strength value and showed the highest mechanical performance. It is also understood in some studies in the literature that the reason for the higher performance of roof/wall elements compared to concrete and glass wastes is that they are more suitable calcined aluminosilicate materials for geopolymerization with their physical and chemical properties (Allahverdi and Najafi, 2009). Eventually, when the compressive strength of the CDWF-8,9,10,11 mixes was analyzed, the findings revealed that concrete waste yielded better results than glass waste. Considering the results obtained in this study, CDWF-9 coded mixture containing 35.56% roof tile, 26.67% red clay brick, 17.78% hollow brick, 15% concrete waste and 5% glass waste was observed as the highest performance mixture with reaching 53.40 MPa compressive strength.

During the development of geopolymer binders, 100% concrete waste was first produced and analyzed under various alkali activator concentrations and curing conditions, as a result, while gaining considerable compressive strength in heat curing, it showed very poor performance when curing under ambient conditions. Concrete waste was then mixed with glass waste and sufficient compressive strength values were not reached as a result of the thermal curing of the produced mixtures. Finally, some samples were produced by adding roof/wall elements to the mixtures, and 100% CDW-based geopolymer paste mixtures were developed that exceeded 50 MPa compressive strengths after heat curing. The optimum ratios of five different CDW materials, which will be the basis of the mortar and concrete mixtures to be produced later in the study, have been determined and important findings have been obtained regarding the geopolymerization kinetics according to the mechanical

properties results obtained. In addition to the mechanical properties, various microstructural analyzes such as SEM, EDX and XRD were performed to observe the gel structure and distribution, void ratio, type of crystalline products and peaks formed in the matrix of these produced geopolymer pastes.

#### **4.2. Development of Geopolymer Mortars**

In the next stage of the study, the development of geopolymer mortar mixtures was planned by adding recycled fine aggregates to the binder precursors obtained from CDW, with their sizes below 4.75 mm and the amount 35% of the binder. The recycled aggregate in different sizes produced by grinding the concrete waste obtained by CDW was applied directly to the mortar mixtures without any treatment process. Three different studies have been carried out within the scope of the development of geopolymer mortar mixtures. The first is the SW-1,9 series, which contains a 100% CDW-based binder and recycled fine aggregate, the second is the SS-1,9 series designed by adding 20% blast furnace slag to the mixtures in the first series, and the third is the SW6-1,4, SS5-1,4 and SS-6-1,4 series produced by adding four different rates of  $\text{Ca(OH)}_2$  to the most performance mixtures of the first two series. The aim of this study is to examine the effect of sodium hydroxide and sodium silicate usage rates on the performance of CDW-based mortar mixtures and, observe the effect of GBFS, which is frequently used in the literature and has very important features for geopolymerization, and investigate the effect of  $\text{Ca(OH)}_2$  addition on the compressive strength of the samples by forming Ca-based structures in the matrix. The mixtures' designs have been based on the findings of the previous study of the development of geopolymer paste, the results obtained in some preliminary studies, the properties of recycled fine aggregates such as water absorption, porosity, adherent cement content and detailed literature review. Contrary to the heat curing process, which can achieve high strength results for geopolymer as a curing method and is very necessary and vital according to other research results, this study focused on ambient curing under laboratory conditions. Heat curing, which has a very important function to accelerate geopolymer reactions, brings high energy consumption, and limited curing conditions. Therefore, the important finding of this study proves that high strengths can be obtained with the optimization of different parameters such as mixture proportion, activator type and ratios under ambient conditions.

In the development of geopolymer mortar mixtures, the SW-1,9 series was produced with a mixture of 100% CDW-based binder and recycled fine aggregates. The design was made in

three different stages including 4M, 8M, and 12M of sodium hydroxide solutions, and each step included three different combinations that containing no sodium silicate, containing sodium silicate equal to the amount of sodium hydroxide, and containing sodium silicate twice the amount of sodium hydroxide. The contents of these mixtures are presented in Table 4.5 and the compressive strength results are presented in Figure 4.5.

**Table 4.5.** Geopolymer mortar mixtures containing all CDW based precursors and recycled fine aggregates

<b>Note: The unit of all materials is kg/m<sup>3</sup>.</b>									
<b>Code</b>	<b>HB</b>	<b>RCB</b>	<b>RT</b>	<b>GW</b>	<b>CW</b>	<b>NaOH (M)</b>	<b>Na<sub>2</sub>SiO<sub>3</sub></b>	<b>Aggregate</b>	<b>Water</b>
<b>SW-1</b>	255	340	425	170	170	4	0	476	476
<b>SW-2</b>	255	340	425	170	170	4	76.16	476	425.68
<b>SW-3</b>	255	340	425	170	170	4	152.32	476	375.36
<b>SW-4</b>	255	340	425	170	170	8	0	476	476
<b>SW-5</b>	255	340	425	170	170	8	152.32	476	375.36
<b>SW-6</b>	255	340	425	170	170	8	304.64	476	274.95
<b>SW-7</b>	255	340	425	170	170	12	0	476	476
<b>SW-8</b>	255	340	425	170	170	12	228.48	476	325.27
<b>SW-9</b>	255	340	425	170	170	12	456.96	476	174.31

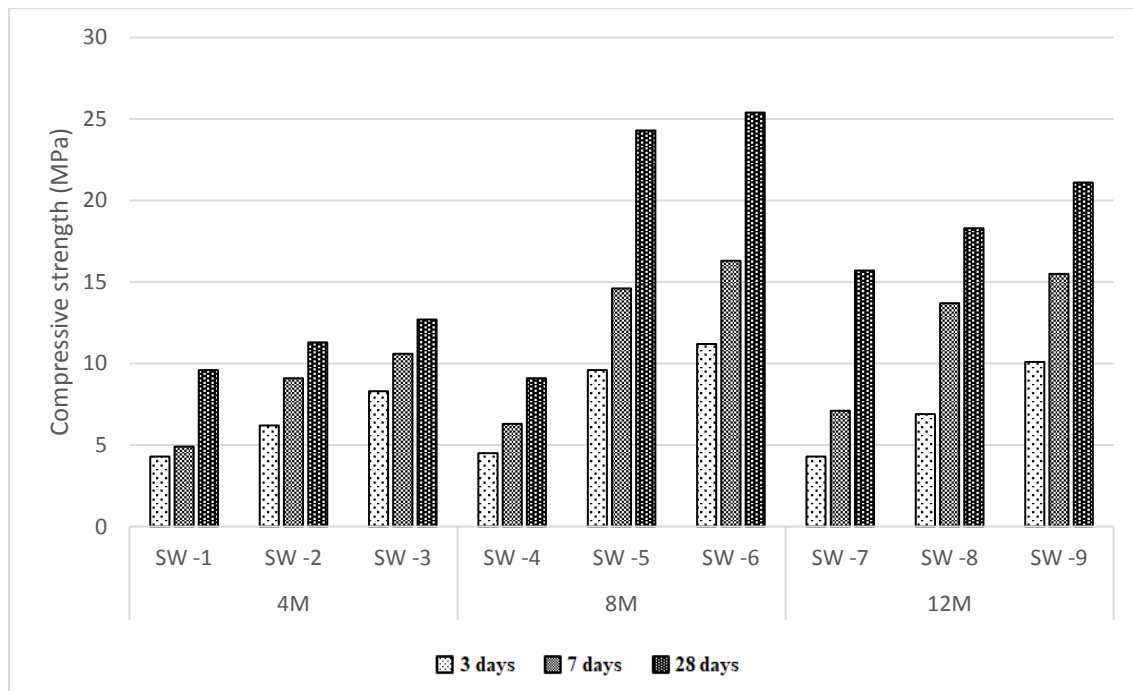


**Figure 4.5.** Compressive strength results of geopolymer mortar mixtures containing all CDW based precursors and recycled fine aggregates

According to the results presented in Figure 4.5, the SW-5 coded mixture where the sodium hydroxide molarity is 8 and the sodium silicate amount is equal to the sodium hydroxide, and the SW-6 coded mixture where the sodium hydroxide molarity is 8 and the sodium silicate amount is twice to the sodium hydroxide exhibiting the highest compressive strengths in this study. In general, mixtures without sodium silicate yielded the lowest strength. However, low compressive strength values were observed in mixtures containing 12M sodium hydroxide solution and excess sodium silicate. Based on these findings, it was found that alkali activator concentrations and the ratios between each other had a great influence on the compressive strength of both, with the ratio increasing until an optimal ratio is achieved, providing a solid matrix by accelerating the aluminosilicate material dissolution. After exceeding this optimum ratio, which may vary depending on the structure and proportion of the material in each mixture, findings such as disrupting the kinetics of the geopolymerization reactions and decrease in strength due to excessive alkali loading to the system are observed. Another result observed in this series is that a high amount of C-origin structure was not found in the matrix of the final product since neither GBFS nor  $\text{Ca}(\text{OH})_2$  were added to the mixtures as a high calcium source. Therefore, the compressive strength of mortar mixtures produced with 100% CDW materials having a high aluminosilicate content could not reach to the desired levels. For this reason, it is planned to add supplementary

materials such as GBFS and  $\text{Ca}(\text{OH})_2$  with high calcium source to achieve at least 30 MPa strength results of these mortar mixtures, which will form the basis of the concrete mixes. In addition to geopolymerization products, it aims at achieving high mechanical performance in the presence of a calcium source by producing CSH or CASH as a secondary hydration product.

In the ongoing phase of the study, new series from SS-1 to SS-9 was produced similarly to the previous series in terms of activator quantity and rates, aggregate, water/binder amount by only adding 20% GBFS the mixtures. The contents of the mixtures are presented in Table 4.6 and the compressive strength results are presented in Figure 4.6.

**Table 4.6.** Geopolymer mortar mixtures produced with the addition of GBFS

<b>Note: The unit of all materials is kg/m<sup>3</sup>.</b>										
<b>Code</b>	<b>HB</b>	<b>RCB</b>	<b>RT</b>	<b>GW</b>	<b>CW</b>	<b>GBFS</b>	<b>NaOH (M)</b>	<b>Na<sub>2</sub>SiO<sub>3</sub></b>	<b>Aggregate</b>	<b>Water</b>
<b>SS-1</b>	204	272	340	136	136	272	4	0	476	476
<b>SS-2</b>	204	272	340	136	136	272	4	76.16	476	425.68
<b>SS-3</b>	204	272	340	136	136	272	4	152.32	476	375.36
<b>SS-4</b>	204	272	340	136	136	272	8	0	476	476
<b>SS-5</b>	204	272	340	136	136	272	8	152.32	476	375.36
<b>SS-6</b>	204	272	340	136	136	272	8	304.64	476	274.95
<b>SS-7</b>	204	272	340	136	136	272	12	0	476	476
<b>SS-8</b>	204	272	340	136	136	272	12	228.48	476	325.27
<b>SS-9</b>	204	272	340	136	136	272	12	456.96	476	174.31

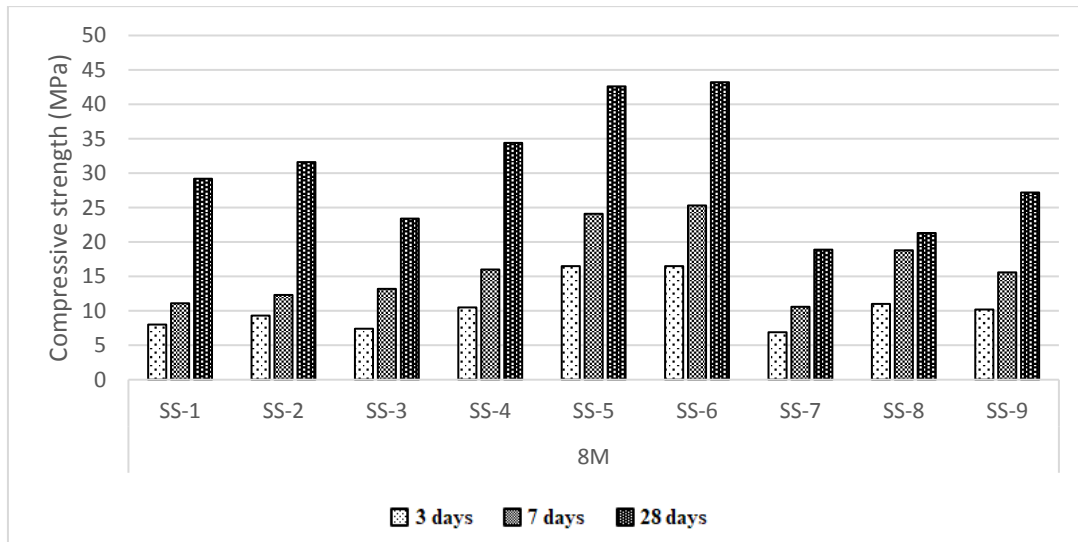


**Figure 4.6.** Compressive Strength results of geopolymer mortar mixtures produced with the addition of GBFS

Considering the results given in Figure 4.6, in the series produced with the addition of 20% GBFS to CDW-based binders, a high compressive strength result was achieved with 43.2 MPa after 28 days of ambient curing of SS-6 coded mixture. Taking into account of the compressive strength of the SS-6 coded mixture produced with the addition of 20% GBFS to the SW-6 coded mixture produced in the previous study, it is clearly seen that the addition of GBFS improved compressive strength by approximately 70%. As it is known, with the dissolution of calcium types from blast furnace slag, it is supported with the development of CSH structures from the beginning of the geopolymerization reactions, and the aluminosilicate material then reacts to form a high Al gel, resulting in NASH and CSH gels formed in the matrix (Yip et al., 2005). These two types of reaction products, that form a very solid, homogeneous and low void structure in the matrix, provide high compressive strength samples to be manufactured as in this study. Moreover, another important finding observed in this study is that the compression strength of the samples is substantially improved when the curing time is extended to 28 days relative to the 7 days curing time. This result shows that the GBFS can contribute to the compressive strength even in the long term with the products it forms as a result of the continuous hydration process in the presence of free and non-evaporable water in the mixture at a later age.

At this stage of the study, the best performing mixtures (SW-6, SS-5, SS-6) from the SW-1.9 and SS-1.9 series were selected and  $\text{Ca}(\text{OH})_2$  was added to these mixtures in powder

form with 2.5%, 5%, 7.5% and 10% of the binder amount. As it is known,  $\text{Ca(OH)}_2$ , which is one of the two products released as a result of cement hydration, reacts with these materials that have pozzolanic behavior such as GBFS, silica fume, fly ash, metakaolin, and creates more C-S-H gels at a later age. In addition, it has been proven in some studies in the literature that by dissolving  $\text{Ca(OH)}_2$  as  $\text{Ca}^+$  and  $\text{OH}^-$  in the system, it will contribute to the mechanical properties of the mixture by creating strong products such as CASH and CSH as a result of both increasing alkalinity and providing extra calcium to the system (Cheng and et al., 1992). The mixtures planned within the scope of the study are produced with the code SW-6-1,4 SS-5-1,4 and SS-6-1,4, and the contents of these mixtures are presented in Table 4.7 and the compressive strength results are presented in Figure 4.7.

**Table 4.7.** Geopolymer mortar mixtures produced with the addition of  $\text{Ca(OH)}_2$

**Note: The unit of all materials is  $\text{kg/m}^3$ .**

Code	HB	RCB	RT	GW	CW	GBFS	$\text{Ca(OH)}_2$	NaOH (M)	$\text{Na}_2\text{SiO}_3$	Aggregate	Water
SW6-1	255	340	425	170	170	0	34	8	304.64	476	274.95
SW6-2	255	340	425	170	170	0	68	8	304.64	476	274.95
SW6-3	255	340	425	170	170	0	102	8	304.64	476	274.95
SW6-4	255	340	425	170	170	0	136	8	304.64	476	274.95
SS5-1	204	272	340	136	136	272	34	8	152.32	476	375.36
SS5-2	204	272	340	136	136	272	68	8	152.32	476	375.36
SS5-3	204	272	340	136	136	272	102	8	152.32	476	375.36
SS5-4	204	272	340	136	136	272	136	8	152.32	476	375.36
SS6-1	204	272	340	136	136	272	34	8	304.64	476	274.95
SS6-2	204	272	340	136	136	272	68	8	304.64	476	274.95
SS6-3	204	272	340	136	136	272	102	8	304.64	476	274.95
SS6-4	204	272	340	136	136	272	136	8	304.64	476	274.95

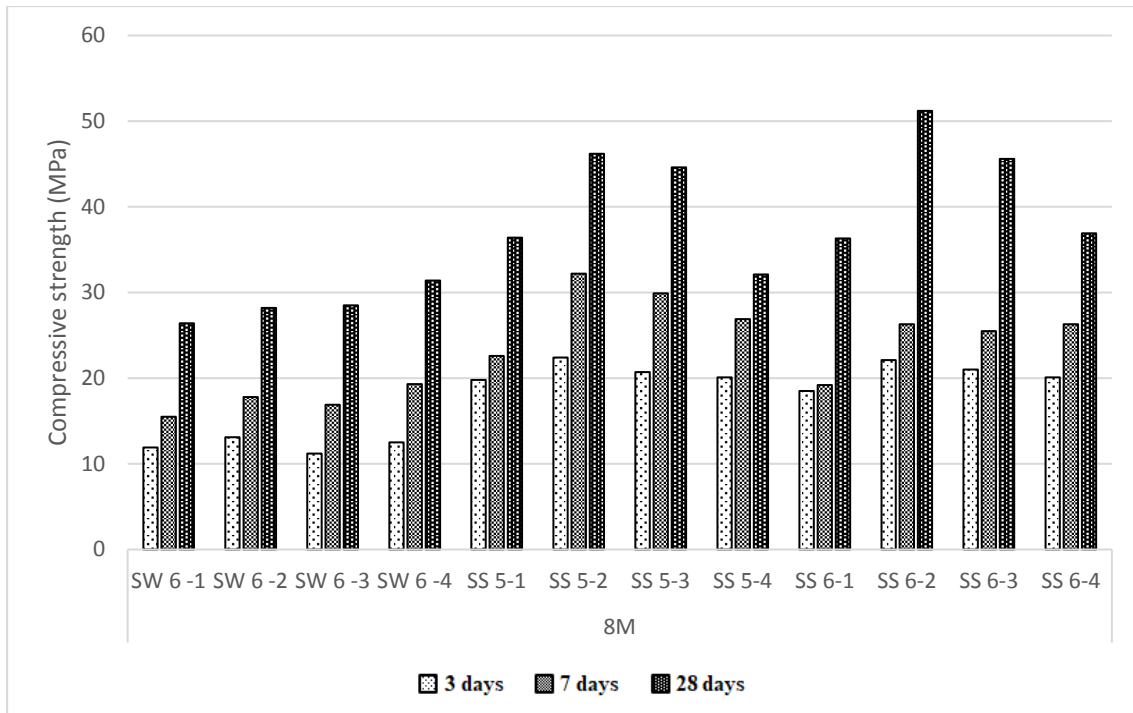


**Figure 4.7.** Compressive strength results of geopolymer mortar mixtures produced with the addition of  $\text{Ca}(\text{OH})_2$

According to the results obtained in Figure 4.7, it is observed that the addition of  $\text{Ca}(\text{OH})_2$  to the mixtures has a quite positive effect on the compressive strength of the mixtures. Especially with the addition of 5%  $\text{Ca}(\text{OH})_2$ , the SS-6-2 coded mixture was the highest compressive mixture with 51.2 MPa in the development of geopolymeric mortar mixtures. Especially with the addition of 5%  $\text{Ca}(\text{OH})_2$ , the SS-6-2 coded mixture showed the highest compressive strength result with 51.2 MPa in the development of geopolymeric mortar mixtures. Considering the compressive strength results of four mixtures designed by adding  $\text{Ca}(\text{OH})_2$  to 100% CDW based mixtures, the compressive strength increased gradually with the increase of  $\text{Ca}(\text{OH})_2$  substitution in their mixtures. As mentioned earlier, this is explained by the formation of Ca-based structures in the matrix with the increased calcium content. In SS-5-1,4 and SS-6-1,4 mixtures containing CDW-based precursor material and GBFS, the addition of 5%  $\text{Ca}(\text{OH})_2$  gave the highest strength results, and the increased amount of  $\text{Ca}(\text{OH})_2$  did not contribute to the compressive strength of these mixtures. This is also stated in some literature studies that there is a ratio in certain limits between the aluminosilicate content of the binders in the geopolymerization reactions and the amount of calcium included in the system, where this ratio is above or below these certain limits, the kinetics of the



geopolymerization reactions will be disrupted and lead to negative effects on the mechanical properties of the final product. (Temuujin et al., 2009).

Within the scope of the development of geopolymer mortar mixtures, the highest compressive strength of 25.4 MPa was achieved as a result of the producing SW-1,9 series by mixing 100% CDW-based precursor materials and recycled fine aggregates obtained from concrete wastes. Considering the harmful effects of cement and concrete to nature, the results obtained from these mixtures, which are produced entirely from CDW and contain no cement, natural aggregates and additives, have shown that CDW can be an alternative building material with the alkaline activation used appropriate and optimum rates. Subsequently, SS-1,9 series was produced by adding a 20% GBFS, which is industrial waste material and can establish strong and stable bonds in the matrix with its high calcium content. The highest compressive strength in this series was obtained from the SS-6 coded sample with 43.2 MPa. In contrast to the heat curing, the relatively poor performance of the mortar mixtures produced with CDW-based binder materials in the ambient curing was overcome by the addition of GBFS. In addition,  $\text{Ca}(\text{OH})_2$  has been applied to the mixtures in varying amounts and it has been planned that they provide the mixture additional calcium source and to ensure that continuous strength gain by pozzolanic reactions in later years. In the last series planned for this purpose, as a result of curing under ambient conditions, a very high strength result as 51.2 MPa was obtained. Considering concretes usually with 30 MPa compressive strength in terms of structurally, within the scope of this study carried out to develop alternative products to traditional concrete, the strength results exceeding 50 MPa in ambient conditions have been reached in 28 days in the study of developing geopolymer mortar mixtures that form the basis of geopolymer concrete mixtures. For the geopolymer concrete mixes to be produced after this stage, the mixes with the highest performances have been designed by making use of the knowledge and experience obtained from the development of geopolymer paste and mortar mixtures and as a result of various preliminary studies and literature reviews.

### **4.3. Development of Geopolymer Concretes**

In the final stage of the study, numerous experiments were carried out with the addition of 4.75-16 mm coarse aggregate in the developed geopolymer mortar mixtures within the scope of CDW-based geopolymer concrete development. While the water/binder ratio was kept

constant at 0.35 throughout the study, the amount of aggregate was determined after various experiments.

In the first stage of the study, it was examined the influence of inert material, which is approximately 5% in the recycled aggregate and has a size between 0-100 microns and not sufficient to act as neither aggregate nor binder and negatively affects the workability of the mixtures. Two mixtures were designed in this preliminary analysis, the recycled aggregate was used without any treatment in one of them (N-0) and the inert content of the recycled aggregate was removed by a sieving process in the other (N-1). The content and compressive strength results of the mixtures are given in Table 4.8.

**Table 4.8.** Experiment to examine the effect of inert material between 0-100 microns in the recycled aggregate

<b>Note: The unit of all materials is kg/m<sup>3</sup>.</b>									
<b>Code</b>	<b>HB</b>	<b>RCB</b>	<b>GBFS</b>	<b>Ca(OH)<sub>2</sub></b>	<b>NaOH (M)</b>	<b>Aggregate</b>	<b>Water</b>	<b>Heat Curing Conditions (°C – hr)</b>	<b>Compressive Strength Results (MPa)</b>
<b>N-0</b>	400	400	200	125	15	1000	350	115 – 72	24.6
<b>N-1</b>	400	400	200	125	15	1000	350	115 – 72	26.2

According to the compressive strength of the mixtures in Table 4.8, The compressive strength of the N-0 coded mixture containing aggregate without any treatment and 15 moles of the sodium solution was resulted in compressive strength of 24,6 MPa by applying 72 hours and 115 ° C thermal curing. The compressive strength of the N-1 code was 26.2 MPa which provided the same content and curing conditions of the mixture with the elimination of 0–100 micron inert materials. According to the results, it is seen that this inert material between 0-100 microns has a negative effect on both compressive strength and workability. However, it has been concluded that there is no need for any sieving process in future studies since the sieving process in large-scale productions will lead to high labor demand and the presence of inert material affects the strength results in a quite small amount.

In the following study, fly ash was included in the mix instead of blast furnace slag, and three series were designed to examine the increase in the amount of fly ash and aggregates. In the first mixture of the series (N-2), fly ash was used in 20% of the amount of binder, while aggregate was used equally with the total amount of binder. In the second mixture (N-3) of the series, the amount of fly ash was kept constant while the amount of aggregate was doubled. In the final mixture (N-4) of the series, this time the amount of fly ash was doubled, while the aggregate was used equally with the total amount of binder as in the first mixture. The designed mixtures were subjected to a 115 ° C heat curing process for 72 hours after casting. The contents of the mixtures and their compressive strength results are presented in Table 4.9.

**Table 4.9.** Investigation of fly ash and aggregate amount in the scope of geopolymer concrete development

<b>Note: The unit of all materials is kg/m<sup>3</sup>.</b>										
<b>Code</b>	<b>HB</b>	<b>RCB</b>	<b>RT</b>	<b>CW</b>	<b>FA</b>	<b>NaOH (M)</b>	<b>Aggregate</b>	<b>Water</b>	<b>Heat Curing Conditions (°C – hr)</b>	<b>Compressive Strength Results (MPa)</b>
<b>N-2</b>	200	200	200	200	200	15	1000	350	115 – 72	34.1
<b>N-3</b>	200	200	200	200	200	15	2000	350	115 – 72	31.1
<b>N-4</b>	150	150	150	150	400	15	1000	350	115 – 72	37.6

According to the results presented in Table 4.9, it was observed that the compressive strength of the mixes was above 30 MPa with the thermal curing process. As stated before, it is concluded that the calcium content is not vital when the reactions are accelerated by heat curing, and fly ash has been shown to perform better than GBFS due to its high aluminosilicate content and spherical shape. However, as the compressive strength of the N-4 coded mixture is approximately 7% higher than the compressive strength of the N-2 coded mixture, it has been concluded that the high substitution of fly ash does not have a serious contribution to the mixture's compressive strength. In addition, by comparing the compressive strength of N-2 and N-3 coded mixtures, it is concluded that the increase in aggregate amount negatively affects the compressive strength. These findings gave an important idea for the mix designs to be made in the later stage of the study.

In the development of geopolymer concrete, after the 30 MPa compressive strength was exceeded with thermal curing applications, preliminary studies were conducted for ambient curing in laboratory conditions. In this context, different mixtures have been designed by changing various parameters such as precursor type and amount, activator type and concentration, and the effect of these parameters on the performance of the final product has been examined. The contents of the mixtures designed in this study are presented in Table 4.10 and the compressive strength results are presented in Table 4.11.

**Table 4.10.** Mixtures produced by changing various parameters in the development of geopolymer concrete

**Note: The unit of all materials is kg/m<sup>3</sup>.**

Code	HB	RCB	RT	GW	CW	GBFS	Ca(OH) <sub>2</sub>	NaOH (M)	Na <sub>2</sub> SiO <sub>3</sub>	Aggregate	Water
N-5	150	200	250	0	200	200	0	12	0	1000	350
N-6	150	200	250	100	100	200	0	12	0	1000	350
N-7	150	200	250	100	100	200	0	8	224	1000	202.15
N-8	150	200	250	100	100	200	0	5	250	1000	185
N-9	150	200	250	100	100	200	100	8	224	1000	202.15
N-10	200	270	330	100	100	0	100	15	0	1000	350

**Table 4.11.** Compressive strength results of mixtures produced by changing various parameters in the development of geopolymer concrete

Code	Compressive Strength Results (MPa)	Ambient Curing (day)
N-5	21.2	14
N-6	19.4	
N-7	25.3	
N-8	22.1	
N-9	28.6	
N-10	14.2	

In this series, the mixtures produced by changing some parameters were examined as a result of their compressive strength after 14 days of ambient curing. According to the compressive strength results of the N-5 coded mixture and N-6 coded mixture designed to investigate of usage of glass waste, it was observed that the use of glass waste had a slightly negative effect on the performance of the samples. Furthermore, it was observed that the mixture with N-7 code, where sodium silicate was used to be 2 times the amount of sodium hydroxide, showed approximately 20% more compressive strength than the mixture with N-6 code where sodium silicate was not used. This indicates that the use of sodium silicate has a significant positive effect on the ambient curing, as seen in the development of geopolymer mortar mixtures. Unlike the N-7 coded mixture, the sodium hydroxide solution was decreased to 5M in the N-8 coded mixture while the amount of silicate was increased approximately 11.6%. Considering the compressive strength of these two mixtures, lowering the sodium hydroxide molarity had a negative effect on the system. The fact that sodium hydroxide, which plays the most important role in dissolving the aluminosilicate content of the waste materials, remained below certain molarity, had an adverse effect on the system despite the increase of sodium silicate. According to the compressive strength result of the mixture with N-9 code produced with the addition of 10%  $\text{Ca(OH)}_2$  to the mixture with N-7 code, it was observed that the addition of  $\text{Ca(OH)}_2$  had a significant contribution to the compressive strengths. As a result, the mixture with code N-9 reached the highest compressive strength result in this series, with a compressive strength of 28.6 MPa after 14 days of ambient curing. Finally, as shown in previous studies, the mixture with N-10 code produced with a completely CDW-based binder material showed the lowest strength results due to reasons such as insufficient calcium source and not using sodium silicate. The use of only  $\text{Ca(OH)}_2$  as a source of calcium and its ineffectiveness in the absence of GBFS caused the mixture with N-10 code to perform poorly.

Throughout the N-1,10 series produced within the scope of the development of geopolymer concrete mixtures, the behavior of parameters that significantly affect the strength results of concrete samples such as oven curing and 14-day ambient curing, varying activator ratios, precursor material type and quantities were examined. Following this preliminary analysis, important results have been obtained for the highest performing CDW-based geopolymer concrete mixtures that are finally to be produced in the following phases in ambient conditions.

According to the knowledge and experience gained in the development of geopolymer concrete mixtures, some productions have been made by determining the mixing ratios so that the materials will perform at the highest performance. During these productions, it has been observed that some cracks are formed, which are thought to be caused by drying and autogenous shrinkage that cause the samples to deteriorate from early ages to the next ages. In the ongoing stages of the study, a number of attempts have been made to prevent these cracks. After a literature review, it has been concluded that curing conditions will have a beneficial impact on shrinking and improve the composition of the mixture. As a result of the researches, it has been concluded that increasing the humidity level in the curing of the samples has a positive effect against shrinkage and cracks formation, and rapid-drying should be prevented in the production of crack-free geopolymer samples (Zuhua et al., 2009; Perera et al., 2007). Additionally, various curing trials such as air curing, water curing and polyethylene-sealed curing have been carried out on slag-based samples activated with powder sodium silicate and hydrated lime in the literature. According to the results obtained, there were no visible cracks in the water and polyethylene-sealed samples, so the samples cured in this way showed higher compressive strengths than the samples cured in dry air. Crack formation and related strength decreases have been attributed to the very dry surface (Collins and Sanjayan, 2001). In this context, by increasing the number of samples produced, moisture cure applications were carried out besides the dry environment cure. The contents of the mixtures are presented in Table 4.12 and the compressive strength results are presented in Table 4.13.

**Table 4.12.** Study on the shrinkage behavior of samples in the development of geopolymer concrete

**Note: The unit of all materials is kg/m<sup>3</sup>.**

Code	HB	RCB	RT	GW	CW	GBFS	SFA	Ca(OH) <sub>2</sub>	NaOH (M)	Na <sub>2</sub> SiO <sub>3</sub>	Aggregate	Water	SR
E-1	150	200	250	100	100	150	50	0	8	224	1000	202.15	0
E-2	150	200	250	100	100	150	50	60	8	224	1000	202.15	0
E-3	150	200	250	100	100	150	50	0	8	224	2000	202.15	0
E-4	150	200	250	100	100	150	50	0	8	224	1000	202.15	40

**Table 4.13.** Compressive strength results in the study on the shrinkage behavior of samples in the development of geopolymer concrete

Code	Compressive Strength Results (MPa)					
	Ambient Curing			Moisture Curing		
	3 days	7 days	28 days	3 days	7 days	28 days
<b>E-1</b>	13.5	17.1	25.1	11.3	19.4	34.2
<b>E-2</b>	14.2	22.5	30.1	12.1	24.1	39.1
<b>E-3</b>	12.1	19.3	29.9	9.8	22.7	33.8
<b>E-4</b>	11.8	18.9	25.7	10.6	21.6	31.2

According to the results obtained in Table 4.13, it was concluded that moisture cure had a positive effect on the compressive strength of the mixtures. In parallel with the information obtained from various literature studies, rapid drying of the sample was prevented along with the moisture curing, and consequently, the crack problem caused by shrinkage stresses was eliminated. In addition, the other three mixtures with various additions to prevent shrinkage and crack formation have shown a higher mechanical performance than the reference mixture E-1. Cracks occurring in a low-humidity environment are more prominent in their later ages, leading to serious reductions in the compressive strength of the samples. Considering the results of this study, 39.1 MPa compressive strength has been achieved by designing the mixture content for the best performance and subjecting it to moisture-curing for 28 days, thereby significant progress was made in the development of CDW-based geopolymer concrete mixtures. After this study, the behavior of the materials used in concrete mixes and curing processes are better understood, and in the next stage, the final 7 mixes are prepared to contain concrete and beam samples.

At the final stage, the GC-1,7 series was designed within the scope of development of geopolymer concrete with construction and demolition waste. In the mixture coded GC-1, while completely CDW-based materials were used as binder material and aggregate, sodium hydroxide was prepared as 8 moles and sodium silicate was included in the mixture as 2 times the amount of sodium hydroxide. GC-2 coded mixture was prepared by adding 7.5% Ca(OH)<sub>2</sub> to the GC-1 coded mixture. Unlike GC-1 coded mixture, GC-3 coded mixture was designed by adding 20% blast furnace slag and 5% Ca(OH)<sub>2</sub> to CDW-based materials. In

addition, sodium hydroxide / sodium silicate ratio of GC-3 coded mixture was adjusted as equal. In contrast to the GC-4 code mixture, the substitution of GBFS was reduced from 20% to 15%, and the remaining 5% was completed with the fly ash. In the GC-5 coded mixture designed to contain no sodium silicate, the amount of the alkaline content was adjusted by increasing the molarity of the sodium hydroxide solution to 12. The GC-6 coded mixture was designed to be the same as the content and activator amount of the GC-4 coded mixture, and the aggregate amount was doubled as the only difference. Finally, unlike the GC-4 coded mixture, the GC-7 mixture was designed to have a sodium silicate/sodium hydroxide ratio of 2. These 7 mixtures are designed to ultimately observe the behavior of parameters that directly affect compressive strengths such as precursor, aggregate, alkali activator type and quantities in different proportions used throughout the study. The contents of the mixtures produced in this series are presented in Table 4.14 and the compressive strength results are presented in Table 4.15.

**Table 4.14.** Final mixtures in the development of geopolymer concrete

**Note: The unit of all materials is kg/m<sup>3</sup>.**

Code	HB	RCB	RT	GW	CW	GBFS	FA	Ca(OH) <sub>2</sub>	NaOH (M)	Na <sub>2</sub> SiO <sub>3</sub>	Aggregate	Water
GC-1	187.5	250	312.5	125	125	0	0	0	8	224	1000	202.15
GC-2	187.5	250	312.5	125	125	0	0	75	8	224	1000	202.15
GC-3	150	200	250	100	100	200	0	50	8	112	1000	276.1
GC-4	150	200	250	100	100	150	50	50	8	112	1000	276.1
GC-5	150	200	250	100	100	150	50	100	12	0	1000	350
GC-6	150	200	250	100	100	150	50	50	8	112	2000	276.1
GC-7	150	200	250	100	100	150	50	50	8	224	1000	202.15



**Table 4.15.** Compressive strength results of final mixtures in the development of geopolymer concrete

	Compressive Strength Results (MPa)				Flexural Strength Results (MPa)
	Concrete				Beam
	Moisture Curing		Water Curing		Moisture Curing
Code	7 days	28 days	7 days	28 days	28 days
<b>GC-1</b>	7.1	25.3	6.2	20.3	4.4
<b>GC-2</b>	9.4	26.1	8.3	23.1	4.8
<b>GC-3</b>	15.3	30.6	16.4	24.5	5.2
<b>GC-4</b>	16.1	32.2	15.3	25.6	5.3
<b>GC-5</b>	10.4	25.1	6.8	18.7	4.2
<b>GC-6</b>	12.6	34.9	11.3	27.6	5.9
<b>GC-7</b>	23.4	39.6	17.5	33.8	6.5

7 and 28 days of compressive strength results of the concrete and beam samples produced in the GC-1.7 series were presented in Table 4.15. Considering the results obtained, the compressive strength of the GC-1 mixture, which was produced by using CDW-based materials together with sodium hydroxide and sodium silicate as alkali activator resulted as 7.1 MPa in 7 days and 25.3 MPa in 28 days under the moisture curing. In the water cure, a decrease of approximately 20% was observed in the compressive strength of the samples. Produced by adding 7.5% Ca (OH) 2 to the GC-1 coded mixture, the GC-2 coded mixture reached 26.1 MPa compressive strength at the end of 28 days in the moisture cure. The GC-3 mixture produced with the addition of 20% GBFS showed a compressive strength performance above 30 MPa (30.6 MPa). In order to eliminate the workability and setting time problems by increasing of the sodium silicate amount, 5% fly ash was added to the mixtures and the GC-4 coded mixture produced in this context reached 32.2 MPa compressive strength at the end of 28 days, and it was observed that it was also better in terms of workability compared to previous mixtures. GC-5 coded mixture produced without the use of sodium silicate showed the lowest compressive strengths for 28 days of moisture

curing, and in addition to sodium hydroxide, sodium silicate was found to be required to obtain strong properties. Furthermore, in contrast to the moisture cure, GC-5 coded mixture has shown very poor performance in the water cure. In the mixture with the GC-6 code, where the aggregate amount is twice the amount of binder, the compressive strength of 34.9 MPa has been reached after 28 days of moisture cure. Unlike the GC-6 coded mixture, the GC-7 coded mixture, where the aggregate ratio was used equal to the binder amount, reached the compressive strength of 39.6 MPa at the end of the 28-day moisture cure and became the final concrete mixture of the study. Although some loss of strength has been observed at the end of the water curing, the issue of the water curing damaging geopolymer products by completely dissolving its structure, which is frequently mentioned in geopolymer researches, has been overcome in this study.

The flexural strength of beam samples produced within the scope of the development of geopolymer concrete mixtures showed parallel performances according to the compressive strengths of the concrete mixture as expected. With a flexural strength of 6.5 MPa, the beam sample produced with GC-7 coded mixture had the highest performance of that series. As a consequence of this series, it was found that significant flexural strengths can be achieved by the reinforcement applied to the column and beam structures that will be produced in the future on a large scale.

In the literature, when geopolymer concrete samples with compressive strengths similar to concrete produced with Portland cement are produced as beams and their flexural strengths are analyzed, results showed that flexural strengths of geopolymer beams have reached higher levels compared to flexural strengths of beams produced with Portland cement. This has been associated with the matrix formed as a result of geopolymerization, being more ductile than Portland cement systems by different microstructure. (Susan A. et al., 2012). The samples produced in this study also had similar behavior compared to Portland cement beams in the literature, although no Portland cement reference beam samples were produced. In general, the concrete samples obtained using completely CDW-based material are still experiencing a situation that can be improved based on the findings, although they are very good results in comparison with the studies in the literature. It is also very important to evaluate the properties of these waste materials, which will be obtained from different sources, and formulate accordingly. However, it has been observed that better results can be obtained within the scope of “green concrete” production by adding industrial wastes such

as GBFS or fly ash to CDW based waste materials. In addition, it has been concluded from the detailed literature reviews and studies conducted throughout the study that using sodium hydroxide together with sodium silicate as an alkali activator has a very positive effect on the geopolymer mechanism instead of using sodium silicate alone.

#### 4.4. Micro-Mechanical Analysis

##### 4.4.1. X-ray diffraction (XRD) Analysis

The XRD-Analysis was conducted on several samples to determine phase types and quantities of the crystals formed after the powdered CDW-based paste, mortar and concrete samples developed for the purpose of the study, and to analyze the amorphous material content in the mixture. Each phase observed as a result of XRD analysis creates a unique diffraction model. For example, quartz, cristobalite and glass are different phases of SiO<sub>2</sub>. Although they are chemically the same as this phase, their atomic order differs. Amorphous materials such as glass do not form diffraction peaks. The results of XRD analysis to examine the crystal phases formed in this context are presented below.

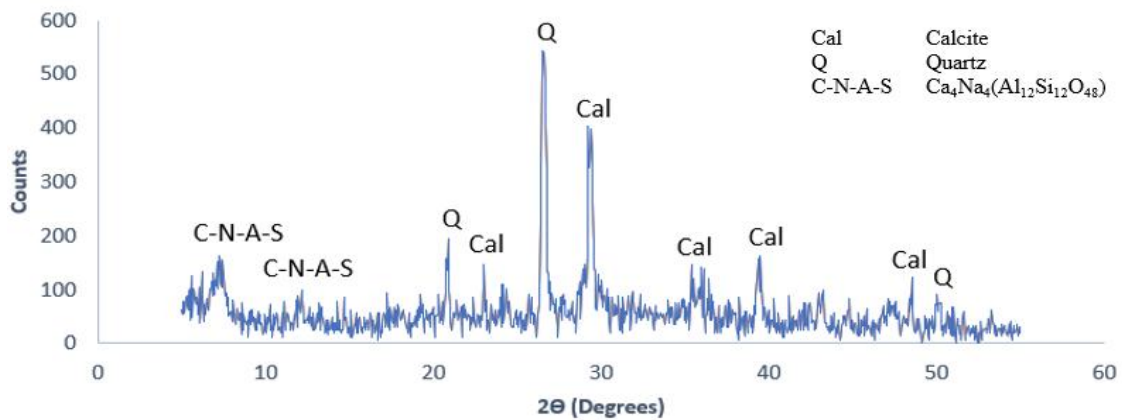


**Figure 4.8.** XRD analysis of WCF-1 mixture after heat curing at 75 ° C for 72 hours

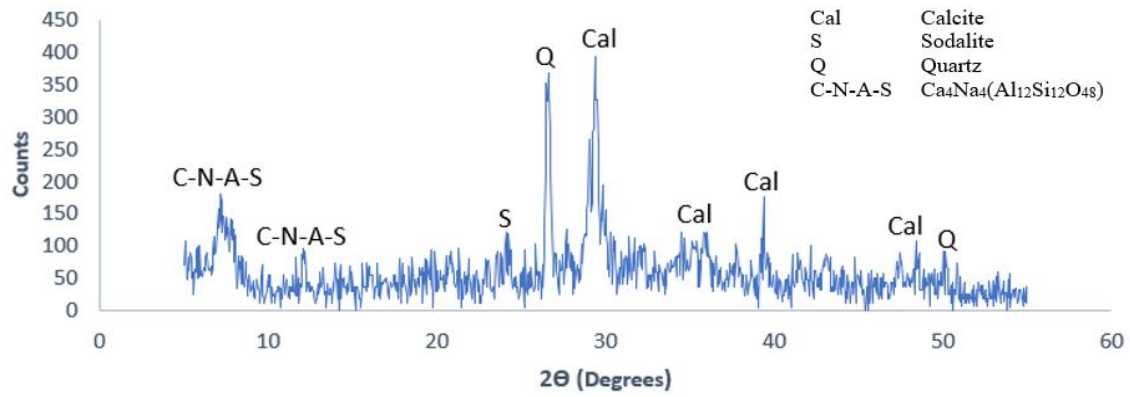


**Figure 4.9.** XRD analysis of WCF-9 mixture after heat curing at 125 °C for 48 hours

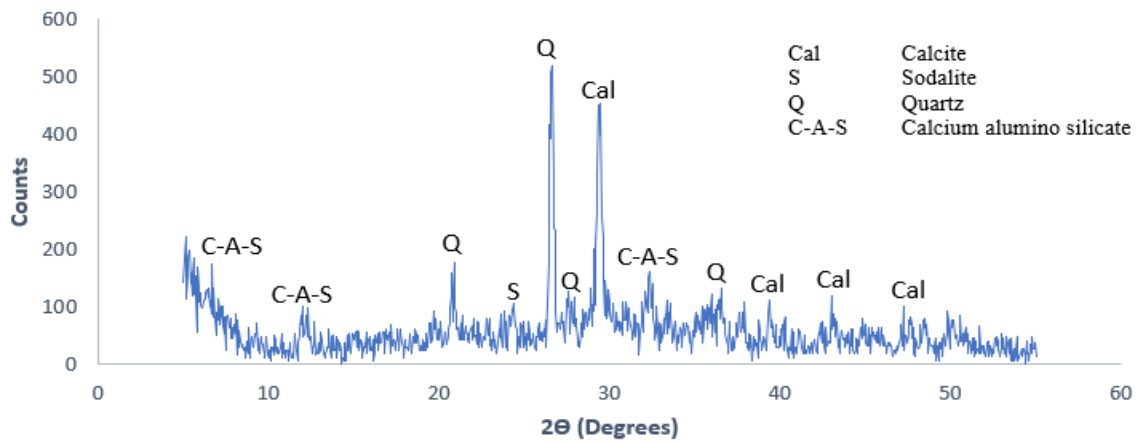


**Figure 4.10.** XRD analysis of WCF-S-6 mixture after 28 days of ambient curing

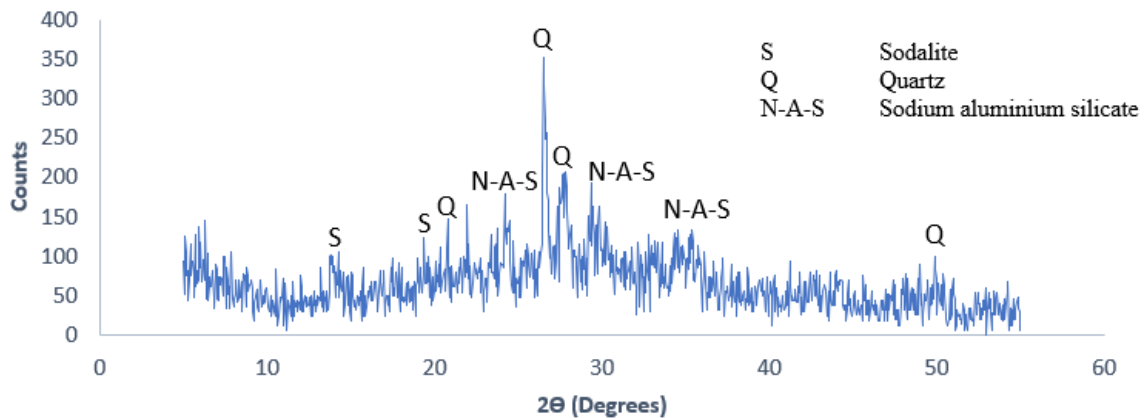


**Figure 4.11.** XRD analysis of CDWF-1 mixture after heat curing

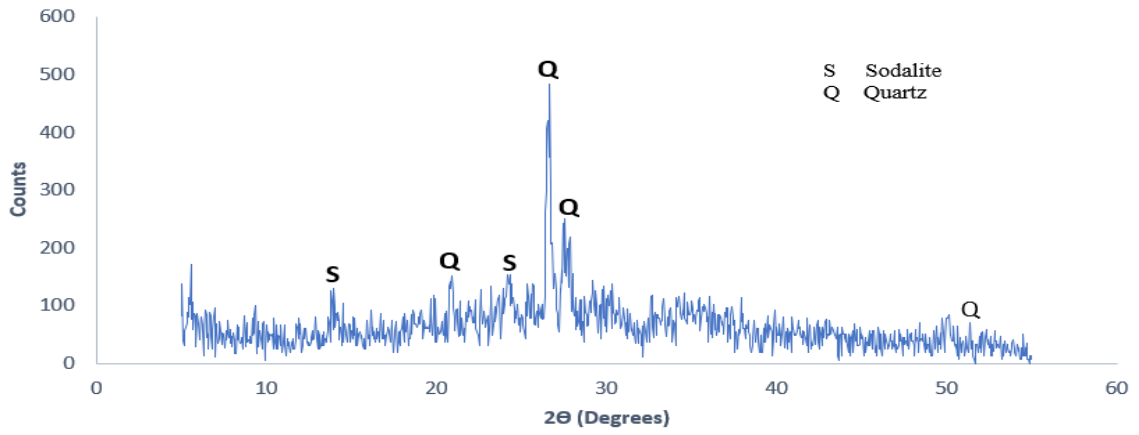


**Figure 4.12.** XRD analysis of CDWF-9 mixture after heat curing

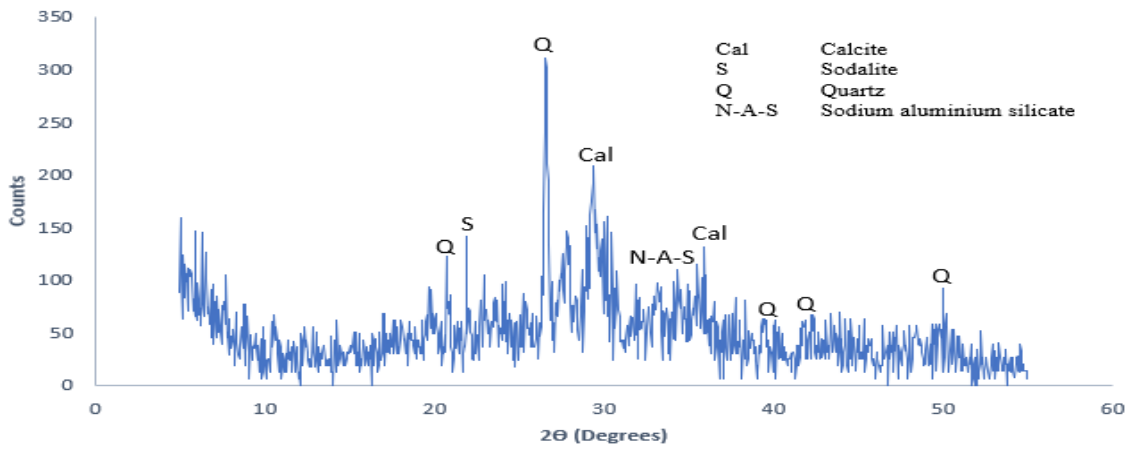


**Figure 4.13.** XRD analysis SW-6 mixture after 28 days of ambient curing

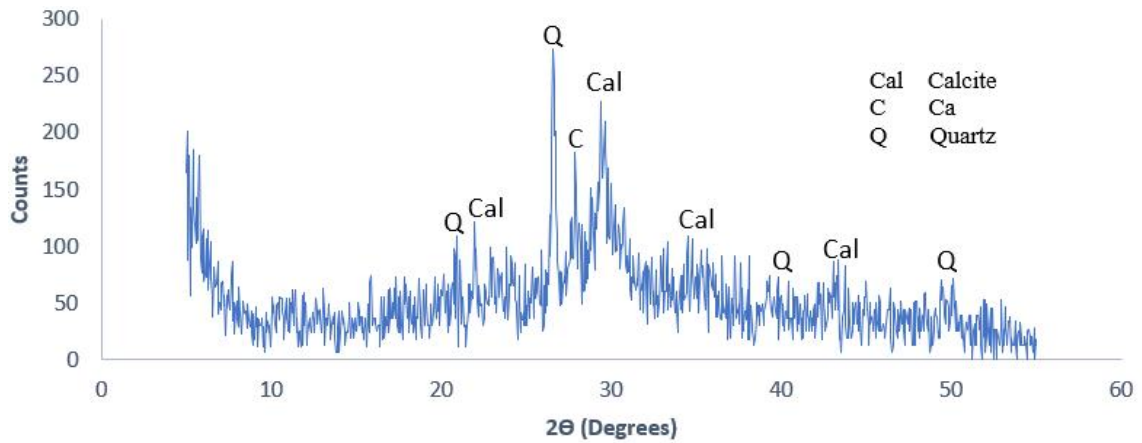


**Figure 4.14.** XRD analysis SS-6 mixture after 28 days of ambient curing

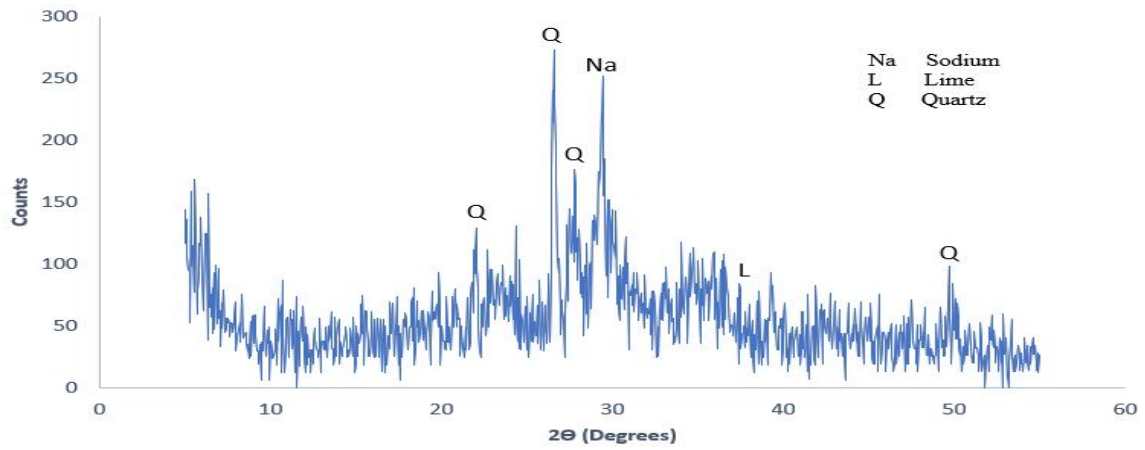


**Figure 4.15.** XRD analysis SS6-2 mixture after 28 days of ambient curing

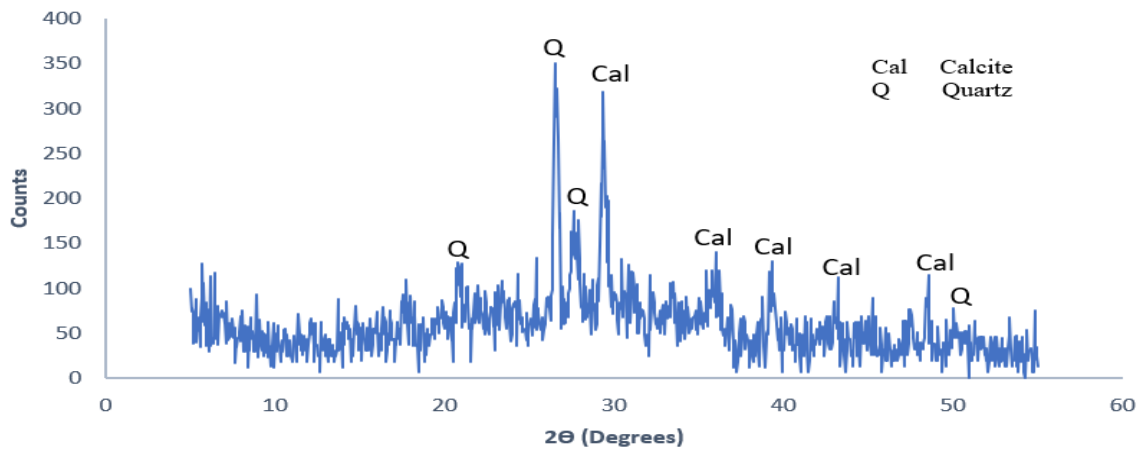


**Figure 4.16.** XRD analysis E-2 mixture after 28 days of ambient curing

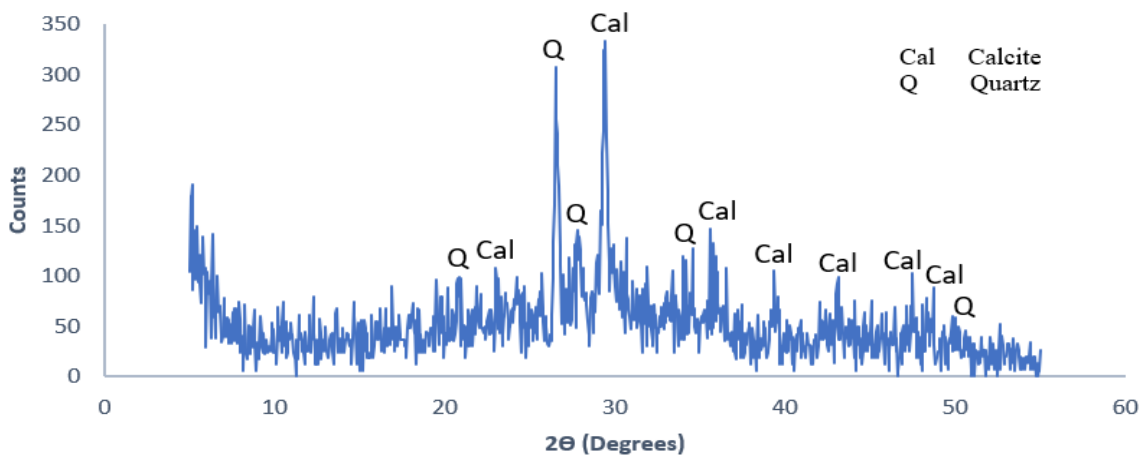


**Figure 4.17.** XRD analysis GC-7 mixture after 28 days of moisture curing

The quartz phase detected in all samples with XRD analysis is a highly reactive crystal phase. In the XRD analysis results of the concrete waste in powder form, the quartz crystal phase

determined at an angle of  $20.75^\circ$ ,  $26.65^\circ$  and  $50.15^\circ$  of  $2\theta$  was determined at the same angular intervals for WCF-1 produced by activating the concrete waste with alkali and It was observed that their phase density remained almost at the same level as a result of alkali activation. This may be related to the fact that the WCF-1 mixture cannot fully perform geopolymerization reactions and shows low compressive strength results. Phases such as quartz and mullite are generally known as crystal phases that are not affected by geopolymerization reactions (Van Jaarsveld et al., 1998). CNAS (Tetracalcium Tetrasodium Tectododecaalumododecacilicate), another crystal structure formed as a result of geopolymerization in the WCF-1 mixture, generally has a nanometric level within the amorphous aluminosilicate gel with 3D structure (Palomo et al., 2004). The formation of the zeolite structure occurs as a result of the formation of the aluminosilicate gel followed by crystallization to the zeolite. The calcite phases seen in the results of the analysis are thought to occur in the existing structure of concrete waste or due to carbonation reactions during the aging of the geopolymer matrix. When the XRD analysis of the WCF-2 mixture is examined, it is observed that similar crystal phase peaks are formed with the WCF-1 mixture. However, the decrease in the density of the quartz peaks indicates that geopolymer reactions occur more effectively. In addition, in the WCF-2 mixture, a sodalite peak was found in a similar way to the studies performed in the literature, but the chemical reactions that triggered the formation of the sodalite peak in the matrix as a result of the geopolymer reactions could not be detected exactly (Komnitsas et al., 2007; Zaharaki et al., 2010). Crystal structure peaks were determined for the CAS(H) gel structure with the XRD results of the WCF-S-6 mixture using sodium silicate to contribute to curing under ambient conditions. Although this provides evidence that geopolymerization reactions occur, the similarity of dense peaks of the crystalline phases such as quartz and calcite and raw material can be associated with the low mechanical performance of the WCF-S-6 mixture in the ambient cure. In the development of geopolymer paste, CDWF-1, which has an average level of compressive strength performance, has been found crystalline peaks of the NAS(H) gel structure seen in geopolymer systems using low calcium precursors as well as similar crystal phases found in other mixtures. According to the XRD results for the CDWF-9 mixture, which exhibits higher compressive strengths than the CDWF-1 mixture, crystal phase formations are reduced. The quartz phase has seen at an angle of  $26.65^\circ$  of  $2\theta$  of the precursor and the sodalite peaks that can be seen in the matrix after the geopolymerization reactions are the crystal structures detected in the mixture in a small amount. The hump structure formed in the XRD spectrum as a result of the high rate of geopolymer reactions is clearly visible

between 20 ° and 40 ° for SW-6, SS-6, SS6-2 mixtures. This illustrates the obvious relation between the increase in compression strength and the decrease in the peaks of the XRD crystalline phases. These peaks are crystal structure peaks for quartz, calcite, sodalite and NAS(H) gel for SW-6 mixture. When the SS-6 and SS6-2 mixtures are examined, it is seen that the crystal peak densities of the SS6-2 mixture containing calcium hydroxide in the XRD spectrum are lower compared to the SS-6 mixture and thus the high compressive strength is associated with decreasing peak densities. In addition, the SS6-2 mixture, which shows the highest compressive strength among these three mixtures, is the mixture with the least crystal peak. The formation of the hump structure is observed for the mixtures of E2 and GC7. In addition to the same activator types and ratios used for these two mixtures, a similar structure can be clearly seen in the XRD micrographs. In both mixtures, the same crystalline phases were detected at almost the same angles with similar phase densities.

#### **4.4.2. Scanning Electron Microscope (SEM) and Energy Dispersive X-Ray (EDX) Analysis**

Within the scope of the study, SEM analysis was conducted to examine detailed reaction products of various paste, mortar and concrete samples. Besides SEM analysis, EDX analysis was performed to determine the atomic structure of the reaction products to selected points of the sample. In this context, SEM and EDX analysis results of various samples are presented below.



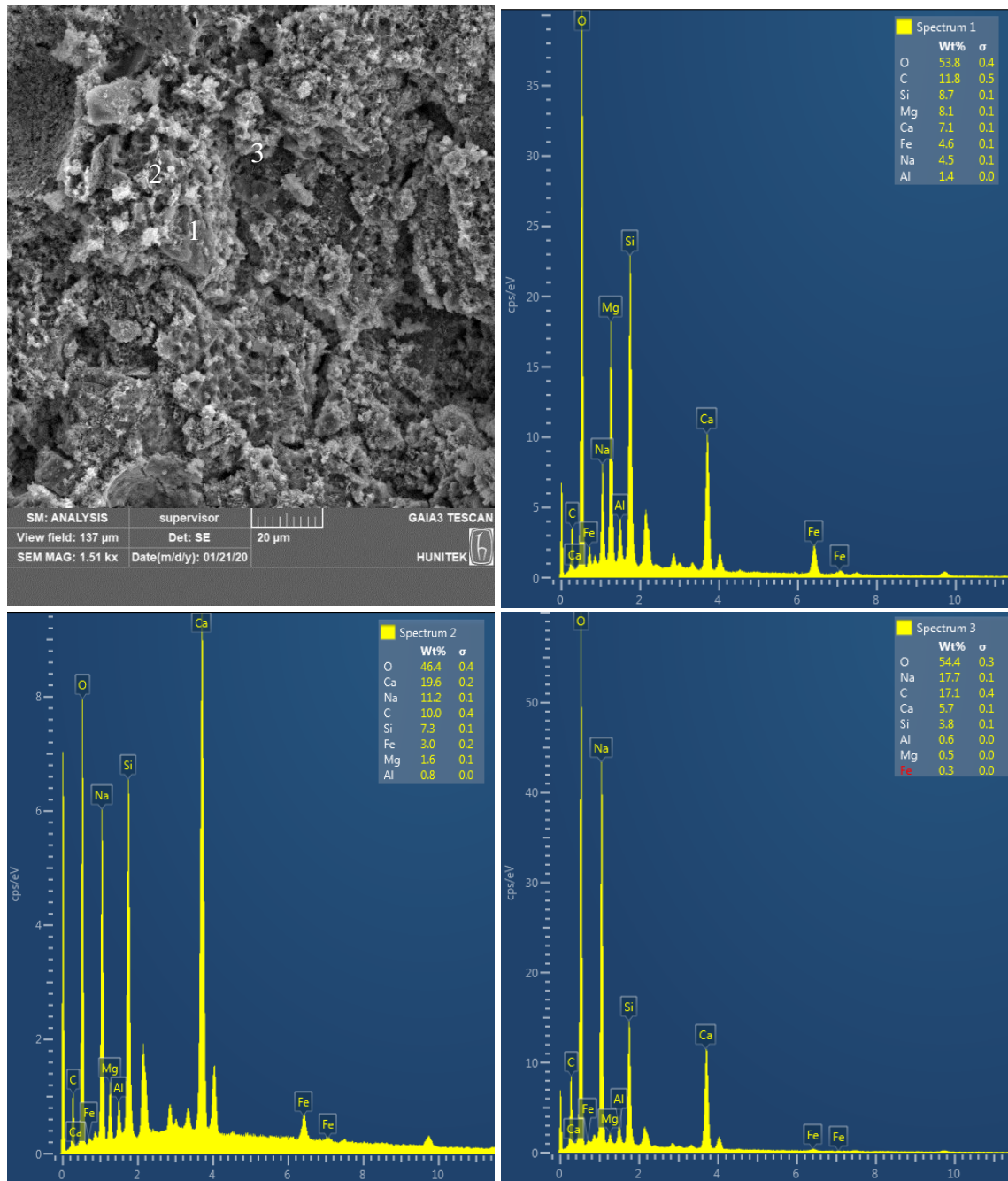


**Figure 4.18.** SEM-EDX analysis of WCF-1 mixture (75 ° C for 72 hr)

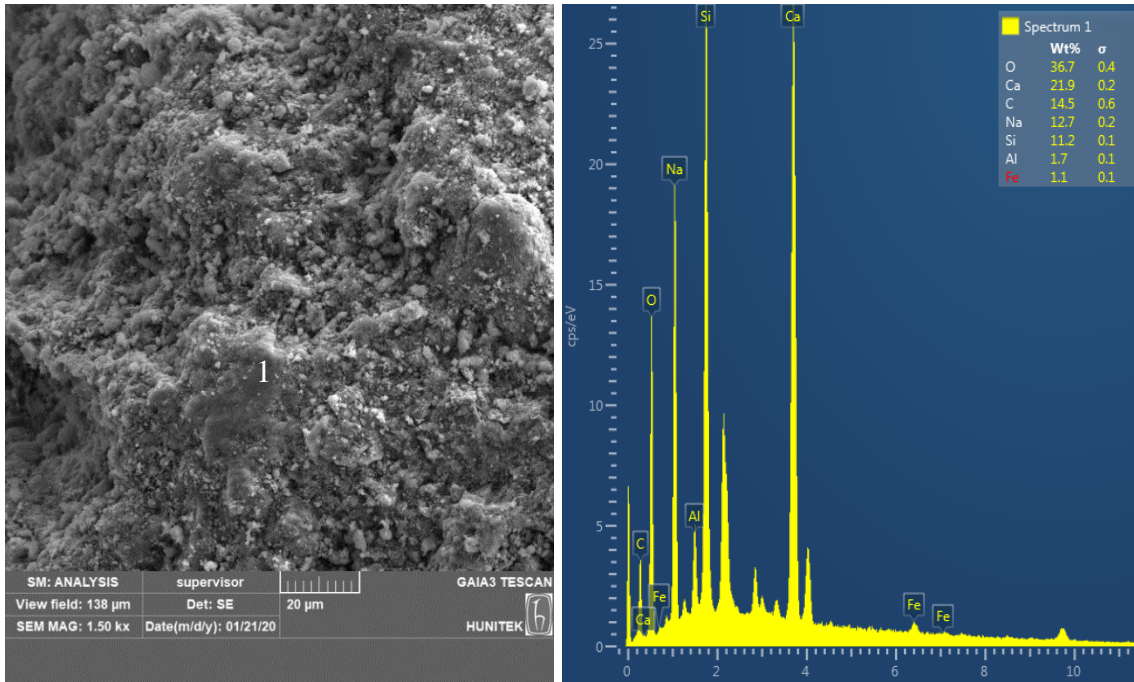


**Figure 4.19.** SEM-EDX analysis of WCF-9 mixture (125 ° C for 48 hr)

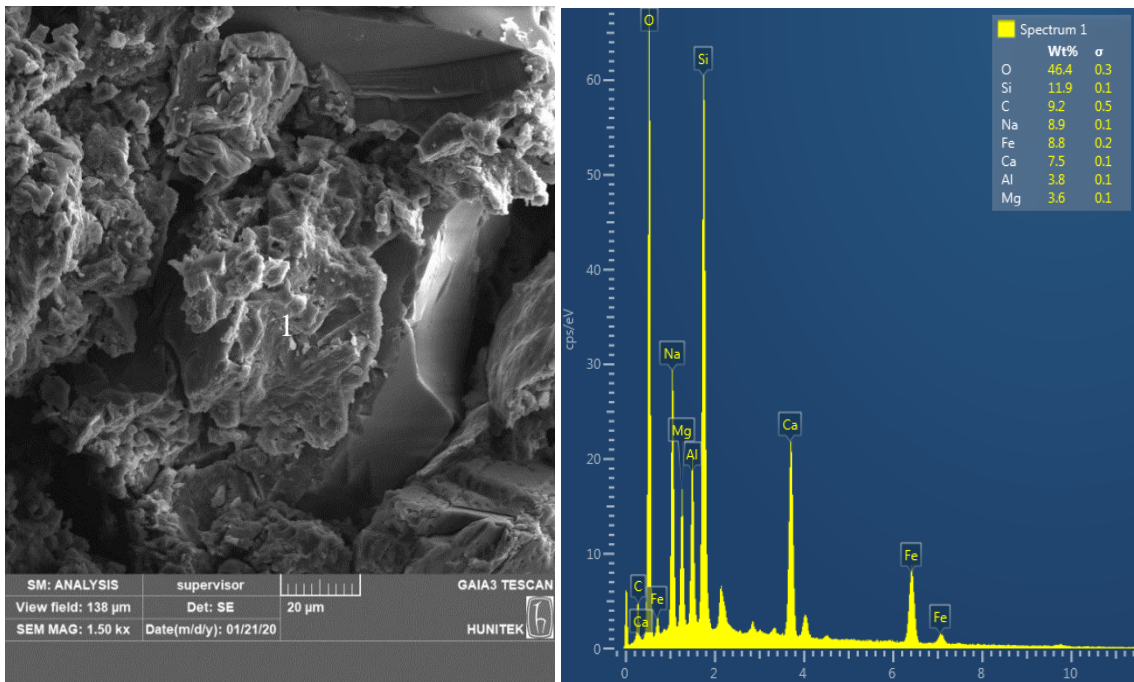


**Figure 4.20.** SEM-EDX analysis of WCF-S-6 mixture (28 days at ambient)

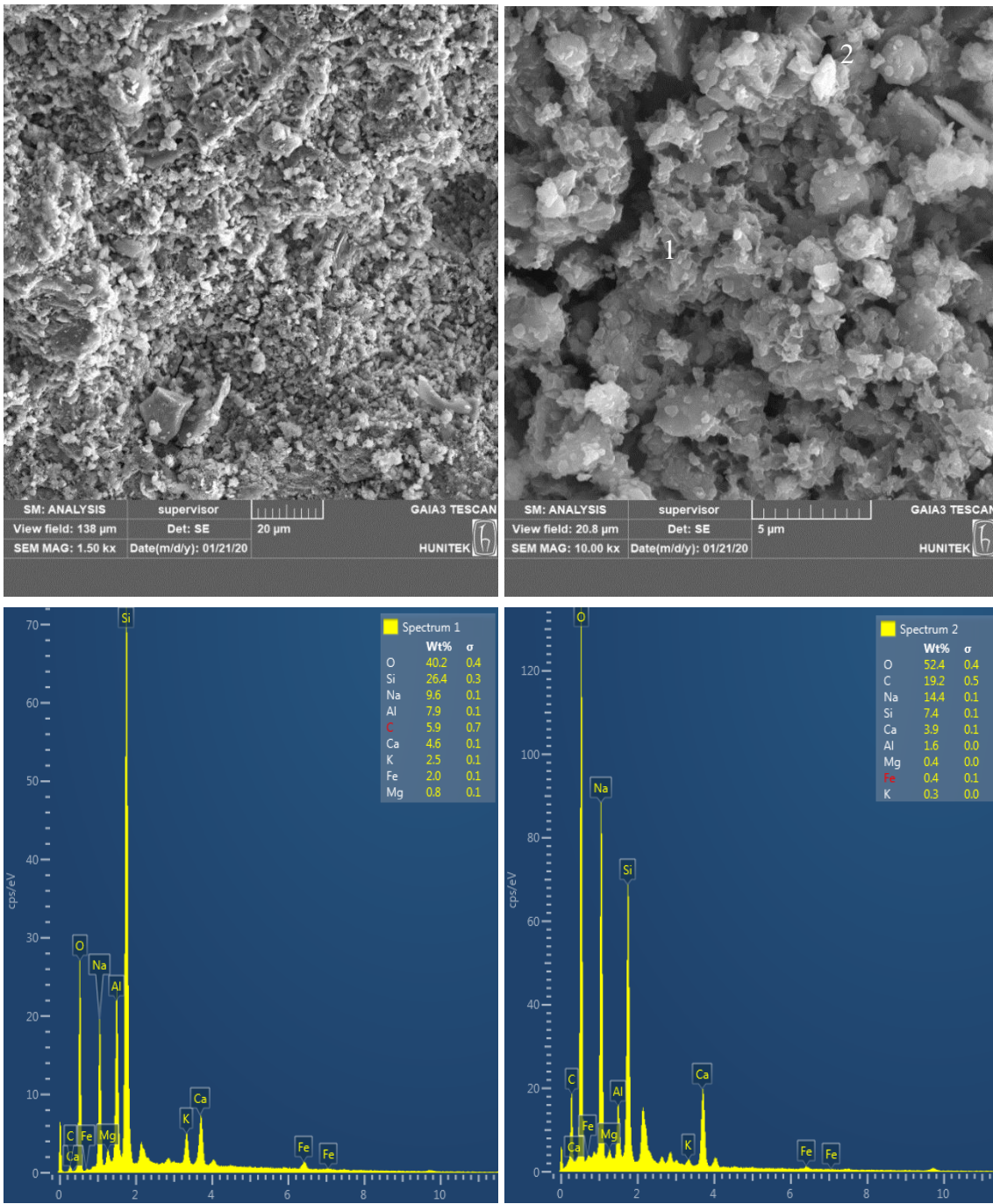


**Figure 4.21.** SEM-EDX analysis of CDWF-1 mixture after heat curing



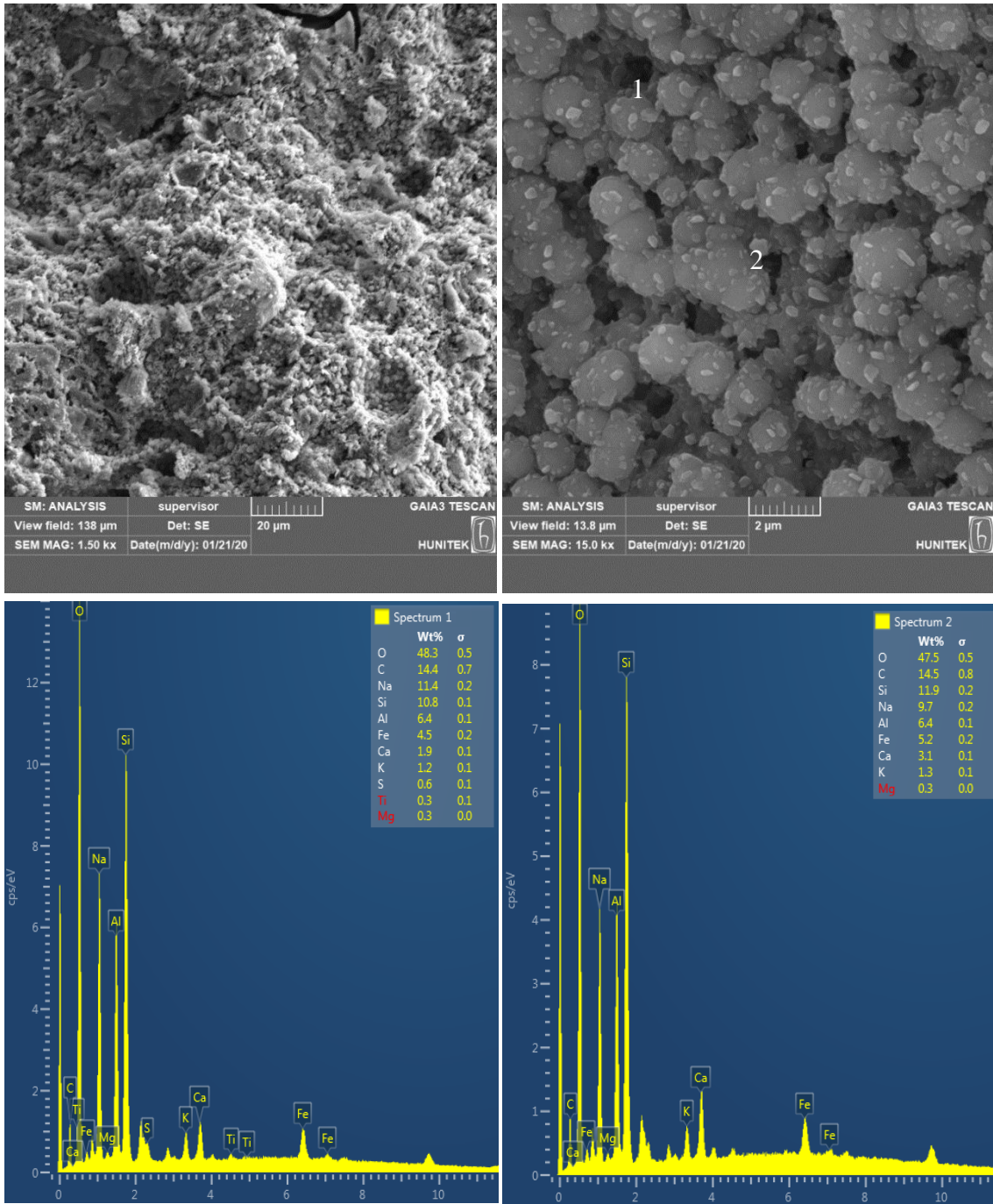


**Figure 4.22.** SEM-EDX analysis of CDWF-9 mixture after heat curing

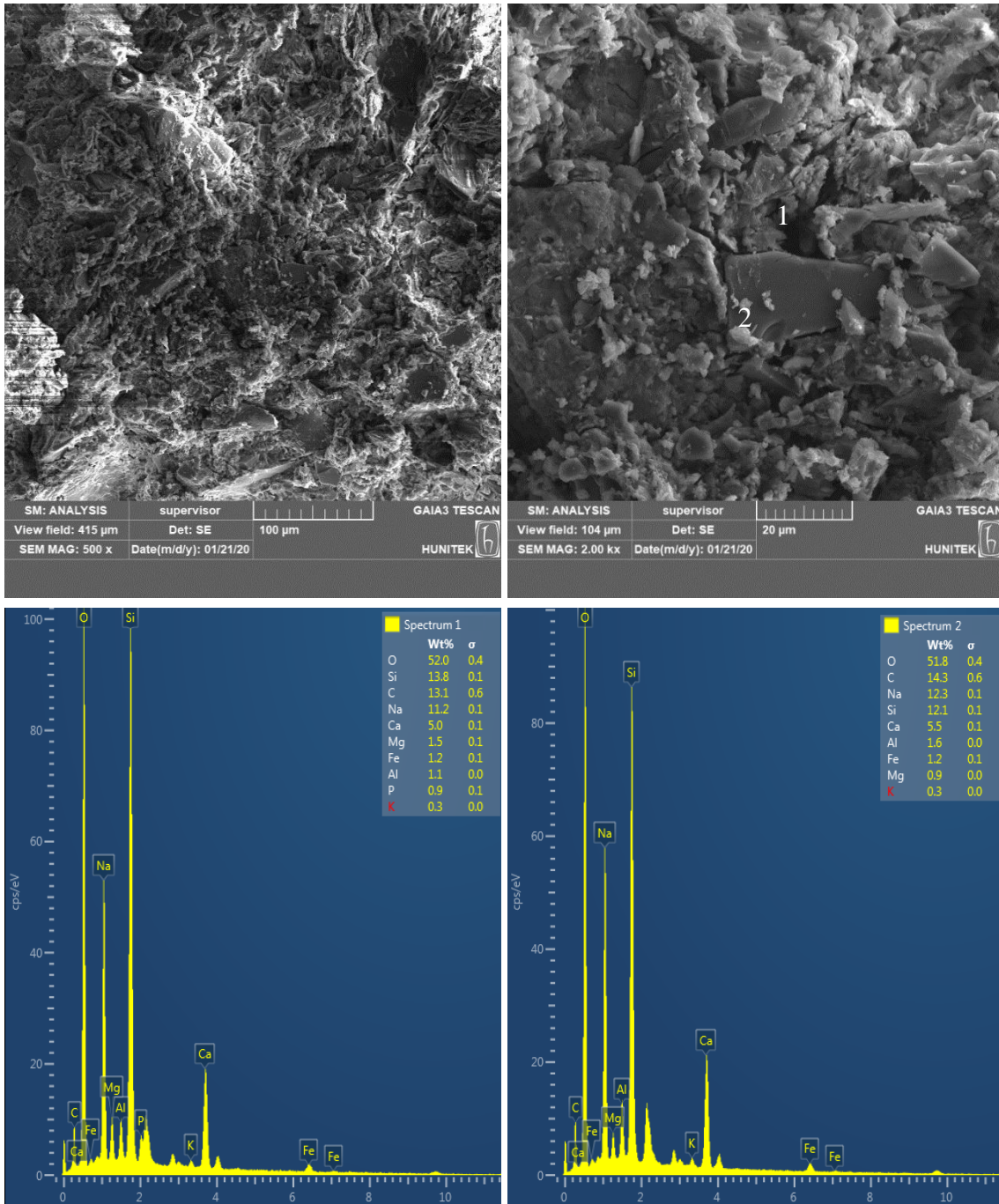


**Figure 4.23.** SEM-EDX analysis SW-6 mixture (28 days at ambient)

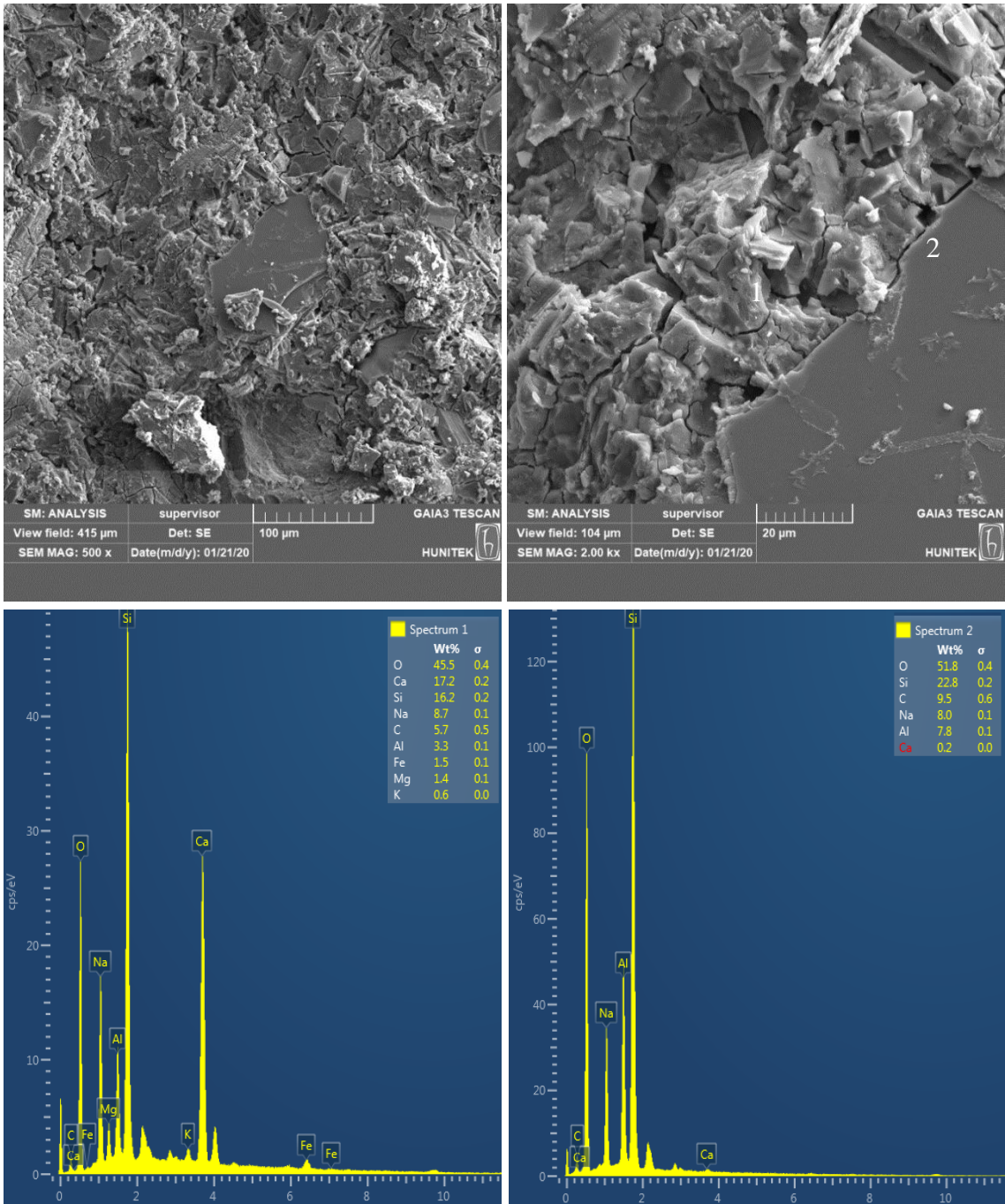
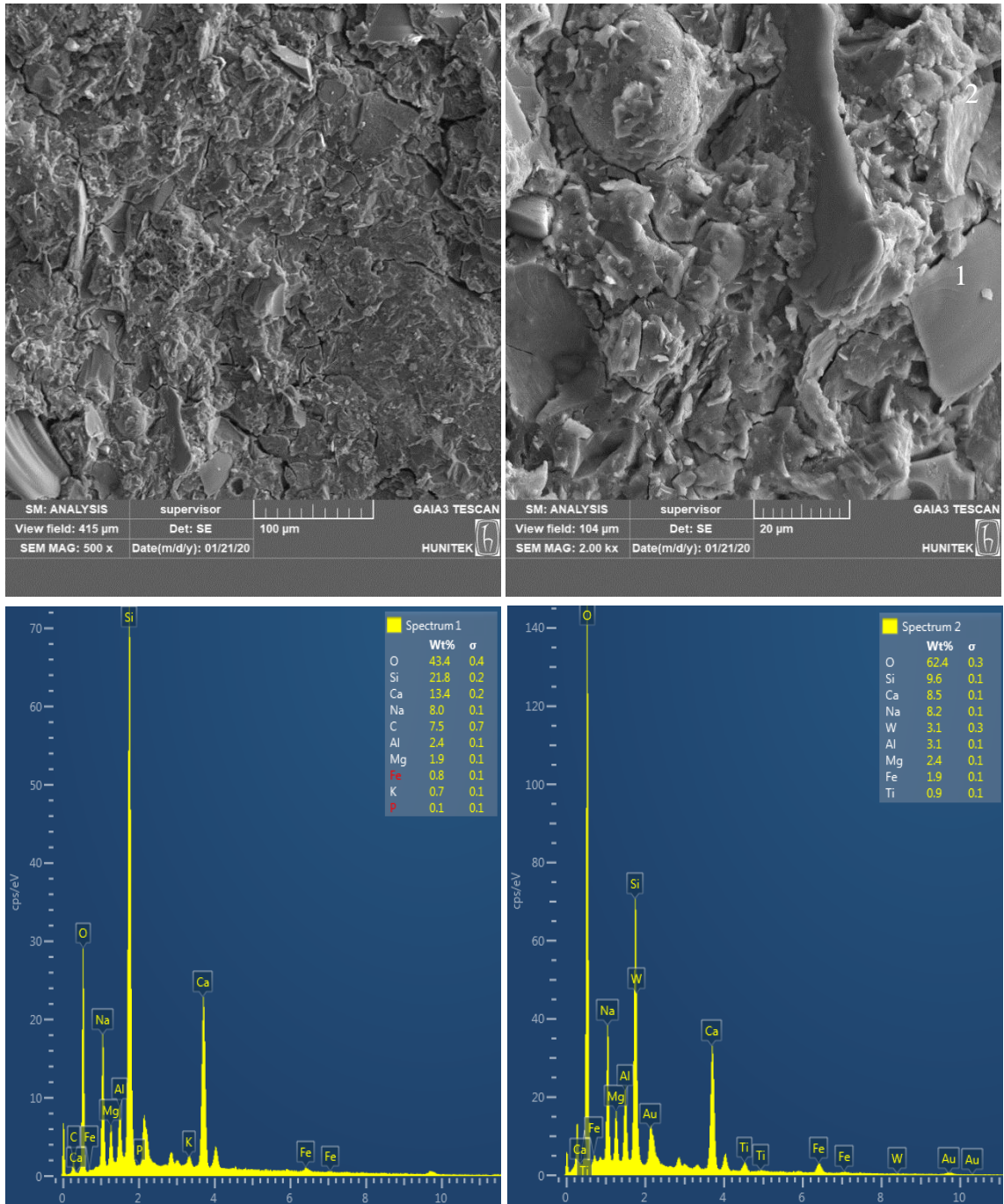
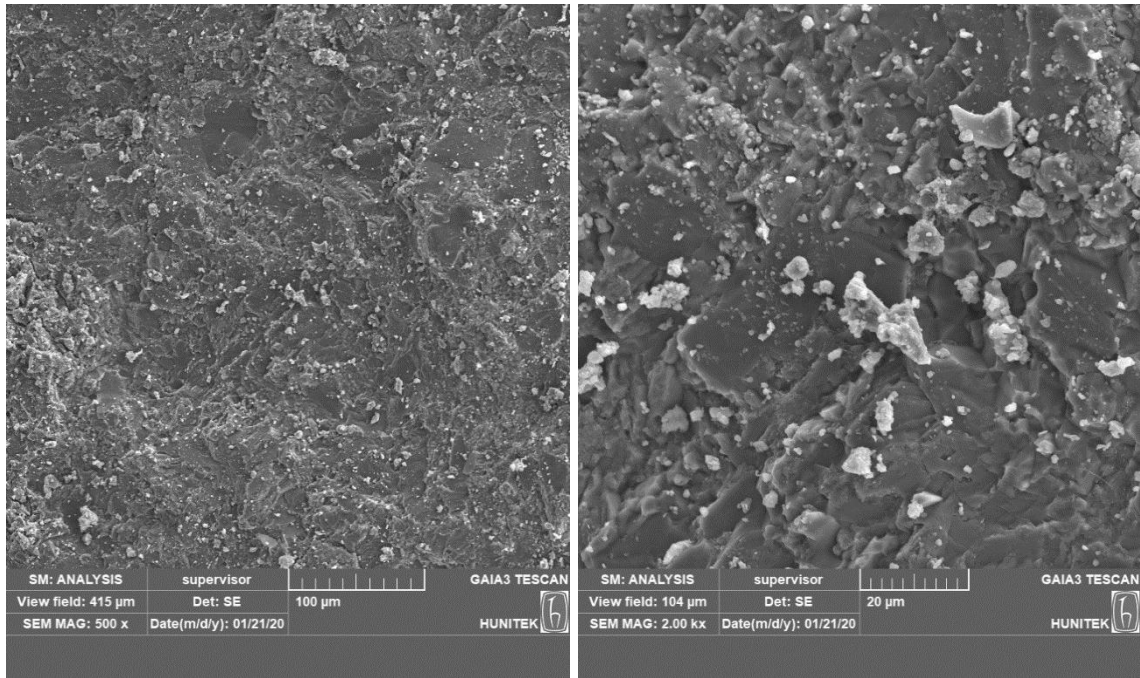


Figure 4.24. SEM-EDX analysis SS-6 mixture (28 days at ambient)





**Figure 4.25.** SEM-EDX analysis SS6-2 mixture (28 days at ambient)



**Figure 4.26.** SEM analysis E-2 mixture (28 days at ambient)

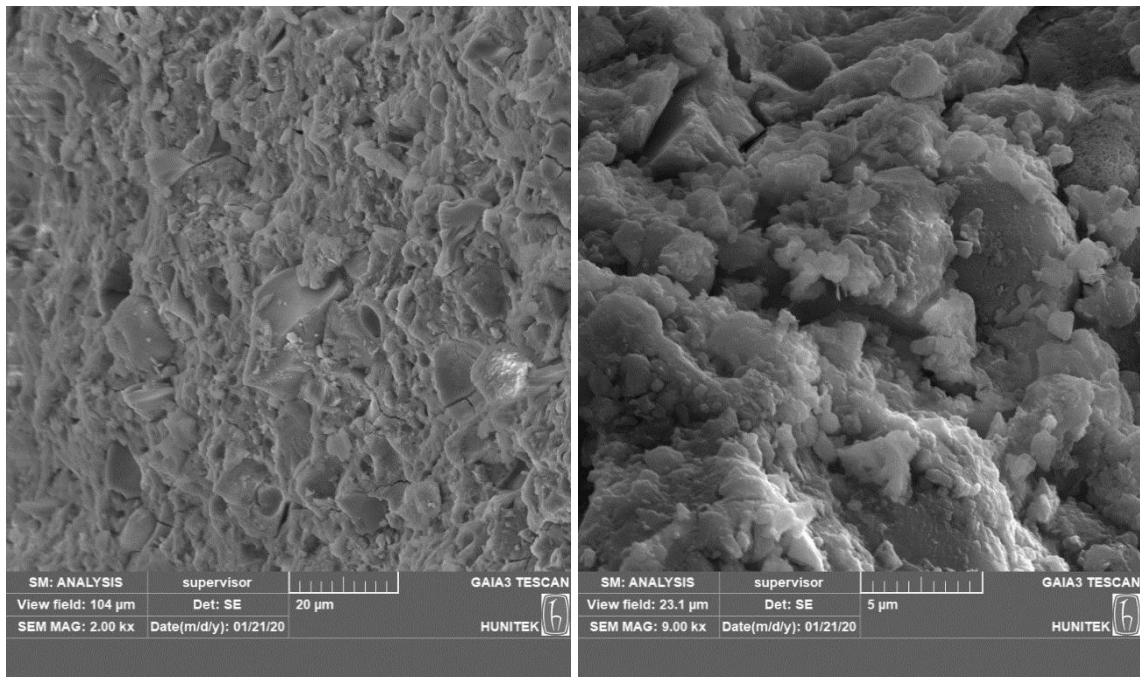


**Figure 4.27.** SEM analysis GC-7 mixture (28 days at ambient)

By examining the SEM and EDX images, significant changes and concentrations were observed in the microstructures of the geopolymer samples with changes in the precursors, alkali activators and curing conditions. A non-homogenous and porous structure was observed while examining the SEM picture of the WCF-1 coded mixture shown in Figure



3.18. When analyzing various points in EDX analyzes, the variation of sodium peaks indicates that alkaline activation is not homogenous enough and there are unreacted sodium hydroxide particles. In addition, the variability in the calcium peaks shows that the concrete waste is partially dissolved, and all these results support the WCF-1 coded mixture to yield low strength. In SEM and EDX images of the WCF-9 coded mixture (Figure 4.19), it was observed that a more homogeneous matrix was obtained than the WCF-1 coded mixture. In addition, it was concluded that the molecules forming the bonds in the matrix are distributed more regularly and the expected peaks are formed by EDX analysis of this mixture. An extremely irregular and porous matrix was seen when looking at the SEM image of the WCF-S-6 coded mixture as seen in Figure 4.20. This situation leads to a better understanding of the coded WCF-S-6 mixture with insufficient geopolymerisation reaction and low strength results. However, a regular and balanced molecular distribution was found by EDX analysis taken from a dense point. Considering the SEM and EDX results of the mixture coded in CDWF-1 in Figure 4.21, the inclusion of all other CDW-based binder material in addition to concrete waste provided a more dense and homogeneous matrix. In the image taken at 9.00 kx magnification, reaction products and non-reacting products and alkalis surrounding these products are found. This effect, leading to weakness in the matrix by not participating in the reaction, has also been observed in the literature (Alehyen et al., 2017). The most important parameter supporting this effect is EDX analysis results from different regions. While in some regions, balanced rates of silicon, sodium and aluminum peaks were observed, in some regions thought to be unresponsive, the sodium peak was high. When we look at the SEM and EDX analysis of the CDWF-9 coded mixture presented in Figure 4.22, a more dense matrix was found compared to the CDWF-1 coded mixture. According to the compressive strength results in the series where all CDW-based binder materials are used together (Figure 4.4), the CDWF-9 coded mixture, which reaches the highest strength, has a similar NASH gel distribution as a result of EDX analysis from different regions. However, since high calcium content materials such as GBFS and  $\text{Ca}(\text{OH})_2$  are not used in this mixture, calcium peaks are quite low as a result of EDX analysis. SEM and EDX analyses of SW-6, SS-6 and SS-6-2 coded mixtures, which are produced with recycled fine aggregate, are presented in Figure 4.23, Figure 4.24 and Figure 4.25 respectively. Among these 3 mixtures, which have the highest compressive strength performance in their series, less calcium-based structures are encountered in the mixture with SW-6 code, while silicon, sodium and carbon-based structures are quite balanced and regular. In the SS-6 and SS-6-2 coded mixtures, calcium-based CASH structures were formed with NASH gel in the matrix, which positively

affected the compressive strength of the mixtures. When looking at the SEM images of the mortar mixtures, in addition to the intense and homogeneous matrix in general, porous and micro-cracked structures were encountered at the interface transition zone between aggregate and geopolymer binder. This situation proves the existence of more than one interface transition zone between the geopolymer paste and the recycled aggregate, as previously stated, which weaken the matrix. SEM analysis images of E-2 coded and GC-7 coded concrete samples are presented in Figure 4.26 and Figure 4.27 respectively. After 28 days of ambient moisture curing, a very regular, homogeneous and dense matrix was detected with SEM images from the E-2 coded and GC-7 coded mixtures which showing 39.1 MPa and 39.6 MPa compressive strength, respectively. Even though the presence of unreacted solid precursors is observed, a matrix was obtained in which microcracking and porosity are quite minimal.

#### **4.5. Durability Studies of CDW-Based Geopolymer Concrete**

Throughout the study, only mechanical and micro-mechanical analysis results of geopolymer concrete mixtures, which were successfully developed in the process from powder form to concrete, are not sufficient in terms of performance. In addition to these mechanical properties, it is necessary to examine the durability properties of the produced geopolymer concretes to simulate environmental conditions. In this context, various durability tests have been performed to measure the resistance of sulfate, sorptivity, rapid chloride permeability test (RCPT) and resistance of wetting-drying cycles to a number of final mixtures.

In order to conduct durability tests, two of the concrete mixtures developed during the study were selected. One of them is the F coded mixture which has the highest compressive strength among CDW based mixtures containing GBFS and fly ash, while the other is the W coded mixture producing with 100% CDW based binder. The contents of the mixtures are presented in Table 4.16.

**Table 4.16.** Mixtures produced for durability studies

**Note: The unit of all materials is kg/m<sup>3</sup>.**

Code	HB	RCB	RT	GW	CW	GBFS	FA	Ca(OH) <sub>2</sub>	NaOH (M)	Na <sub>2</sub> SiO <sub>3</sub>	Aggregate	Water
F	150	200	250	100	100	150	50	50	8	224	1000	202.15
W	187.5	250	312.5	125	125	0	0	75	8	224	1000	202.15

From the mixture designs presented in Table 4.16, three samples of 50 mm in height and 100 mm in diameter cylinders were produced for RCPT and sorptivity tests, while three samples of 10x10x10 cm cubes were produced for resistance of wetting-drying cycle and resistance to sulphate tests. The casted samples were left to water curing for one week in order to gain sufficient strength before the test. The procedure and results of the durability tests applied to the samples in question are detailed below.

#### **4.5.1. Resistance to Sulphate**

Samples produced to measure resistance to sulphate attack were immersed in sodium sulphate solution according to ASTM C 1012 after gaining sufficient strength for one-week water curing. The samples immersed in the sulphate solution were removed from the solution to measure their mass and compressive strength every 7 days up to 21 days. The mass and compressive strengths of the specimens are presented in Figure 4.28 and Figure 4.29, respectively.

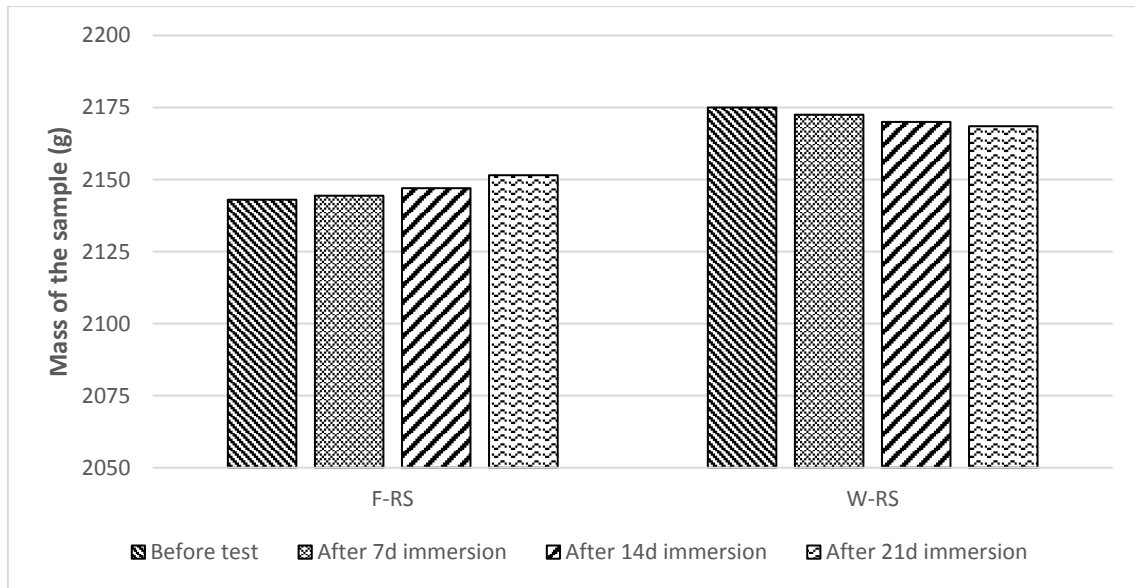


**Figure 4.28.** Masses of the samples for Resistance to Sulphate

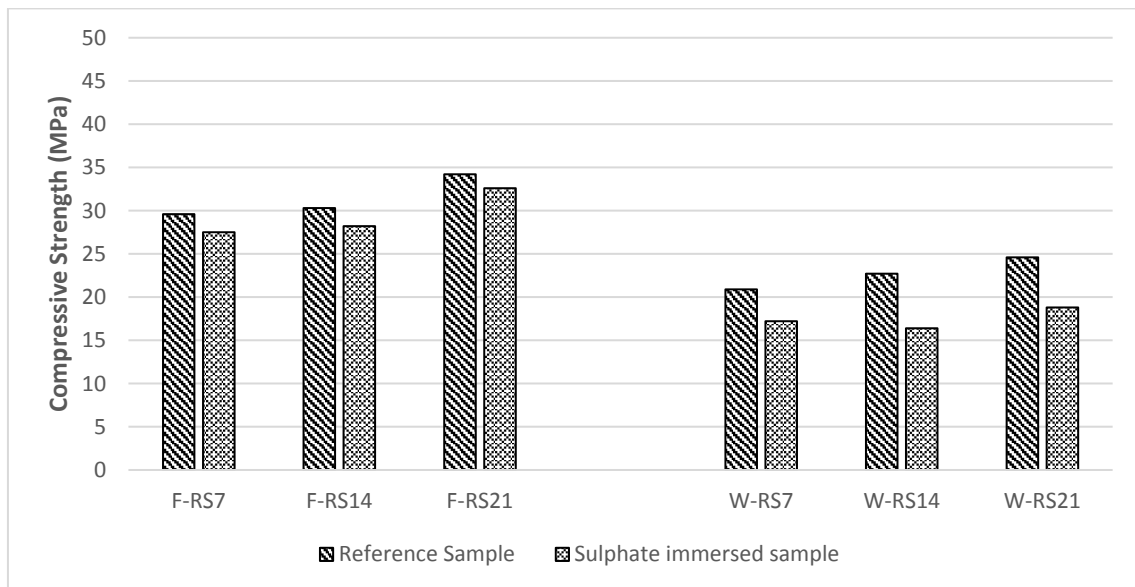


**Figure 4.29.** Compressive strength results of the samples for Resistance to Sulphate

Surface cracks, erosion or spalling were not observed visually in the samples soaked in sodium sulphate solution within the scope of sulphate resistance test. Considering the sample mass presented in Figure 4.28, no significant mass changes in the samples was observed in parallel with no visual degradation. In addition, while a small amount of weight change (approximately average 0.14%) has a tendency to increase in F-coded samples, a small amount of weight change (approximately average 0.1%) has a tendency to decrease in W-coded samples. According to the results presented in Figure 4.29, there was a slight decrease in compressive strength in all concretes immersed in sodium sulfate solution in comparison

to the reference sample. Although sodium sulfate has the potential to act as an alkali activator, there is no increase in compressive strength by not observing geopolymer reactions due to sodium sulfate. According to the studies conducted in the literature to measure Sulphate resistance of geopolymer concretes, the results obtained within the scope of this study remained within acceptable limits and it was concluded that both F-coded and W-coded samples were resistant to sulphate. In this context, studies to analyze the sulfate resistance of geopolymer concrete have also been observed in some previous researches that the sulphate resistance of geopolymer concrete is higher than that of Portland cement concrete (Partha et al., 2013).

#### 4.5.2. The Resistance to Wetting–Drying Cycles

Samples produced to be subjected to the wetting-drying cycle were dried and weighed first after gaining sufficient strength after a week of water curing, then kept in 18 hours of water and 6 hours in a 70 ° C oven every day to measure their mass and compressive strength for 7, 14 and 21 days. In this context, the results of the mass and compressive strength of the samples as a result of the wetting-drying cycles are presented in Figure 4.30 and Figure 4.31, respectively.

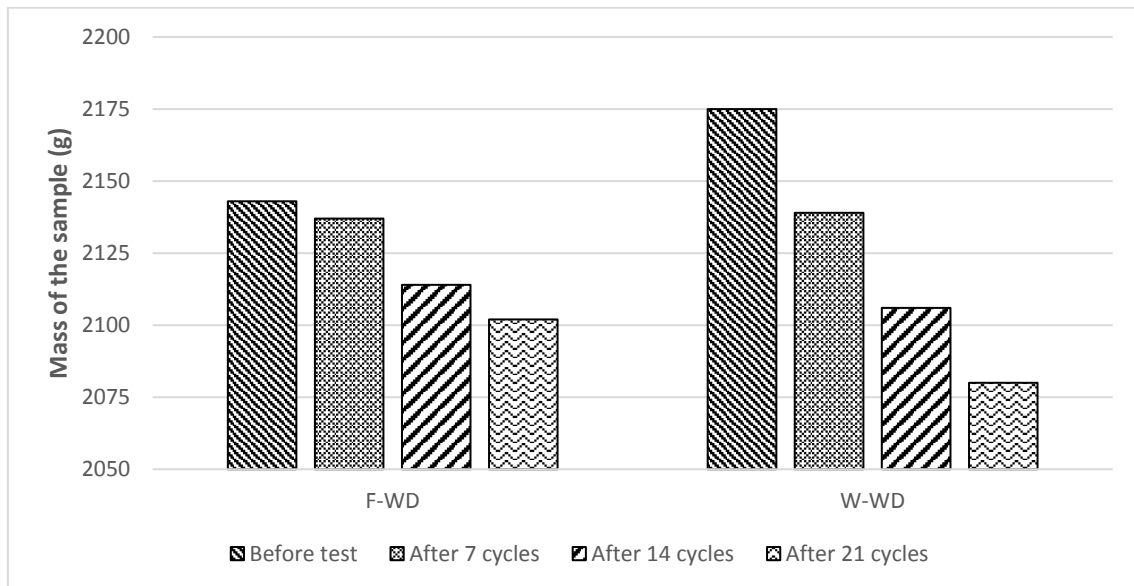


**Figure 4.30.** Masses of the samples for Wetting-Drying Cycles

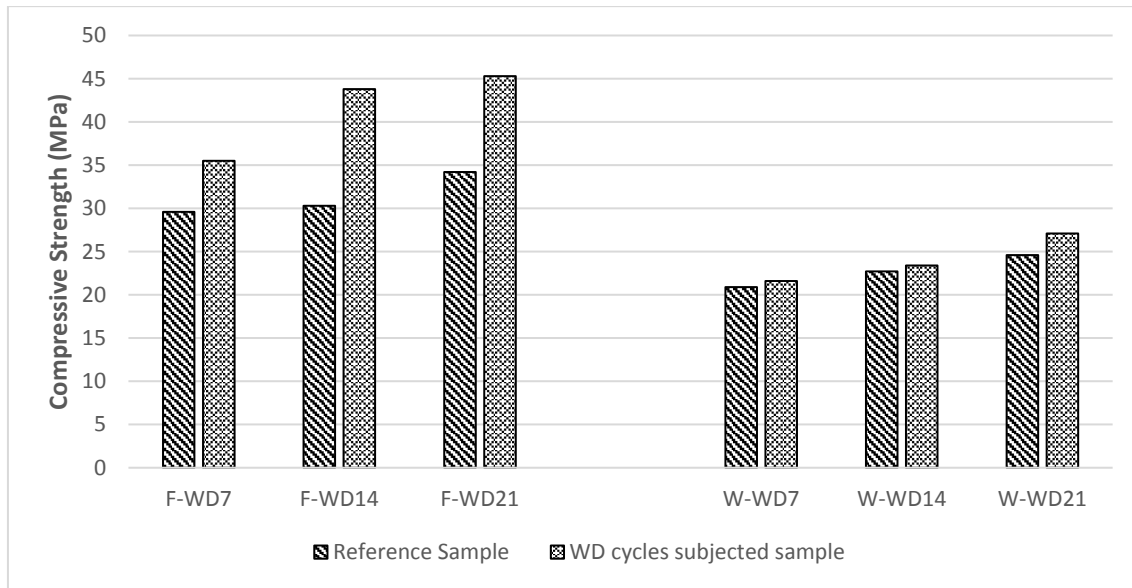


**Figure 4.31.** Compressive strength results of the samples for Wetting-Drying Cycles

In the samples produced within the scope of the wetting-drying experiment, surface cracks were begun to occur at the end of each cycle, and as the number of cycles increased, the number and depth of cracks were increased. These cracks were more apparently observed in W-coded samples compared to F-coded samples. As shown in Figure 4.30, significant mass losses were experienced in samples exposed to the wetting-drying cycle. Nevertheless, according to the results presented in Figure 4.31, despite these negative effects on the visual properties of the samples, their compressive strength increased after the wetting-drying cycles. For samples placed in the oven for 6 hours in each cycle, a temperature of 70 ° C had a positive effect on ongoing reaction kinetics. In this context, the compressive strength of the sample not subjected to the wetting-drying cycle of the mixture coded F-WD21, was 34.2 MPa in 28 days, while the compressive strength of the sample subjected 21 times to the wetting-drying cycle after 7 days of curing was 45.3 MPa. However, the compressive strength changes of W-coded mixtures can be neglected. Consequently, the geopolymer concrete samples, which have been exposed to wetting-drying cycles in extreme conditions, have proved to be resistant to the wetting-drying cycle. However, for a study were done by Şinasi et al. (2020), an increment in compressive strength was observed after the wetting-drying cycles of the geopolymers produced with GBFS and, the researchers stated that the possible reasons for this were the positive effect of the thermal curing process and the fact that the blast furnace slag caught the free chloride ion in the environment and caused an increase in compressive strength over time.

### 4.5.3. Rapid Chloride Permeability Test

Samples produced as cylinders were subjected to RCPT test according to ASTM C 1202 standard at days 7,14,21 and 28 after gaining sufficient strength after a week of water curing. The results of the Coulomb values obtained after the RCPT test are presented in Figure 4.32.

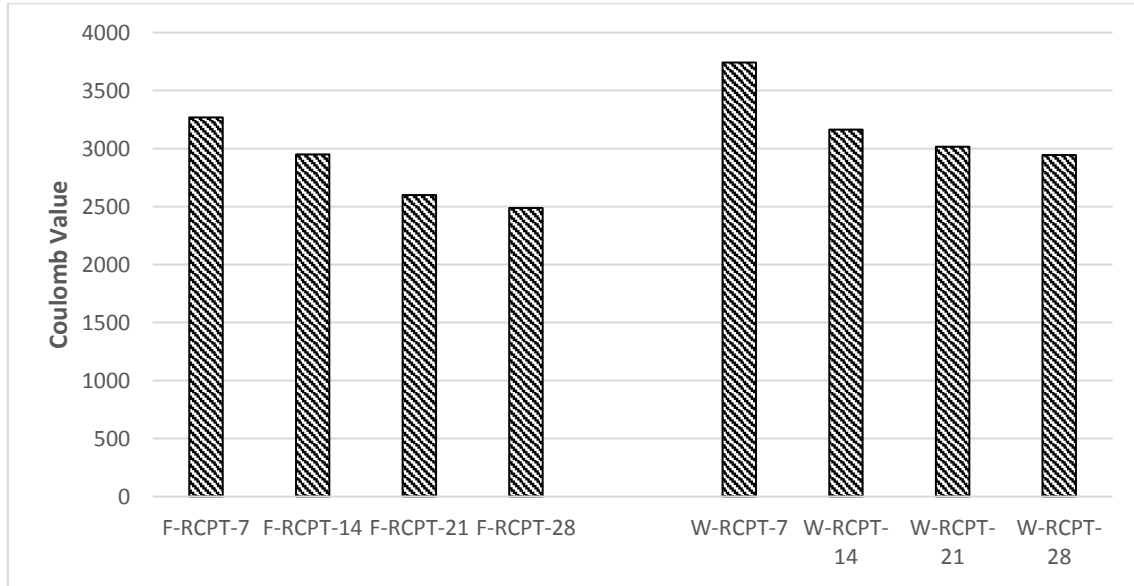


**Figure 4.32.** Coulomb values of the samples for RCPT

As the result of RCPT, the Coulomb values of F-coded samples started from 3269 on the 7th day and decreased to 2488 on the 28th day, while the Coulomb values of the W-coded samples decreased from 3742 on the 7th day to 2944 on the 28th day. Considering the classification of Coulomb values between 2000 and 4000 as moderate and values over 4000 as high in ASTM C 1202 Standard, the values obtained in this study remained within acceptable limits. In addition, Şinasi et al. (2020) found that geopolymer concrete produced with blast furnace slag performed better than Portland cement concrete as a result of RCPT analysis.

### 4.5.4. Sorptivity Test

Samples produced as cylinders were subjected to Sorptivity test according to ASTM C 1585 standards at days 7,14,21 and 28 after gaining sufficient strength after a week of water curing. The results of the absorption values (I) obtained after the sorptivity test are presented in Figure 4.33 for F-coded samples, and Figure 4.34 for W-coded samples.

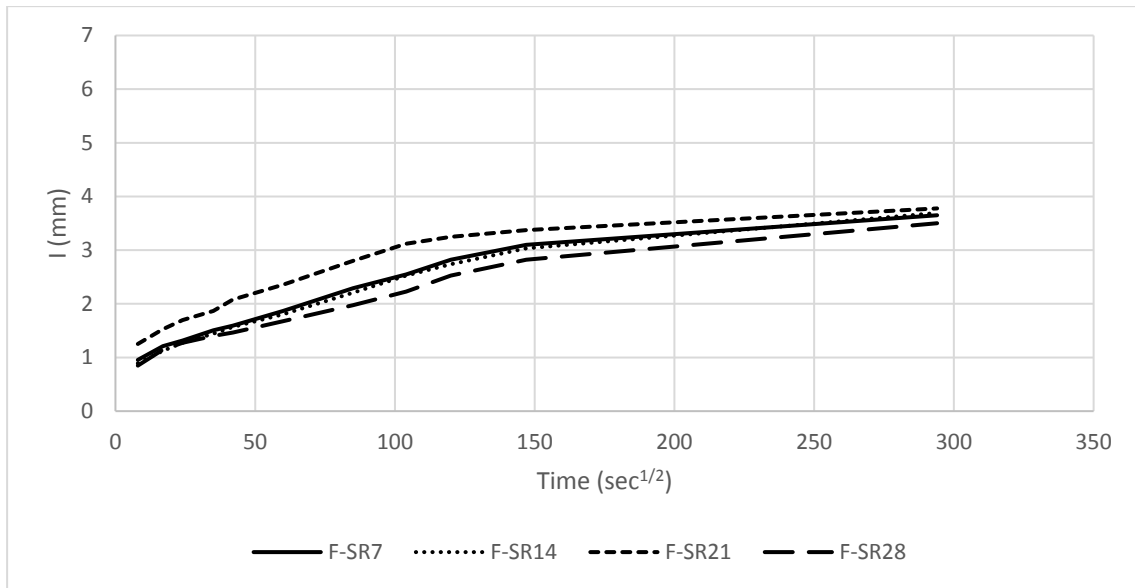


**Figure 4.33.** Absorption results of the F-coded samples for Sorptivity test

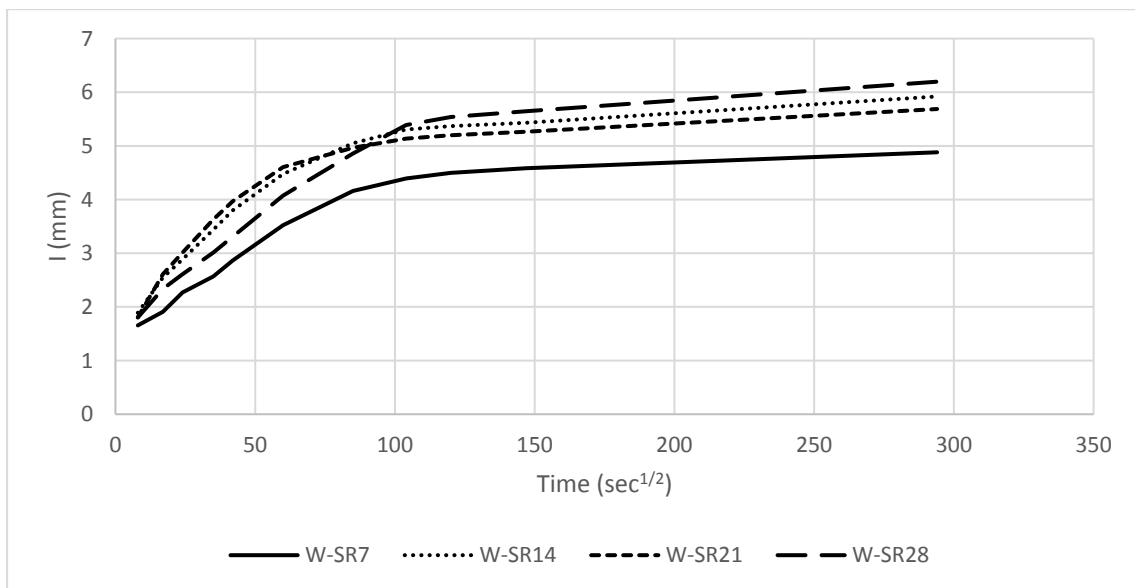


**Figure 4.34.** Absorption results of the W-coded samples for Sorptivity test

Problems such as erosion and efflorescence over time were observed on the surfaces of the samples subjected to the sorptivity test. In general, within the scope of the sorptivity test, while F-coded samples absorb 30 grams of water after 24 hours, this number has reached 45 grams in W-coded samples. According to absorption values of the F-coded samples (Figure 4.33) and W-coded samples (Figure 4.34) at the end of the sorptivity test, the F-coded samples had a lower absorption value than the W-coded samples, which showed that the F-coded samples performed better. Although Portland cement concrete was not produced for



any comparison, Salmabanu and Urvashi (2015) concluded that geopolymer concrete made of fly ash exhibited better performance against absorption than control concrete after the sorptivity test.

## 5. CONCLUSION

Within the scope of the study, it was aimed to develop concrete mixtures by the geopolymerization technology by using the materials obtained from construction and demolition waste (CDW) such as hollow brick (HB) red clay brick (RCB), roof tile (RT), glass waste (GW) and concrete waste (CW). The following conclusions have been drawn on the basis of the experimental research report in the study from the obtaining process of the materials aforementioned to the development of the final product with the desired properties:

- In the production of geopolymer paste with the single use of concrete waste as an aluminosilicate source, the compressive strength of concrete waste prepared with 19M sodium hydroxide solution reached a maximum value of 34.2 MPa after 48 hours of oven curing at 125 °C. Compressive strength value remained at 16.9 MPa as a result of 28 days of curing, and consequently, these results have remained far away from reaching the final product under ambient conditions as one of the most important objectives in the study.
- In the ongoing process, mixtures produced by combining concrete waste with glass waste reached 36.3 MPa compressive strength value after 48 hours of heat curing at 125 °C. The addition of glass waste did not have enough positive effects on mechanical performance was associated with the fact that glass waste had a coarse particle size and was unbalanced in terms of Si/Al ratio, which is one of the most important parameters in the geopolymerization mechanism.
- Within the scope of the development of geopolymer paste mixtures, 53.40 MPa compressive strength was reached after the thermal cure application to the samples produced with various mixtures containing all CDW-based waste materials. According to this result, it was observed that CDW-based waste materials have significant binding capacity in case of optimizing mixing and curing properties.
- In the development of the CDW-based geopolymer mortars, the compressive strengths of the SW series, which are produced based on 100% CDW, remained at a maximum value of 25.4 MPa, and sufficient strength could not be achieved. Afterward, 20% GBFS was added to the mixtures by aiming the formation of stronger structures in the matrix by providing some CSH and CASH gel formation to the geopolymer structure of the addition of calcium-based material in long-term

curing, and their compressive strengths reached quite high values such as 43.2 MPa after 28 days of curing. In another geopolymer mortar mixture series produced by adding calcium hydroxide ( $\text{Ca}(\text{OH})_2$ ) as a tertiary activator to the mixture in order to achieve Si/Al - Ca balance and to obtain a stronger matrix with pozzolanic reactions, the compressive strength results reached a maximum of 51.2 MPa in 28 days ambient curing and with these results, it was achieved a very important point within the scope of developing products that may be an alternative to traditional cemented systems.

- According to the results of the development of geopolymer mortar studies, it is clearly seen that the alkali activator type and concentration have a significant effect on final performance. Samples produced without  $\text{Na}_2\text{SiO}_3$  showed poor performance as a result of a 28-day ambient cure, while the use of relatively high levels of NaOH and  $\text{Na}_2\text{SiO}_3$  also had negative effects on reaction kinetics. In this context, the best results were obtained in cases where the  $\text{Na}_2\text{SiO}_3/\text{NAOH}$  ratio was used as 2 with 8M sodium hydroxide solution.
- In the development of CDW-based geopolymer concrete, the mixtures in which the aggregate amount is equal to the binder amount, the  $\text{Na}_2\text{SiO}_3/\text{NAOH}$  ratio is 2, usage of  $\text{Ca}(\text{OH})_2$ , fly ash and GBFS is %5, %5 and %15, respectively, showed the best performance in terms of compressive strength as 39.6 MPa after 28 days moisture curing. In addition, surface cracks due to drying shrinkage were observed in geopolymer concrete samples and it was concluded that moisture curing and water curing are the most important factors in preventing these cracks. Also in the case of water curing which can causes to a high amount of compressive strength losses and degradation of samples, the addition of fly ash and GBFS had a positive effect on the stabilization of concretes.
- SEM / EDX and XRD analyzes were performed on various samples produced during the study and it was observed that smoother, homogeneous and crack-free structures were formed in SEM images of the high performing samples. The chemical composition of the structures formed in the geopolymer matrix was observed by EDX analysis, and the atomic structure of the mixtures with higher compressive strength was found to be more stable in terms of NASH and CASH gel compositions. In addition, as a result of XRD analysis, it was observed that various phases in the precursor (eg quartz, dolomite, kyanite) decreased as a result of geopolymer reactions and various new phases (eg calcite, NASH gel) were formed. These kinds of changes

and decreases are associated with the dissolution and polycondensation stages of precursors to form a geopolymer product.

- In the durability studies of CDW-based geopolymer concretes, after sulphate immersion of samples in order to measure the resistance of sulphate, a negligible quantity increment on the mass of samples and slightly decrease on compressive strength of samples was observed. As a result of exposure of the samples to the wetting-drying cycle, although some crack formation was observed on the sample surface, the thermal curing process applied during drying stage had a positive effect on the compressive strength of the samples. It was also observed that the developed geopolymer concrete samples were within the acceptable limits comparing to the structural concrete properties as a result of RCPT and sorptivity tests. After a series of durability tests conducted, it was concluded that the developed geopolymer concrete samples are durable as much as the conventional cemented concrete against environmental conditions.
- Overall, the excessive consumption of raw materials and excessive CO<sub>2</sub> emissions that affect negatively the environment and the climate, which a major issue in all countries of the world in recent years, have become an inevitable necessity to minimized. Considering the damages of traditional Portland cement to the environment, the development of eco-friendly "green" building materials will be a very important objective for future generations as well as today. In this context, with this thesis prepared after comprehensive studies, CDW-based geopolymer concrete mixtures that provide the opportunity to minimize these damages and having properties equivalent to conventional concrete in terms of mechanical, micro-mechanical and durability properties have been developed. The most significant result of this analysis is that the final product, which developed in order to reduce damage to the atmosphere and debris pollution generated last years, will be used in building systems in large-scale in the following years.

## REFERENCES

- Abbas A, Fathifazl G, Isgor OB, Razaqpur AG, Fouriner B, Foo S. Environmental benefits of green concrete. *EIC Clim Change Technol 2006 IEEE*; 10–12 May **2006**:1–8.
- Ahmari, S., Ren, X., Toufigh, V., & Zhang, L. (2012). Production of geopolymeric binder from blended waste concrete powder and fly ash. *Construction and Building Materials*, 35, 718-729.
- Allahverdi, A., & Kani, E. N. (2009). Construction wastes as raw materials for geopolymer binders. *International Journal of Civil Engineering*, 7(3), 154-160.
- Allahverdi, A., & Kani, E. N. (2013). Use of construction and demolition waste (CDW) for alkali-activated or geopolymer cements. In *Handbook of recycled concrete and demolition waste* (pp. 439-475). Woodhead Publishing.
- Allahverdi, Ali & Najafi, Ebrahim. (2009). Construction Wastes as Raw Materials for Geopolymer Binders. *International Journal of Civil Engineering*. 7. 154-160.
- Arslan, H, Salgın, B, & Coşgun, N .2012. Construction and demolition waste management in Turkey. INTECH Open Access Publisher.
- Badogiannis, E., Kakali, G. and Tsivilis, S. (2005) Metakaolin as supplementary cementitious material. Optimization of kaolin to metakaolin conversion. *Journal of Thermal Analysis and Calorimetry*, 81, 457–462. doi: 10.1007/s10973-005-0806-3.
- Bai, Y., Collier, N., Milestone, N. and Yang, C.: The potential for using slags activated with near neutral salts as immobilisation matrices for nuclear wastes containing reactive metals. *J. Nucl. Mater.* 413(3), 183-192 (2011)
- Barrer, R. M. and Mainwaring, D. E. (1972a) Chemistry of soil minerals. Part XI . Hydrothermal transformations of metakaolinite in potassium hydroxide. *Journal of the Chemical Society – Dalton Transactions*, 1254–1265. doi: 10.1039/DT9720001254.
- Barrer, R. M. and Mainwaring, D. E. (1972b) Chemistry of soil minerals. Part XIII . Reactions of metakaolinite with single and mixed bases. *Journal of the Chemical Society – Dalton Transactions*, 2534–2546. doi: 10.1039/DT9720002534.
- Bell, J. L., Sarin, P., Provis, J. L., Haggerty, R. P., Driemeyer, P. E., Chupas, P. J., van Deventer, J. S. J. and Kriven, W. M. (2008) Atomic structure of a cesium aluminosilicate geopolymer: A pair distribution function study, *Chemistry of Materials*, 20, 4768–4776.
- Ben Haha, M., Le Saout, G., Winnefeld, F. and Lothenbach, B.: Influence of activator type on hydration kinetics, hydrate assemblage and microstructural development of alkali activated blast-furnace slags. *Cem. Concr. Res.* 41(3), 301- 310 (2011)

- Ben Haha, M., Le Saout, G., Winnefeld, F. and Lothenbach, B.: Influence of activator type on hydration kinetics, hydrate assemblage and microstructural development of alkali activated blast-furnace slags. *Cem. Concr. Res.* 41(3), 301- 310 (2011)
- Palacios, M. and Puertas, F.: Effectiveness of mixing time on hardened properties of waterglass-activated slag pastes and mortars. *ACI Mater. J.* 108(1), 73-78 (2011)
- Ben Haha, M., Lothenbach, B., Le Saout, G. and Winnefeld, F.: Influence of slag chemistry on the hydration of alkali-activated blast-furnace slag — Part II: Effect of Al<sub>2</sub>O<sub>3</sub>. *Cem. Concr. Res.* 42(1), 74-83 (2012)
- Ben Haha, M., Lothenbach, B., Le Saout, G. and Winnefeld, F.: Influence of slag chemistry on the hydration of alkali-activated blast-furnace slag -- Part I: Effect of MgO. *Cem. Concr. Res.* 41(9), 955-963 (2011)
- Benharrats, N., Belbachir, M., Legrand, A.P. and D’Espinose de la Caillerie, J.-B.: <sup>29</sup>Si and <sup>27</sup>Al MAS NMR study of the zeolitization of kaolin by alkali leaching. *Clay Miner.* 38(1), 49-61 (2003)
- Bernal, S. A., de Gutiérrez, R. M., & Provis, J. L. (2012). Engineering and durability properties of concretes based on alkali-activated granulated blast furnace slag/metakaolin blends. *Construction and Building Materials*, 33, 99-108.
- Bernal, S.A., Provis, J.L., Mejía de Gutierrez, R. and Rose, V.: Evolution of binder structure in sodium silicate-activated slag-metakaolin blends. *Cem. Concr. Compos.* 33(1), 46-54 (2011)
- Bernal, S.A., Provis, J.L., Walkley, B., San Nicolas, R., Gehman, J.D., et al. 2013. Gel nanostructure in alkaliactivated binders based on slag and fly ash, and effects of accelerated carbonation. *Cem. Concr. Res.* 53:127–44
- Bernal, S.A., Skibsted, J. and Herfort, D.: Hybrid binders based on alkali sulfateactivated Portland clinker and metakaolin. In: Palomo, A., (ed.) XIII International Congress on the Chemistry of Cement, Madrid. CD-ROM proceedings. (2011)
- Bingöl, Ş., Bilim, C., Atiş, C. D., & Durak, U. (2020). Durability Properties of Geopolymer Mortars Containing Slag. *Iranian Journal of Science and Technology, Transactions of Civil Engineering*, 1-9.
- Bortnovsky, O., Dědeček, J., Tvarůžková, Z., Sobalík, Z. and Šubrt, J.: Metal ions as probes for characterization of geopolymer materials. *J. Am. Ceram. Soc* 91(9), 3052-3057 (2008)
- Brindle, J. H. and McCarthy, M. J. (2006) Chemical constraints on fly ash glass compositions. *Energy and Fuels*, 20, 2580–2585. doi:10.1021/ef0603028.
- Brouwers, H. J. H. and van Eijk, R. J. (2002) Fly ash reactivity: Extension and application of a shrinking core model and thermodynamic approach. *Journal of Materials Science*, 37, 2129–2141. doi:10.1023/A:1015206305942.
- BS 8500-2 (2002), Concrete—complementary British Standard to BS EN 206-1, part 2: specification for constituent materials and concrete. British Standards Institution.

- C.L. Sabine, R.A. Feely, N. Gruber, R.M. Key, K. Lee, J.L. Bullister, et al. The oceanic sink for anthropogenic CO<sub>2</sub> *Science*, 305 (16 July **2004**), pp. 367-371
- Cheng, Q. H., Tagnit-Hamou, A. ve Sarkar, S. L. (**1992**). Strength and microstructural properties of waterglass activated slag. *Materials Research Society Symposium Proceedings*, 245, 49–54.
- Cheng-Yi, H., Feldman, R.F. (**1985**) Hydration reactions in Portland cement– silica fume blend. *Cem Concr Res* 15:585–592
- Chindapasirt, P., Chareerat, T. and Sirivivatnanon, V. (**2007**) Workability and strength of coarse high calcium fly ash geopolymer. *Cement and Concrete Composites*, 29, 224–229. doi:10.1016/j.cemconcomp.2006.11.002.
- Cho, H., Felmy, A.R., Craciun, R., Keenum, J.P., Shah, N. and Dixon, D.A.: Solution state structure determination of silicate oligomers by <sup>29</sup>Si NMR spectroscopy and molecular modeling. *J. Am. Chem. Soc.* 128(7), 2324-2335 (**2006**)
- Cohen, M.D., Bentur, A. (**1988**) Durability of Portland cement–silica fume pastes in magnesium sulfate and sodium sulfate solutions. *ACI Mater J* 85(3):148–157
- Collins, F. ve Sanjayan, J. G. (**2001**). Microcracking and strength development of alkali-activated slag concrete. *Cement and Concrete Composites*, 23 (4-5), 345–352.
- Corinaldesi V., Moriconi G. (**2009b**), “Influence of mineral additions on the performance of 100 % recycled aggregate concrete. *Constr Build Mater* 23(8):2869–2876.
- Costa U, Ursella P (**2003**) Construction and demolition waste recycling in Italy, WASCON 2003—Progress on the road to sustainability. San Sebastian, Spain, pp 231–239
- Criado, M., Fernandez-Jimenez, A., de la Torre, A.G., Aranda, M.A.G., Palomo, A. **2007**. An XRD study of the effect of the SiO<sub>2</sub>/Na<sub>2</sub>O ratio on the alkali activation of fly ash. *Cem. Concr. Res.* 37:671–79
- Criado, M., Fernández-Jiménez, A., de la Torre, A.G., Aranda, M.A.G. and Palomo, A.: An XRD study of the effect of the SiO<sub>2</sub>/Na<sub>2</sub>O ratio on the alkali activation of fly ash. *Cem. Concr. Res.* 37(5), 671-679 (**2007**) 29
- Criado, M., Fernandez-Jimenez, A., Palomo, A., Sobrados, I., Sanz, J.. **2008**. Alkali activation of fly ash. Effect of the SiO<sub>2</sub>/Na<sub>2</sub>O ratio. Part II. <sup>29</sup>Si MAS-NMR survey. *Microporous Mesoporous Mater.* 109:525–34
- Criado, M., Palomo, A. and Fernández-Jiménez, A.: Alkali activation of fly ashes. Part 1: Effect of curing conditions on the carbonation of the reaction products. *Fuel* 84(16), 2048-2054 (**2005**)
- Criado, M., Palomo, A., Fernández-Jiménez, A. **2005**. Alkali activation of fly ashes. Part 1. Effect of curing conditions on the carbonation of the reaction products. *Fuel* 84:2048–54
- Davidovits, J. (**1982**) Mineral polymers and methods of making them, US Patent 4,349,386.

- Davidovits, J. (1982a) The need to create a new technical language for the transfer of basic scientific information. Transfer and Exploitation of Scientific and Technical Information, EUR 7716. Luxembourg, Commission of the European Communities.
- Davidovits, J. (1991) Geopolymers – Inorganic polymeric new materials. *Journal of Thermal Analysis*, 37, 1633–1656. doi:10.1007/BF01912193.
- Davidovits, J. (1993) Geopolymer cements to minimize carbon-dioxide green house warming. *Ceram Trans* 37:165–82
- Davidovits, J. (2008) *Geopolymer Chemistry and Applications*, Saint-Quentin, France, Institut Géopolymère.
- Davidovits, J.: Geopolymers - Inorganic polymeric new materials. *J. Therm. Anal.* 37(8), 1633-1656 (1991)
- De Juan M.S., Gutiérrez P.A. (2009), “Study on the influence of attached mortar content on the properties of recycled concrete aggregate” *Constr Build Mater* 23(2):872–877.
- Deb, P., Nath, P., & Sarker, P. (2013). Sulphate Resistance of Slag Blended Fly Ash Based Geopolymer Concrete. In *Concrete 2013: Proceedings of the 26th Biennial National Conference of the Concrete Institute of Australia*. Concrete Institute of Australia.
- Demortier, A., Gobeltz, N., Lelieur, J.P. and Duhayon, C.: Infrared evidence for the formation of an intermediate compound during the synthesis of zeolite Na-A from metakaolin. *Int. J. Inorg. Mater.* 1(2), 129-134 (1999)
- Duran Atış C., Bilim C., Çelik Ö. and Karahan, O. (2009), ‘Influence of activator on the strength and drying shrinkage of alkali-activated slag mortar’, *Constr. Build. Mater.* 23(1), 548–555.
- Duxson, P. and Provis, J. L. (2008) Designing precursors for geopolymer cements. *Journal of the American Ceramic Society*, 91, 3864–3869. doi:10.1111/j.1551–2916.2008.02787.x
- Duxson, P., Lukey, G.C., Separovic, F. and van Deventer, J.S.J.: The effect of alkali cations on aluminum incorporation in geopolymeric gels. *Ind. Eng. Chem. Res.* 44(4), 832-839 (2005)
- Duxson, P., Mallicoat, S. W., Lukey, G. C., Kriven, W. M. and van Deventer, J. S. J. (2007b) The effect of alkali and Si/Al ratio on the development of mechanical properties of metakaolin-based geopolymers. *Colloids and Surfaces A – Physicochemical and Engineering Aspects*, 292, 8–20. doi:10.1016/j.colsurfa.2006.05.044.
- Duxson, P., Mallicoat, S.W., Lukey, G.C., Kriven, W.M. and van Deventer, J.S.J.: The effect of alkali and Si/Al ratio on the development of mechanical properties of metakaolin-based geopolymers. *Colloids Surf. A* 292(1), 8-20 (2007)
- Duxson, P., Provis, J. L., Lukey, G. C., Mallicoat, S. W., Kriven, W. M. and van Deventer, J. S. J. (2005b) Understanding the relationship between geopolymer composition, microstructure and mechanical properties. *Colloids and Surfaces A –*



Physicochemical and Engineering Aspects, 269, 47–58.  
doi:10.1016/j.colsurfa.2005.06.060.

- Duxson, P., Provis, J.L., Lukey, G.C., Mallicoat, S.W., Kriven, W.M. and van Deventer, J.S.J.: Understanding the relationship between geopolymer composition, microstructure and mechanical properties. *Colloids Surfaces A* 269(1-3), 47-58 (2005)
- Duxson, P., Provis, J.L., Lukey, G.C., van Deventer, J.S.J., Separovic, F. and Gan, Z.H.: <sup>39</sup>K NMR of free potassium in geopolymers. *Ind. Eng. Chem. Res.* 45(26), 9208-9210 (2006)
- Engelhardt, G., Jancke, H., Hoebbel, D. and Wieker, W.: Strukturuntersuchungen an Silikatanionen in wäßriger Lösung mit Hilfe der <sup>29</sup>Si-NMR-Spektroskopie. *Z. Chemie* 14(3), 109-110 (1974)
- Escalante-Garcia, J., Fuentes, A.F., Gorokhovskiy, A., Fraire-Luna, P.E. and Mendoza-Suarez, G.: Hydration products and reactivity of blast-furnace slag activated by various alkalis. *J. Am. Ceram. Soc.* 86(12), 2148-2153 (2003)
- Etxeberria M., Mari A., Vázquez E. (2007a), “Recycled aggregate concrete as structural material” *Mater Struct* 40(5):529–541.
- Feng, D., Tan, H. and van Deventer, J. S. J. (2004) Ultrasound enhanced geopolymerisation. *Journal of Materials Science*, 39, 571–580. doi: 10.1023/B:JMSC.0000011513.87316.5c.
- Fernández-Jiménez A. (2000), ‘Cementos de escorias activadas alcalinamante: influencia de las variables y modelización del proceso’, PhD Thesis, Universidad Autónoma de Madrid, Spain.
- Fernández-Jiménez A. and Palomo A. (2003), ‘Characterisation of fly ashes: potential reactivity as alkaline cements’, *Fuel* 82, 2259–2265.
- Fernández-Jiménez, A. and Palomo, A.: Mid-infrared spectroscopic studies of alkali-activated fly ash structure. *Micropor. Mesopor. Mater.* 86(1-3), 207-214 (2005)
- Fernández-Jiménez, A. and Puertas, F.: Alkali-activated slag cements: Kinetic studies. *Cem. Concr. Res.* 27(3), 359-368 (1997)
- Fernández-Jiménez, A. and Puertas, F.: Alkali-activated slag cements: Kinetic studies. *Cem. Concr. Res.* 27(3), 359-368 (1997)
- Fernández-Jiménez, A. and Puertas, F.: Effect of activator mix on the hydration and strength behaviour of alkali-activated slag cements. *Adv. Cem. Res.* 15(3), 129-136 (2003)
- Fernández-Jiménez, A., Palomo, A. and Criado, M.: Alkali activated fly ash binders. A comparative study between sodium and potassium activators. *Mater. Constr.* 56(281), 51-65 (2006)
- Fernandez-Jimenez, A., Palomo, A.. 2005. Mid-infrared spectroscopic studies of alkali-activated fly ash structure. *Microporous Mesoporous Mater.* 86:207–14

- Fernández-Jiménez, A., Puertas, F. and Arteaga, A.: Determination of kinetic equations of alkaline activation of blast furnace slag by means of calorimetric data. *J. Thermal Anal. Calorim.* 52(3), 945-955 (1998)
- Fernández-Jiménez, A., Puertas, F., Sobrados, I. and Sanz, J.: Structure of calcium silicate hydrates formed in alkaline-activated slag: Influence of the type of alkaline activator. *J. Am. Ceram. Soc.* 86(8), 1389-1394 (2003)
- Ferreira L., de Brito J., Barra M. (2011), "Influence of pre-saturation of recycled coarse concrete aggregates on structural concretes mechanical and durability properties" *Mag Concr Res* 63(8):617–627.
- Fonseca N., de Brito J., Evangelista L. (2011), The influence of curing conditions on the mechanical performance of concrete made with recycled concrete waste" *Cem Concr Compos* 33(6):637–643.
- Franklin Associates (ed) (1998) Characterization of building-related construction and demolition debris in the United States, Report No. EPA530-R-98-010, prepared for the U.S. Environmental Protection Agency, Municipal and Industrial Solid Waste Division, Office of Solid Waste, USA
- Frondistou-Yannas, S. (1977) "Waste concrete as aggregate for new concrete." *Journal Proceedings*. Vol. 74. No. 8.
- Gartner, E.: Industrially interesting approaches to "low-CO<sub>2</sub>" cements. *Cem. Concr. Res.* 34(9), 1489-1498 (2004)
- Glukhovsky, V.D.: Ancient, modern and future concretes. In: Krivenko, P.V., (ed.) *Proceedings of the First International Conference on Alkaline Cements and Concretes*, Kiev, Ukraine. Vol. 1, pp. 1-9. VIPOL Stock Company (1994)
- Goberis, S., & Antonovich, V. (2004). Influence of sodium silicate amount on the setting time and EXO temperature of a complex binder consisting of high-aluminate cement, liquid glass and metallurgical slag. *Cement and concrete research*, 34(10), 1939-1941.
- Gomes, S. and François, M. (2000) Characterization of mullite in silicoaluminous fly ash by XRD, TEM, and <sup>29</sup>Si MAS NMR. *Cement and Concrete Research*, 30, 175–181. doi:10.1016/S0008-8846(99)00226-4.
- Gonzalez-Fonteboia B, Martinez-Abella F (2008) Concretes with aggregates from demolition waste and silica fume: materials and mechanical properties. *Build Environ* 43(4):429–437
- Granizo, M. L. and Blanco, M. T. (1998) Alkaline activation of metakaolin – An isothermal conduction calorimetry study. *Journal of Thermal Analysis*, 52, 957–965. doi:10.1023/A:1010176321136
- Granizo, M. L., Blanco Varela, M. T. and Martínez-Ramírez, S. (2007) Alkali activation of metakaolins: Parameters affecting mechanical, structural and microstructural

- properties. *Journal of Materials Science*, 42, 2934–2943. doi: 10.1007/s10853-006-0565-y.
- Hack, D. R., & Bryan, D. P. (2006). *Aggregates. Industrial Minerals and Rocks*, Kogel EK, Trivedi NC, Barker JM, Krukowski ST (eds), 7th Edition, Littleton, Colorado, Society for Mining, Metallurgy and Exploration, 1105-1119.
- Hajimohammadi, A., Provis, J.L. and van Deventer, J.S.J.: Time-resolved and spatially-resolved infrared spectroscopic observation of seeded nucleation controlling geopolymer gel formation. *J. Colloid Interf. Sci.* 357(2), 384-392 (2011)
- Hajimohammadi, A., Provis, J.L., van Deventer, J.S.J. 2010. The effect of alumina release rate on the mechanism of geopolymer gel formation. *Chem. Mater.* 22:5199–208
- Halasz, I., Agarwal, M., Li, R. and Miller, N.: Monitoring the structure of water soluble silicates. *Catal. Today* 126, 196-202 (2007)
- Halasz, I., Agarwal, M., Li, R.B. and Miller, N.: What can vibrational spectroscopy tell about the structure of dissolved sodium silicates? *Microporous Mesoporous Mater.* 135(1-3), 74-81 (2010)
- Hansen T.C., Narud H. (1983), “Strength of recycled concrete made from crushed concrete coarse aggregate” *Concr Int* 5(1):79–83.
- Heller-Kallai, L. and Lapides, I.: Reactions of kaolinites and metakaolinites with NaOH - comparison of different samples (Part 1). *Appl. Clay Sci.* 35, 99-107 (2007)
- Hemmings, R. T. and Berry, E. E. (1988) On the glass in coal fly ashes: Recent advances. *Fly Ash and Coal Conversion By-Products: Characterization, Utilization, and Disposal IV*, Warrendale, PA, Mccarthy, G. J. (Ed.), 3–38.
- Hendriks, C. A., Worrell, E., De Jager, D., Blok, K., & Riemer, P. (1998, August). Emission reduction of greenhouse gases from the cement industry. In *Proceedings of the fourth international conference on greenhouse gas control technologies* (pp. 939-944). Interlaken, Austria, IEA GHG R&D Programme.
- Henry, J., Towler, M. R., Stanton, K. T., Querol, X. and Moreno, N. (2001) Characterisation of the glass fraction of a selection of European coal fly ashes. *Journal of Chemical Technology and Biotechnology*, 79, 540–546.
- Higgins, D. (1991) The historical development of GGBS. *Concrete*, 25, 7-9.
- JZ, Li P, Qin W. Study on bond–slip between recycled aggregate concrete and rebars. *J Tongji Univ* 2006 34:13–6 [in Chinese].
- Katz A (2003) Properties of concrete made with recycled aggregate from partially hydrated old concrete. *Cem Concr Res* 33(5):703–711
- Keyte, L. M., Lukey, G. C. and van Deventer, J. S. J. (2005) The effect of coal ash glass chemistry on the tailored design of waste-based geopolymeric products. *WasteEng 2005*, Albi, France, Nzihou, A. (Ed.), CD-ROM proceedings.

- Khan, M. I., & Siddique, R. (2011). Utilization of silica fume in concrete: Review of durability properties. *Resources, Conservation and Recycling*, 57, 30–35. doi:10.1016/j.resconrec.2011.09.016
- Khater, H. M. (2013). Effect of silica fume on the characterization of the geopolymer materials. *International Journal of Advanced Structural Engineering*, 5(1), 12.
- Klemm, W. A. (1989) Cementitious materials: historical notes. In J. P. Skalny (ed.), *Materials Science of Concrete /*, The American Ceramic Society, Westerville, pp. 1-26.
- Knight, C.T.G., Balec, R.J. and Kinrade, S.D.: The structure of silicate anions in alkaline solutions. *Angew. Chem. Int. Ed.* 46, 8148-8152 (2007)
- Komnitsas, K., & Zaharaki, D. (2015). Co-utilization of construction and demolition with industrial wastes for the production of geopolymer. In *Inter. Conference on Industrial Waste & Wastewater Treatment & Valorization*, President Hotel, Athens (pp. 21-23).
- Komnitsas, K., Zaharaki, D., Vlachou, A., Bartzas, G., & Galetakis, M. (2015). Effect of synthesis parameters on the quality of construction and demolition wastes (CDW) geopolymers. *Advanced Powder Technology*, 26(2), 368-376.
- Kriven, W. M., Bell, J. L. and Gordon, M. (2003) Microstructure and microchemistry of fully-reacted geopolymers and geopolymer matrix composites. *Ceramic Transactions*, 153, 227–250.
- Kurt, C. and Bittner, J.: Sodium hydroxide. In: *Ullmann's Encyclopedia of Industrial Chemistry*, Wiley-VCH Verlag (2006)
- Lampris, C., Lupo, R., & Cheeseman, C. R. (2009). Geopolymerisation of silt generated from construction and demolition waste washing plants. *Waste Management*, 29(1), 368-373.
- Lippiatt, B., & Ahmad, S. (2004, May). Measuring the life-cycle environmental and economic performance of concrete: the BEES approach. In *Proceedings of the International Workshop on Sustainable Development and Concrete Technology* (pp. 213-230).
- Lloyd, R. R. (2008) PhD Thesis, Department of Chemical and Biomolecular Engineering, University of Melbourne, Australia.
- Lloyd, R.R., Provis, J.L., Smeaton, K.J. and van Deventer, J.S.J.: Spatial distribution of pores in fly ash-based inorganic polymer gels visualised by Wood's metal intrusion. *Micropor. Mesopor. Mater.* 126(1-2), 32-39 (2009)
- Luhar, S., & Khandelwal, U. (2015). Durability studies of fly ash based geopolymer concrete. *Int. J. Eng. Res. Appl.*, 5(8–4), 17-32.
- Lukey, G. C., Mendis, P. A., van Deventer, J. S. J. and Sofi, M. (2006) Advances in inorganic polymer concrete technology. In Day, K. W. (Ed.) *Concrete Mix Design, Quality Control and Specification*, 3rd Edition. London, Routledge.

- Maage, M. (1989) Efficiency factors for condensed silica fume in concrete. In: Third international conference on fly ash, silica fume, slag and natural pozzolans in concrete, Trondheim, Norway, 1989. American Concrete Institute Publication SP 114-70, Detroit
- Mackenzie, K. J. D. (2003) What are these things called geopolymers? A physico-chemical perspective. *Ceramic Transactions*, 153, 175–186.
- MacKenzie, K. J. D., Brown, I. W. M., Meinhold, R. H. and Bowden, M. E. (1985) Outstanding problems in the kaolinite-mullite reaction sequence investigated by  $^{29}\text{Si}$  and  $^{27}\text{Al}$  solid-state nuclear magnetic resonance: I. Metakaolinite. *Journal of the American Ceramic Society*, 68, 293–297. doi: 10.1111/j.1151-2916.1985.tb15228.x.
- Malhotra, V. M. (1976), “Use of recycled concrete as a new aggregate” Energy, Mines and Resources Canada.
- Milestone, N.B.: Reactions in cement encapsulated nuclear wastes: Need for toolbox of different cement types. *Adv. Appl. Ceram.* 105(1), 13-20 (2006)
- Mills T.H, Showalter E, Jarman D. (1999) A Cost Effective Waste Management Plan. *Cost Engineering* 41 (3): 35–43.
- Monnin, C. and Dubois, M.: Thermodynamics of the  $\text{LiOH}+\text{H}_2\text{O}$  system. *J. Chem. Eng. Data* 50(4), 1109-1113 (2005)
- Myers R.J., Bernal S.A., San Nicolas R. and Provis J.L. (2013), ‘Generalized structural description of calcium–sodium aluminosilicate hydrate gels: the cross-linked substituted tobermorite model’, *Langmuir*, 29, 5294–5306.
- Nagataki S, Gokce A, Saeki T (2000), “Effects of recycled aggregate characteristics on the performance parameters of recycled aggregate concrete” In: Proceedings of the fifth CANMET/ACI international conference on durability of concrete, Barcelona, pp 51–71.
- Nagataki S, Gökçe A, Saeki T, Hisada M (2004), “Assessment of recycling process induced damage sensitivity of recycled concrete aggregates” *Cem Concr Res* 34(6):965–971.
- Najafi Kani E , Allahverdi A and Provis J L ( 2012 ), ‘ Efflorescence control in geopolymer binder based on natural pozzolan ‘, *Cement and Concrete Composites* , 34 ( 1 ), 25 – 33 .
- Neville, A. (1975) *High Alumina Cement Concrete*, John Wiley & Sons, New York.
- Nocuń-Wczelik, W.: Heat evolution in alkali activated synthetic slag–metakaolin mixtures. *J. Thermal Anal. Calorim.* 86(3), 739-743 (2006)
- Nordström, J., Nilsson, E., Jarvol, P., Nayeri, M., Palmqvist, A., Bergenholtz, J. and Matic, A.: Concentration- and pH-dependence of highly alkaline sodium silicate solutions. *J. Colloid Interf. Sci.* 356(1), 37-45 (2011)
- Nugteren, H. W. (2007) Coal fly ash: From waste to industrial product. *Particle and Particle Systems Characterisation*, 24, 49–55. doi:10.1002/ppsc.200601074.

- Oh, J.E., Monteiro, P.J.M., Jun, S.S., Choi, S. and Clark, S.M.: The evolution of strength and crystalline phases for alkali-activated ground blast furnace slag and fly ash-based geopolymers. *Cem. Concr. Res.* 40(2), 189-196 (2010)
- Oliveira MB, Vázquez E (1996), "The influence of retained moisture in aggregates from recycling on the properties of new hardened concrete" *Waste Manage (Oxf)* 16(1–3):113–117.
- Oyler, D.C. Use of a sodium silicate gel grout for plugging horizontal methane drainage holes. Vol. 8843. US Dept. of the Interior, Bureau of Mines, 1984.
- P. De Silva, K. Sagoe-Crenstil, V. Sirivivatnanon, Kinetics of geopolymerization: Role of Al<sub>2</sub>O<sub>3</sub> and SiO<sub>2</sub>, *Cem. Concr. Res.* 37 (2007) 512–518.
- Pacheco-Torgal, F., & Jalali, S. (2010). Reusing ceramic wastes in concrete. *Construction and Building Materials*, 24(5), 832-838.
- Palomo, A., Alonso, S., Fernández-Jiménez, A., Sobrados, I., Sanz, J. 2004. Alkaline activation of fly ashes:
- Palomo, A. and Glasser, F. P. (1992) Chemically-bonded cementitious materials based on metakaolin. *British Ceramic Transactions and Journal*, 91, 107–112.
- Palomo, A., Alonso, S., Fernández-Jiménez, A., Sobrados, I. and Sanz, J.: Alkaline activation of fly ashes: NMR study of the reaction products. *J. Am. Ceram. Soc.* 87(6), 1141-1145 (2004)
- Palomo, A., Banfill, P.F.G., Fernández-Jiménez, A. and Swift, D.S.: Properties of alkali-activated fly ashes determined from rheological measurements. *Adv. Cem. Res.* 17(4), 143-151 (2005)
- Palomo, A., Macias, A., Blanco, M.T. and Puertas, F.: Physical, chemical and mechanical characterisation of geopolymers. In: *Proceedings of the 9th International Congress on the Chemistry of Cement*, New Delhi, India. Vol. 5, pp. 505-511. National Council for Cement and Building Materials (1992)
- Patel, S and Patel CG. 2016. "Cost Optimization of The Project by Construction Waste Management." *International Research Journal of Engineering and Technology (IRJET)*, 05 (03), 734-740.
- Pelster, S.A., Schrader, W. and Schüth, F.: Monitoring temporal evolution of silicate species during hydrolysis and condensation of silicates using mass spectrometry. *J. Am. Chem. Soc.* 128(13), 4310-4317 (2006)
- Pereira L (2002) Construction and demolition waste recycling: the case of the Portuguese northern region (in Portuguese). Master Thesis in Civil Engineering, Minho University, Braga, Portugal
- Perera, D. S., Nicholson, C. L., Blackford, M. G., Fletcher, R. A. and Trautman, R. A. (2004) Geopolymers made using New Zealand flyash. *Journal of the Ceramic Society of Japan*, 112, S108–S111

- Perera, D. S., Uchida, O., Vance, E. R., & Finnie, K. S. (2007). Influence of curing schedule on the integrity of geopolymers. *Journal of materials science*, 42(9), 3099-3106.
- Petry, D.P., Haouas, M., Wong, S.C.C., Aerts, A., Kirschhock, C.E.A., Martens, J.A., Gaskell, S.J., Anderson, M.W. and Taulelle, F.: Connectivity analysis of the clear sol precursor of silicalite: are nanoparticles aggregated oligomers or silica particles? *J. Phys. Chem. C* 113(49), 20827-20836 (2009)
- Phair, J.W. and van Deventer, J.S.J.: Effect of the silicate activator pH on the microstructural characteristics of waste-based geopolymers. *Int. J. Miner. Proc.* 66(1-4), 121-143 (2002)
- Phair, J.W., van Deventer, J.S.J. (2002) Characterisation of fly-ash based geopolymeric binders activated with sodium aluminate. *Ind Eng Chem Res* 41:4242–4251
- Poon C.S (2007) Reducing Construction Waste. *Waste Management* 27: 1715–1716.
- Poon C.S., Shui Z.H., Lam L. (2004a), “Effect of microstructure of ITZ on compressive strength of concrete prepared with recycled aggregates” *Constr Build Mater* 18(6):461–468.
- Poon C.S., Shui Z.H., Lam L., Fok H., Kou S.C. (2004b),” Influence of moisture states of natural and recycled aggregates on the slump and compressive strength of concrete” *Cem Concr Res* 34(1):31–36.
- Provis J. and van Deventer J.S.J. (eds) (2009), *Geopolymers: structure, processing, properties and industrial applications*, Woodhead Publishing Limited, Cambridge.
- Provis, J. L., & Van Deventer, J. S. (Eds.). (2013). *Alkali activated materials: state-of-the-art report*, RILEM TC 224-AAM (Vol. 13). Springer Science & Business Media.
- Provis, J. L., Lukey, G. C. and Van Deventer, J. S. J. (2005) Do geopolymers actually contain nanocrystalline zeolites? – A re-examination of existing results. *Chemistry of Materials*, 17, 3075–3085. doi:10.1021/cm050230i.
- Provis, J. L., Lukey, G. C. and van Deventer, J. S. J. (2005b) Do geopolymers actually contain nanocrystalline zeolites? – A re-examination of existing results. *Chemistry of Materials*, 17, 3075–3085. doi:10.1021/cm050230i.
- Provis, J.L., Duxson, P., Lukey, G.C., Separovic, F., Kriven, W.M. and van Deventer, J.S.J.: Modeling speciation in highly concentrated alkaline silicate solutions. *Ind. Eng. Chem. Res.* 44(23), 8899-8908 (2005)
- Provis, J.L., Lukey, G.C. and van Deventer, J.S.J.: Do geopolymers actually contain nanocrystalline zeolites? - A reexamination of existing results. *Chem. Mater.* 17(12), 3075-3085 (2005)
- Provis, J.L., Rose, V., Bernal, S.A. and van Deventer, J.S.J.: High resolution nanoprobe X-ray fluorescence characterization of heterogeneous calcium and heavy metal distributions in alkali activated fly ash. *Langmuir* 25(19), 11897- 11904 (2009)

- Provis, J.L., Rose, V., Bernal, S.A. and van Deventer, J.S.J.: High resolution nanoprobe X-ray fluorescence characterization of heterogeneous calcium and heavy metal distributions in alkali activated fly ash. *Langmuir* 25(19), 11897- 11904 (2009)
- Provis, J.L., Rose, V., Winarski, R.P. and van Deventer, J.S.J.: Hard X-ray nanotomography of amorphous aluminosilicate cements. *Scripta Mater.* 65(4), 316-319 (2011)
- Provis, J.L., Yong, S.L. and Duxson, P.: Nanostructure/microstructure of metakaolin geopolymers. In: Provis, J.L. and van Deventer, J.S.J. (eds.) *Geopolymers: Structure, Processing, Properties and Industrial Applications*, pp. 72-88. Woodhead, Cambridge, UK (2009)
- Fernández-Jiménez, A. and Palomo, A.: Nanostructure/microstructure of fly ash geopolymers. In: Provis, J.L. and van Deventer, J.S.J. (eds.) *Geopolymers: Structure, Processing, Properties and Industrial Applications*, pp. 89-117. Woodhead, Cambridge, UK (2009)
- Provis, J.L., Yong, S.L. and Duxson, P.: Nanostructure/microstructure of metakaolin geopolymers. In: Provis, J.L. and van Deventer, J.S.J. (eds.) *Geopolymers: Structure, Processing, Properties and Industrial Applications*, pp. 72-88. Woodhead, Cambridge, UK (2009)
- Provis, J.L.: Activating solution chemistry for geopolymers. In: Provis, J.L. and van Deventer, J.S.J. (eds.) *Geopolymers: Structure, Processing, Properties and Industrial Applications*, pp. 50-71. Woodhead, Cambridge, UK (2009)
- Puertas F., Palacios M., Manzano H., Dolado J.S., Rico A. and Rodríguez J. (2011), 'A model for the C-A-S-H gel formed in alkali-activated slag cements', *J. Eur. Ceram. Soc.* 31(12), 2043–2056.
- Puertas, A. Barba, M. Gazulla, M. Gómez, M. Palacios, S. Martínez, Residuoscerámicos para su posible uso como materia prima en la fabricación de Clinkerde cemento portland: caracterización y activación alcalina, *Mater. Constr.* 56(2006) 7–84
- Puertas, F., Palacios, M., Manzano, H., Dolado, J.S., Rico, A. and Rodríguez, J.: A model for the C-A-S-H gel formed in alkali-activated slag cements. *J. Eur. Ceram. Soc.* 31(12), 2043-2056 (2011)
- R. Redden, N. Neithalath, Microstructure, strength, and moisture stability of alkali activated glass powder-based binders, *Cem. Concr. Compos.* 45 (2014) 46
- R.A. Feely, C.L. Sabine, K. Lee, W. Berelson, J. Kleypas, V.J. Fabry, et al. Impact of anthropogenic CO<sub>2</sub> on the CaCO<sub>3</sub> system in the oceans *Science*, 305 (16 July 2004), pp. 362-366
- Ramesh, A. and Koziński, J. A. (2001) <sup>29</sup>Si, <sup>27</sup>Al and <sup>23</sup>Na solid-state nuclear magnetic resonance studies of combustion generated ash. *Fuel*, 80, 1603–1610. doi:10.1016/S0016-2361(01)00041-2.



- Ravindrarajah RS, Tam CT (1985) Properties of concrete made with crushed concrete as coarse aggregate. *Mag Concr Res* 37(3):29–38
- Rees, C. A., Provis, J. L., Lukey, G. C. and Van Deventer, J. S. J. (2007) Attenuated total reflectance Fourier transform infrared analysis of fly ash geopolymer gel ageing. *Langmuir*, 23, 8170–8179. doi:10.1021/la700713g.
- Rees, C.A., Provis, J.L., Lukey, G.C., van Deventer, J.S.J. 2007a. Attenuated total reflectance Fourier transform infrared analysis of fly ash geopolymer gel aging. *Langmuir* 23:8170–79
- Rees, C.A., Provis, J.L., Lukey, G.C., van Deventer, J.S.J. 2007b. In situ ATR-FTIR study of the early stages of fly ash geopolymer gel formation. *Langmuir* 23:9076–82
- Reig, L., Tashima, M. M., Borrachero, M. V., Monzó, J., Cheeseman, C. R., & Payá, J. (2013). Properties and microstructure of alkali-activated red clay brick waste. *Construction and Building Materials*, 43, 98-106.
- Reixach FM, Cuscó AS, Barroso JMG (2000) Situación actual y perspectivas de futuro de los residuos de la construcción. Intitut de Tecnologia de la Construcció de Catalunya (IteC), Catalunya, Spain. (in Spanish)
- Richardson, I.G., Cabrera, J.G. (2000) The nature of C–S–H in model slag cements. *Cem Concr Compos* 22:259–266
- Robayo-Salazar, R. A., Rivera, J. F., & de Gutiérrez, R. M. (2017). Alkali-activated building materials made with recycled construction and demolition wastes. *Construction and Building Materials*, 149, 130-138.
- Rocha, J. and Klinowski, J. (1990) Solid-state NMR studies of the structure and reactivity of metakaolinite. *Angewandte Chemie – International Edition, English*, 29, 553–554. doi: 10.1002/anie.199005531.
- Rocha, J., Adams, J. M. and Klinowski, J. (1990) The rehydration of metakaolinite to kaolinite: Evidence from solid-state NMR and cognate techniques. *Journal of Solid State Chemistry*, 89, 260–274. doi:10.1016/0022-4596(90)90267-2.
- Rowles, M. and O’Connor, B.: Chemical optimisation of the compressive strength of aluminosilicate geopolymers synthesised by sodium silicate activation of metakaolinite. *J. Mater. Chem.* 13(5), 1161-1165 (2003)
- Roy, A., Schilling, P. J. and Eaton, H. C. (1996) Alkali activated class C fly ash cement, U.S. Patent 5,565,028.
- Roy, D.: Alkali-activated cements - Opportunities and challenges. *Cem. Concr. Res.* 29(2), 249-254 (1999)
- Ruiz-Santaquiteria, C., Skibsted, J., Fernández-Jiménez, A., Palomo, A. 2012. Alkaline solution/binder ratio as a determining factor in the alkaline activation of aluminosilicates. *Cem. Concr. Res.* 42:1242–51

- S. Ahmari, X. Ren, V. Toufigh, L. Zhang, Production of geopolymeric binder from blended waste concrete powder and fly ash, *Constr. Build. Mater.* 35 (2012) 718–729. <https://doi.org/10.1016/j.conbuildmat.2012.04.044>.
- S. Alonso, A. Palomo, Alkaline activation of metakaolin and calcium hydroxide mixtures: Influence of temperature, activator concentration and solids ratio, *Mater. Lett.* 47 (2001) 55–62.
- Sabir, B. B., Wild, S. and Bai, J. (2001) Metakaolin and calcined clays as pozzolans for concrete: a review. *Cement and Concrete Composites*, 23, 441–454. doi:10.1016/S0958-9465(00)00092-5.
- Sani D., Moriconi G., Fava G., Corinaldesi V. (2005), “Leaching and mechanical behaviour of concrete manufactured with recycled aggregates” *Waste Manage (Oxf)* 25(2):177–182.
- Santos J., Branco F.A., de Brito J. (2002b), “The use of coarse recycled concrete aggregates in the production of new concrete” (in Portuguese), *Structures 2002*. LNEC, Lisbon, pp 227–236.
- Schmücker, M. and MacKenzie, K. J. D. (2005) Microstructure of sodium polysialate siloxo geopolymer. *Ceramics International*, 31, 433–437. doi:10.1016/j.ceramint.2004.06.006.
- Scrivener, K. L., & Kirkpatrick, R. J. (2008). Innovation in use and research on cementitious material. *Cement and concrete research*, 38(2), 128-136.
- Sealey B.J, Phillips P.S, Hill G.J (2001) Waste Management Issues for the UK Readymixed Concrete Industry. *Resources, Conservation and Recycling* 32 (3–4): 321– 331.
- Sellevoid, E.J., Nilsen, T. (1987) Condensed silica fume in concrete: a world review. In: Malhotra VM (ed) *Supplementary Cementing Materials for Concrete*. CANMET, Ottawa, pp 165–243
- Shi C., Krivenko P.V. and Roy D. (2006), *Alkali-activated cements and concretes*, Taylor & Francis, London.
- Shi, C.: On the state and role of alkalis during the activation of alkali-activated slag cement. In: Grieve, G. and Owens, G., (eds.), *Proceedings of the 11th International Congress on the Chemistry of Cement*, Durban, South Africa, pp. 2097-2105 (2003)
- Skinner, L.B., Chae, S.R., Benmore, C.J., Wenk, H.R. and Monteiro, P.J.M.: Nanostructure of calcium silicate hydrates in cements. *Phys. Rev. Lett.* 104, 195502 (2010)
- Slavík, R., Bednařík, V., Vondruška, M., Skoba, O. and Hanzlíček, T.: Proof of sodalite structures in geopolymers. *Chem. Listy* 99, s471-s472 (2005)
- Smolcyk H.G. (1980), ‘Structure et caractérisation des laitiers’, 7th International Congress of the Chemistry of Cement, Paris, vol. 1, 1–16.

- Sun, Z., Cui, H., An, H., Tao, D., Xu, Y., Zhai, J., & Li, Q. (2013). Synthesis and thermal behavior of geopolymer-type material from waste ceramic. *Construction and Building Materials*, 49, 281-287.
- Taylor, H.F.W (1964) *The chemistry of cements*, 1st edition. Academic Press, London
- Taylor, R., Richardson, I.G. and Brydson, R.M.D.: Composition and microstructure of 20-year-old ordinary Portland cement-ground granulated blastfurnace slag blends containing 0 to 100% slag. *Cem. Concr. Res.* 40(7), 971-983 (2010)
- Temuujin, J. V., Van Riessen, A., & Williams, R. (2009). Influence of calcium compounds on the mechanical properties of fly ash geopolymer pastes. *Journal of hazardous materials*, 167(1-3), 82-88.
- Türkiye İnşaat Malzemeleri Sektör Görünüm Raporu (2011) Türkiye Odalar ve Borsalar Birliği. (In English: Report of Turkey Construction Material Sector Outlook, The Union of Chambers and Commodity Exchanges of Turkey) Available: <http://www.tobb.org.tr/Documents/yayinlar/Türkiye%20İnşaat%20Malzemeleri%200Sek%20tör%20Görünüm%20Raporu.pdf>. Accessed 2012 March 6.
- van Deventer, J. S., Provis, J. L., Duxson, P., & Brice, D. G. (2010). Chemical research and climate change as drivers in the commercial adoption of alkali activated materials. *Waste and Biomass Valorization*, 1(1), 145-155.
- van Deventer, J.S.J., Provis, J.L., Duxson, P., Lukey, G.C. 2007. Reaction mechanisms in the geopolymeric conversion of inorganic waste to useful products. *J. Hazard. Mater.* A139:506–13
- van Jaarsveld, J.G.S. and van Deventer, J.S.J.: Effect of the alkali metal activator on the properties of fly ash-based geopolymers. *Ind. Eng. Chem. Res.* 38(10), 3932-3941 (1999)
- van Jaarsveld, J.G.S., van Deventer, J.G.J (1999a) The effect of metal contaminants on the formation and properties of waste-based geopolymers. *Cem Concr Res* 29(8):1189–1200
- van Jaarsveld, J.G.S., van Deventer, J.S.J (1999b) Effect of the alkali metal activator on the properties of fly ash-based geopolymers. *Ind Eng Chem Res* 38:3932–3941
- Vieira J.P.B., Correia J.R., de Brito J. (2011), “Post-fire residual mechanical properties of concrete made with recycled concrete coarse aggregates” *Cem Concr Res* 41(5):533–541.
- Wang F.S., Rui-Lian S. and Ying-Jing C. (2005), ‘Study on modification of the high-strength slag cement material’, *Cement and Concrete Research* 35, 1344–1348.
- Wang S.D. and Scrivener K.L. (1995), ‘Hydration products of alkali activated slag cement’, *Cem. Concr. Res.* 25(3), 561–571.
- Wang S.D., Pu X.C., Scrivener K.L. and Pratt P.L. (1995), ‘Alkali-activated slag: a review of properties and problems’, *Cem. Concr. Res.* 17(27), 93–102.

- Wang, S.-D., Pu, X.-C., Scrivener, K.L. and Pratt, P.L.: Alkali-activated slag cement and concrete: a review of properties and problems. *Adv. Cem. Res.* 7(27), 93-102 (**1995**)
- Wang, S.D., Scrivener, K.L. and Pratt, P.L.: Factors affecting the strength of alkali-activated slag. *Cem. Concr. Res.* 24(6), 1033-1043 (**1994**)
- Ward, C. R. and French, D. (**2006**) Determination of glass content and estimation of glass composition in fly ash using quantitative X-ray diffractometry. *Fuel*, 85, 2268–2277. doi:10.1016/j.fuel.2005.12.026.
- Wastiels, J., Wu, X., Faignet, S. and Patfoort, G.: Mineral polymer based on fly ash. In: *Proceedings of the 9th International Conference on Solid Waste Management*, Philadelphia, PA. 8pp. Widener University (**1993**)
- Wastiels, J., Wu, X., Faignet, S. and Patfoort, G.: Mineral polymer based on fly ash. *J. Resourc. Manag. Technol.* 22(3), 135-141 (**1994**)
- Weldes, H.H. and Lange, K.R.: Properties of soluble silicates. *Ind. Eng. Chem.* 61(4), 29-44 (**1969**)
- White, C.E., Provis, J.L., Kearley, G.J., Riley, D.P. and van Deventer, J.S.J.: Density functional modelling of silicate and aluminosilicate dimerisation solution chemistry. *Dalton Trans.* 40(6), 1348-1355 (**2011**)
- Williams, P. J., Biernacki, J. J., Rawn, C. J., Walker, L. and Bai, J. (**2005**) Microanalytical and computational analysis of Class F fly ash. *ACI Materials Journal*, 102, 330–337.
- Woodward, R. and Duffy, N., **2011**. Cement and concrete flow analysis in a rapidly expanding economy: Ireland as a case study. *Resour. Conserv. Recycl.* 55, 448-455.
- X.S. Wang Magnetic properties and heavy metal pollution of soils in the vicinity of a cement plant, Xuzhou (China) *J. Appl. Geophys.*, 98 (**2013**), pp. 73-78
- Xiao JZ, Li WG, Sun ZH, Lange DA, Shah SP. Studying interfacial transition zones in recycled aggregate concrete with nanoindentation. *Cem Concr Compos* **2013**;37:276–92.
- Xu, H., Lukey, G. C. and van Deventer, J. S. J. (**2004**) The activation of Class C-, Class F-fly ash and blast furnace slag using geopolymerisation. *Proceedings of 8th CANMET/ ACI International Conference on Fly Ash, Silica Fume, Slag and Natural Pozzolans in Concrete*, Las Vegas, NV, Malhotra, V. M. (Ed.), 797–819.
- Y. Lei, Q. Zhang, C. Nielsen, K. He An inventory of primary air pollutants and CO<sub>2</sub> emissions from cement production in China, **1990–2020**
- Yang, K.-H., Song, J.-K., Ashour, A.F. and Lee, E.-T.: Properties of cementless mortars activated by sodium silicate. *Constr. Build. Mater.* 22(9), 1981-1989 (**2008**)
- Yang, X., Zhu, W. and Yang, Q.: The viscosity properties of sodium silicate solutions. *J. Solution Chem.* 37(1), 73-83 (**2008**)

- Yang, Z. X., Ha, N. R., Jang, M. S., Hwang, K. H., & Lee, J. K. (2009). The effect of SiO<sub>2</sub> on the performance of inorganic sludge-based structural concretes. *Journal of Ceramic Processing Research*, 10(3), 266-268.
- Yazhenskikh, E., Hack, K. and Müller, M. (2008) Critical thermodynamic evaluation of oxide systems relevant to fuel ashes and slags. Part 3: Silica–alumina system. *Calphad*, 32, 195–205. doi:10.1016/j.calphad.2007.05.004.
- Yip, C.K., Lukey, G.C. and van Deventer, J.S.J.: The coexistence of geopolymeric gel and calcium silicate hydrate at the early stage of alkaline activation. *Cem. Concr. Res.* 35(9), 1688-1697 (2005)
- Zhang, B., MacKenzie, K.J.D. and Brown, I.W.M.: Crystalline phase formation in metakaolinite geopolymers activated with NaOH and sodium silicate. *J. Mater. Sci.* 44(17), 4668-4676 (2009)
- Zhang, Y., Sun, W. and Li, Z. (2007) Preparation and microstructure of K-PSDS geopolymeric binder. *Colloids and Surfaces A – Physicochemical and Engineering Aspects*, 302, 473–482. doi:10.1016/j.colsurfa.2007.03.031.
- Zhou, H., Wu, X., Xu, Z. and Tang, M.: Kinetic study on hydration of alkaliactivated slag. *Cem. Concr. Res.* 23(6), 1253-1258 (1993)
- Zuhua, Z., Xiao, Y., Huajun, Z., & Yue, C. (2009). Role of water in the synthesis of calcined kaolin-based geopolymer. *Applied Clay Science*, 43(2), 218-223.